UNIVERSITÀ DEGLI STUDI DI MILANO

Scuola di Dottorato in Scienze Biologiche e Molecolari

XXVI Ciclo

SoxD and *SoxF* genes in hematopoietic and vascular development

Alice Omini

PhD Thesis

Scientific tutor: Monica Beltrame

Academic year: 2013-2014

SSD: BIO/11 – BIO/18

Thesis performed at:

Department of Biosciences

Università degli Studi di Milano

Index

Part I

Abstract

Members of the Sry-related HMG box (SOX) family of transcription factors are found throughout the animal kingdom and play widespread roles during development. SoxF proteins are expressed in endothelial cells during mouse vascular development and they are involved in the regulation of different aspect in vascular development. In the last year, the key role of Sox18 during early lymphatic specification has been well elucidated in mouse. We decided to investigate specifically the role played by *sox18* in zebrafish lymphatic development and the interplay between *sox18* and the central lymphatic growth factor *vegfc*. The external development, the optical clarity and the capacity to easily visualize the vascular tree and the blood circulation using a variety of labelling techniques make the zebrafish a useful model to study vascular morphogenesis *in vivo*. Since the initial description of the zebrafish lymphatic system in 2006 it has emerged as a very potent system to study lymphangiogenesis too. The presented data show that the role of Sox18 in lymphangiogenesis is evolutionarily conserved in zebrafish and suggest an unappreciated crosstalk between Sox18 and one of the most potent lymphangiogenic growth factors.

SoxD proteins are an atypical SOX group because they lack a transrepression or a transactivation domain, however they participate in transcriptional activation and repression in different contexts. Sox13 has been described to interact with Tcf1 in T cells, thereby preventing it from binding to target genes, and influencing T-cell differentiation. In literature, we found some hints that suggested a possible involvement for Sox13 in vascular development. We identified the zebrafish *SOX13* ortholog and, due to our interest in the role of *SOX* genes in vascular development, we decided to verify its potential activity. Zebrafish *sox13* is expressed in the

central nervous system, transiently in the developing vasculature and in primitive erythropoietic tissue. We observed that its knockdown impairs angiogenesis in different vascular beds and intersomitic vessels defects are apparently linked to an improper Notch signalling activation. We discovered also an unproposed role for Sox13 in primitive erythropoieis. We observed that *sox13* knockdown affects primitive erythrocyte maturation.

Altogether, the data collected during my PhD period contributed to the enrichment of the complex network that engages SOX proteins during embryo development.

1. State of the art

The development of an organism consists of a series of events that lead to the formation of a complex multicellular system starting from a zygote. For a correct embryogenesis, the delivery of nutrients, oxygen, cellular and humoral factors to the developing organs and structures is fundamental. Therefore, the establishment of a functional cardiovascular system is one of the earliest events that occurs during organogenesis. An accurate knowledge of the players and the signaling pathways and the mechanisms that regulate the correct patterning of the cardiovascular system is really relevant. In addition, the pathological formation of blood vessels associated with a wide range of human diseases is often regulated by the same or similar processes and molecules implicated in vascular development during embryogenesis (Folkman, 1995).

In the past centuries the study of the cardiovascular system engaged many scientists that used different animal models to examine the anatomy, the physiology and the development of the heart and the vascular vessels. In 1661, Marcello Malpighi accurately described the vascular network of a chicken embryo and in 1905 M. Hoyer illustrated the lymphatic system in early tadpoles (Carmeliet, 2005). In the last two decades the zebrafish has emerged as an innovative model system to go deeper into the mechanisms of cardiovascular development and the players that regulate this process in vertebrates. In 1996, in a large scale screen for mutations affecting zebrafish development, a series of mutants for different aspects of the hematopoiesis has been isolated (Ransom et al., 1996). Since then, zebrafish has been exploited to define the molecular mechanisms that regulate hematopoiesis in vertebrates. In 2006, the existence of a lymphatic system has been demonstrated also in zebrafish through the

characterization of the thoracic duct (TD) and other lymphatic vessels in developing and adult zebrafish (Kuchler et al., 2006; Yaniv et al., 2006). This system share important features of the lymphatic vessels of higher vertebrates including conserved anatomy, characteristic morphology, expression and function of genes important for mammalian lymphatic development and functional features, such as lack of connection to the blood vasculature and ability to clear fluid and macromolecules from surrounding tissues (Yaniv et al., 2006).

1.1 Vascular development in zebrafish

The external development, the optical clarity and the capacity to easily visualize the vascular tree and the blood circulation using a variety of labelling techniques make the zebrafish a useful model to study vascular morphogenesis *in vivo*. Furthermore, the small size of the zebrafish embryo ensures a sufficient supply of oxygen by passive diffusion to survive and develop for several days in condition of absence of blood circulation. Zebrafish has a closed circulatory system which shares many characteristics with those of humans and other higher vertebrates. In particular, the anatomical processes and the molecular mechanisms that regulate the assembly of a primary vascular network and its successive remodelling are highly conserved (Isogai et al., 2001; Isogai et al., 2003).

The primitive vascular network in vertebrate embryos form by *vasculogenesis*. This process consists of *de novo* blood vessel formation by angioblasts aggregation and cavitation (Risau and Flamme, 1995). Subsequently, new blood vessels will form by remodelling and sprouting from this primary plexus through a process called *angiogenesis* (Risau,

1997). Lymphatic capillaries are derived from venous endothelial cells (Sabin, 1902; Alitalo, 2011)(Fig. 1.1).

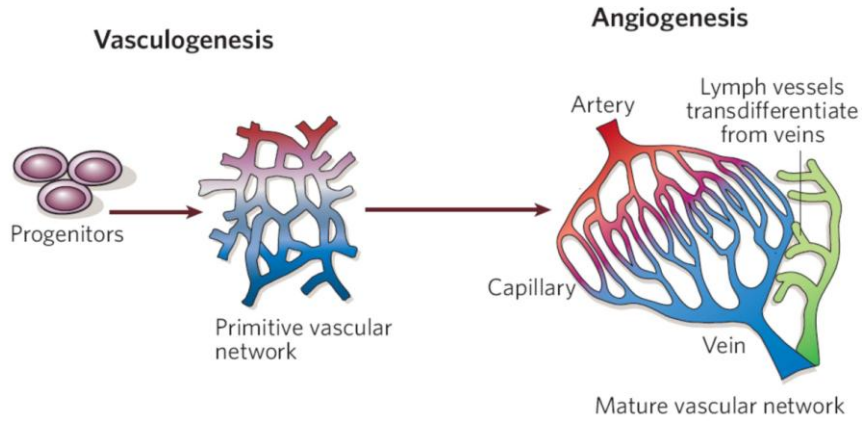

Fig. 1.1: Development of the vascular system in vertebrates. During vasculogenesis, endothelial progenitors give rise to a primitive vascular network, that will be remodeled and expanded during angiogenesis. Lymph vessels develop via trans-differentiation from veins (modified from Carmeliet, 2005).

1.1.1 Vasculogenesis in zebrafish

In zebrafish, as in other vertebrates, endothelial and hematopoietic cells are thought to be derived from a common progenitor, the hemangioblast, which originates from the lateral plate mesoderm (LPM) (Davidson and Zon, 2004). The first evidence of the existence of this cell was provided from the *cloche* mutant, which is characterized by a great reduction in both endothelial and hematopoietic progenitors (Stainier et al., 1995). In addition, genes such as *stem cell leukemia -scl-* and *fetal liver kinase-1/vascular endothelial growth factor receptor 2 –flk1/vegfr2* are required for the formation of both lineages in both zebrafish and mouse (Kallianpur et al., 1994; Kabrun et al., 1997; Liao et al., 1998). During early

somitogenesis, however, endothelial cell precursors, called angioblasts, begin to express genes specific of the endothelial identity (Fouquet et al., 1997). In particular, a series of studies have demonstrated that a set of E26 transformation-specific (ETS) transcription factors are fundamental for endothelial cell specification (well reviewed in Lelievre et al., 2001; Sumanas and Lin, 2006; Pham et al., 2007). Recently, it has been demonstrated that in zebrafish *etv2*/*etsrp* marks two different populations of angioblasts within the posterior LPM (Kohli et al., 2013). These populations originate at different time points and are located at different distances from the dorsal midline. Cell labeling and fate mapping experiments demonstrated that the medial angioblasts correspond to the arterial progenitors of the dorsal aorta (DA), while lateral angioblasts give rise to the venous endothelial cells of the posterior cardinal vein (PCV) (Kohli et al., 2013). Both Vegf and Shh concentrations are important for the proper migration and contribution of both pools of angioblasts to the DA and the PCV (Lawson and Weinstein, 2002). At around the 10 somite stage, the notochord expresses *sonic hodgehog* (*shh*), which induces the expression of the *vascular endothelial growth factor* (*vegf*) by the surrounding somites (Lawson and Weinstein, 2002) (Fig. 1.2). Under the influence of Vegf the medial angioblasts migrate intersomitically to the midline over the endoderm in the anterior to posterior sequence to form the DA. After the 15 somite stage, the lateral precursors initiate migration, with a migrational behavior similar to that of the medial angioblasts, to give rise to the PCV (Kohli et al., 2013) (Fig. 1.2).

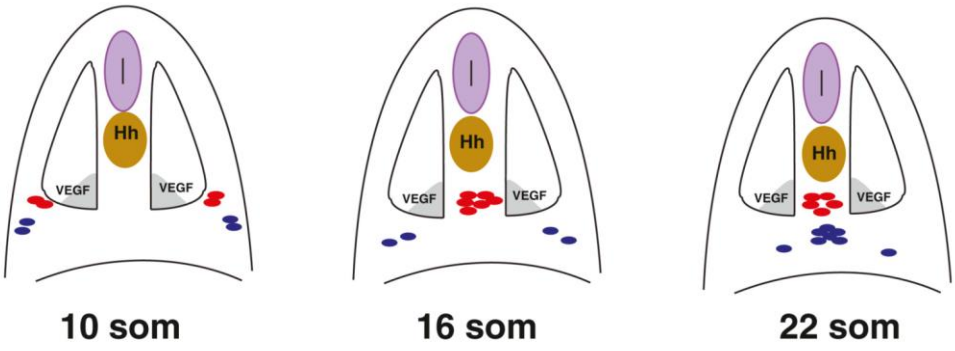

Fig. 1.2: Molecular control of vasculogenesis. During early somitigenesis *shh* expression by the notochord induces *vegf* expression in the somites (10 som). After the 10-somite stage, medial angioblasts migrate to the midline directly to the dorsal position where they differentiate as arterial cells. Shortly after the 15-somite stage, the lateral angioblasts migrate to the ventral position at the midline where they differentiate as venous endothelial cells. (Neural tube in purple, notchord expressing *shh* in brown, *vegf* expressed in the ventral somites, medial angioblasts in red and lateral angioblasts in blue) (Kohli et al., 2013).

An alternative proposed model is that the DA forms by classical vasculogenesis, whereas the formation of the PCV involves an alternative mechanism whereby selective sprouts of venous-fated angioblasts start from the DA, and cell-cell segregation allows distinct arterial and venous vessels to form (Herbert et al., 2009).

At the onset of circulation at around 24 hours post fertilization (hpf) the main axial vessels are formed and luminizated (Isogai et al., 2001). Initially blood flows through a simple single circulatory loop which goes caudally from the heart through the DA and returns rostrally via the PCV (Lawson and Weinstein, 2002)(Fig.1.3).

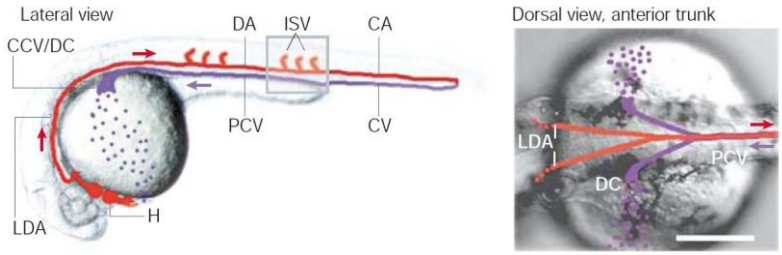

Fig. 1.3: Primary circulation in zebrafish embryo at 30 hpf. Blood leaves the heart (H) and enters the lateral dorsal aorta (LDA), which converge into the dorsal aorta (DA). The circulation flows into the caudal artery (CA), then into the caudal vein (CV) and returns rostrally through the posterior cardinal vein (PCV). Finally, it leaches through the Duct of Cuvier (DC), before returning to the heart (Lawson and Weinstein, 2002).

In the past, it was thought that arteries and veins acquired structurally and functionally distinct features in response to a different blood flow rates and pressure (reviewed in Lawson and Weinstein, 2002). Now, we know that there is a genetic program that specifies artery and vein identity before the onset of circulation. In mice the importance of EphrinB2/ReceptorB4 signaling in arterial-venous differentiation has been demonstrated (Wang et al., 1998). In zebrafish, the Notch pathway acts at a specific step in arterial-venous differentiation to activate an arterial while repressing a venous cell fate program within the presumptive DA. Embryos lacking Notch activity fail to induce arterial specific *ephrinB2a* expression, and exhibit ectopic expression of venous markers (Lawson et al., 2001). COUP-TFII, a member of the orphan nuclear receptor superfamily, is specifically expressed in venous but not arterial endothelium. Ablation of COUP-TFII in endothelial cells enables veins to acquire arterial characteristics, including the expression of Notch signaling molecules. Thus, COUP-TFII has a critical role in repressing Notch signalling to maintain vein identity, which suggests that vein identity is

under genetic control and is not derived by a default pathway (You et al., 2005).

1.1.2 Angiogenesis in zebrafish

After the set up of the primary vascular plexus by vasculogenesis, a mature and more complex network of vessels is obtained by angiogenesis. In the zebrafish embryo, if we limit our attention on the trunk/tail region, the main vessels which are formed through this process are the sub-intestinal vein (SIV) basket, the intersomitic vessels (ISVs), the dorsal longitudinal anastomotic vessels (DLAVs), and the caudal vein plexus (CVP; Fig.1.4). The development of these different types of structures is regulated by the interplay of different molecular pathways.

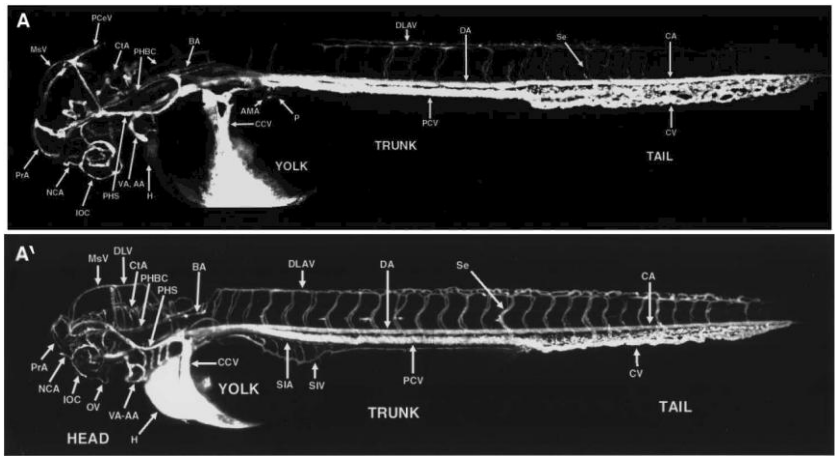

Fig.1.4: Microangiography of zebrafish embryos at 2 and 3 days post fertilization (dpf) (A and A', respectively). Vessels of the trunk-tail region: dorsal longitudinal anastomotic vessel (DLAV), dorsal aorta (DA), intersomitic vessels (Se or ISV), caudal artery (CA), caudal vein (CV), posterior cardinal vein (PCV), sub-intestinal artery (SIA) and vein (SIV) (Isogai et al., 2001).

In zebrafish, as in other vertebrates, ISVs are among the first angiogenic vessels to form (Isogai et al., 2003). When the formation of the DA and the PCV is completed, a set of primary sprouts emerge from the DA and migrate towards the dorsal region of the embryo, following each vertical somites boundary (Fig.1.5A). When they have reached the dorsal portion of the embryo they branch rostrally and caudally to connect with their neighbors to form the DLAV (Fig.1.5B-D). Once this primary set of ISV aorta-derived vessels formation is completed, secondary sprouts begin to emerge from the PCV, growing dorsally alongside the primary ISVs (Fig.1.5C and D). About half of these secondary sprouts connect with the adjacent primary ISV, which looses the connection with the DA and becomes a venous ISV (vISV; Fig1.5D and E). On the other hand, only the primary ISVs which are not attached by the secondary sprouts maintain an arterial identity and constitute the arterial ISVs (aISVs) (Isogai et al., 2003)). The other half of the secondary sprouts stop at the horizontal myoseptum and give rise to a pool of lymphatic precursors, the parachordal lymphangioblasts (PLs; for an accurate description see 1.1.3 section and Fig.1.7) (Bussmann et al., 2010).

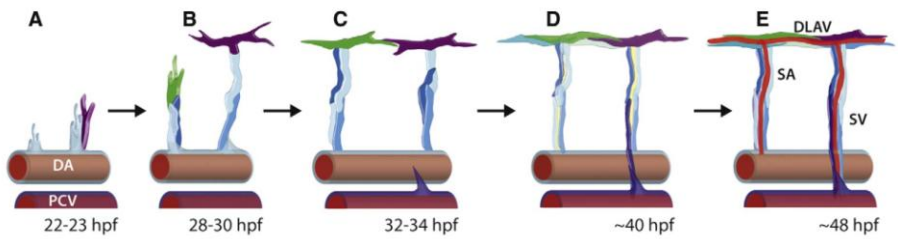

Fig.1.5: ISV and DLAV formation in the zebrafish trunk. Primary sprouts start from the DA and migrate dorsally to form aISV (or SA) and DLAV (A-C). Secondary sprouts originate from the PCV and a half of these connect to primary ISV, forming vISV (or SV; C-E) (Ellertsdottir et al., 2010).

If we analyze the structure of a single ISV sprout, we notice that it is formed by two different types of cells: the tip and the stalk cells. The tip cell is located in the apical portion of the sprout and it is characterized by long dynamic filopodial extensions, indispensible for the correct growth and migration of the vessel (Gerhardt et al., 2003; Siekmann and Lawson, 2007b). The stalk cells are behind the tip cell and are important to make up the base of the sprout and maintain the connection with the vessel of origin (Siekmann and Lawson, 2007a). Regulation of the correct identity of each of these cells is essential for the proper patterning of the vasculature. Tip cell differentiation is induced by VegfA signaling, which induces an endothelial cell to acquire a motile and invasive behavior (Gerhardt et al., 2003). Vegfr2 activation stimulates the up-regulation of the Notch ligand Delta-like4 (Dll4) in the tip cells inducing an up-regulation of the Notch signaling in the neighboring cells, that acquire a stalk cell identity through a lateral inhibition mechanism (Fig. 1.6) (Leslie et al., 2007; Siekmann and Lawson, 2007b; Jakobsson et al., 2010). Notch activation in the stalk cells have the effects to suppress angiogenetic activity and Vegfr-3/Flt4 activity (Siekmann and Lawson, 2007b; Tammela et al., 2008).

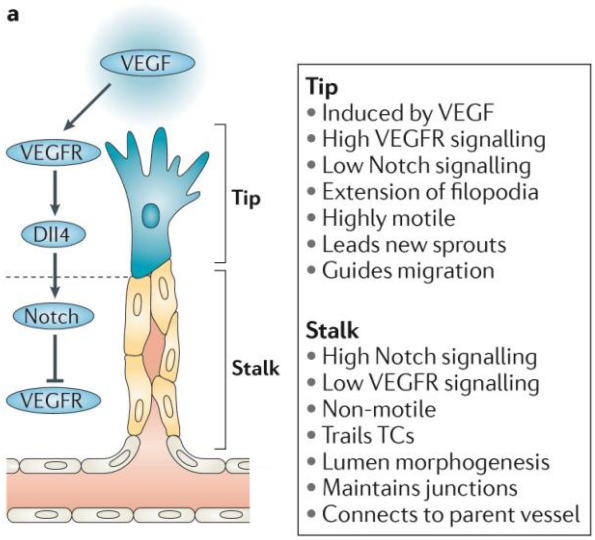

Fig. 1.6: Molecular mechanism of tip and stalk identity acquisition (well reviewed in Herbert and Stainier, 2011).

The caudal vein plexus is formed by a dorsal and a ventral vein interconnected by a series of sprouts which give rise to an honeycomb-like structure (Isogai et al., 2001). Sprouting from the axial vein is mainly regulated by bone morphogenetic protein (BMP) signaling (Wiley et al., 2011). However, also VegfA, which is considered the typical regulator of arterial sprouting, seems to be involved also in CVP remodeling (Rissone et al., 2012).

The SIVs run cranial ward along the yolk or the ventral walls of the intestine on both right and left sides (Isogai et al., 2001). These vessels originate from the duct of Cuvier at 2 dpf, however a partial contribution from also the PCV has been proposed recently (Karina Yaniv lab, unpublished data). During the next 24 hours, these vessels evolve in vascular plexus across most of the dorsal–lateral aspect of the yolk ball and

will provide, together with the supra-intestinal artery, blood supply to absorb the yolk (Nicoli and Presta, 2007). The molecular mechanism that regulates the SIV basket formation is not well characterized as in other districts, however an involvement of BMP signaling has been demonstrated , electing BMP as a main regulator of venous angiogenesis (Wiley et al., 2011).

1.1.3 Lymphangiogenesis in zebrafish

The lymphatic system is a major part of the vascular system. Tissue fluid homeostasis, fat absorption and a role in the immune response are among the most important functions of this apparatus (Tammela and Alitalo, 2010). In mammals, lymphatic precursors arise from the cardinal vein and give rise to the early lymph-sacs (Sabin, 1902; Oliver and Srinivasan, 2010). The mature lymphatic vasculature will form by the remodeling of these structures, and by ballooning from the cardinal vein and migration as single cells (Francois et al., 2012; Hagerling et al., 2013). A venous origin of lymphatic precursors (PLs) has been demonstrated also in zebrafish (Kuchler et al., 2006; Yaniv et al., 2006). As I mentioned above, PLs originate from secondary sprouting which arise from the PCV and transiently reside at the horizontal myoseptum. Precursors that migrate dorsally will form lymphatic intersomitic vessels (ISLVs) and the dorsal longitudinal lymphatic vessels (DLLVs), while those that migrate ventrally will give rise to the thoracic duct (TD; Fig. 1.7) (Bussmann et al., 2010). The TD is the principal lymphatic vessel in the trunk and it is located between the DA and the PCV. Very recently, it has been shown that only cells which reside in the floor of the PCV, and express angioblast markers, give rise to PLs (Karina Yaniv lab, unpublished data).

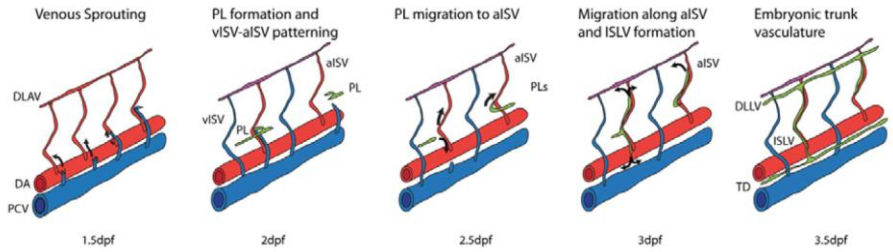

Fig. 1.7: Lymphatic patterning in the zebrafish trunk. Sprouts from the PCV that do not connect to primary ISV migrate to the horizontal myoseptum region where they constitute a pool of PLs. PLs will migrate ventrally or dorsally to form the thoracic duct and ISLVs, respectively, and use arteries as their substrate. ISLVs give ride to the DLLV in the dorsal region (Bussmann et al., 2010).

In zebrafish, the lymphatic system develops under the control of some molecular cues shared with mammals, including the vascular endothelial growth factor VEGFC and its receptor VEGFR3/Flt4. Mammalian VegfC has been identified as potent inducer of lymphatic sprouting (Jeltsch et al., 1997; Saaristo et al., 2002). The knockdown of *vegfc* in zebrafish resulted in marked effects on formation of the TD, and zebrafish *flt4* mutant (*expando*) lacks lymphatics vessels and venous sprouting (Kuchler et al., 2006; Yaniv et al., 2006; Hogan et al., 2009). In the last few years, new zebrafish transgenic lines allow to uncover previously uncharacterised lymphatic vascular beds, such as the facial lymphatics (FLs) the lateral lymphatics (LL) and the intestinal lymphatics (IL) (reviewed in Koltowska et al., 2013).

1.2 Hematopoieis in zebrafish

Hematopoieis is the process through which the blood cellular components are formed. It occurs both during embryonic development and throughout

adulthood to guarantee the production and the renewal of blood cells. Due to these characteristics, in vertebrates, included zebrafish, we can distinguish two different waves of hematopoieis. During the first one, called primitive, erythrocytes and cells of the myeloid lineage are transiently produced; the successive wave, the definitive, gives rise to all blood lineages (erythroid, myeloid and lymphoid) (reviewed by Galloway and Zon, 2003).

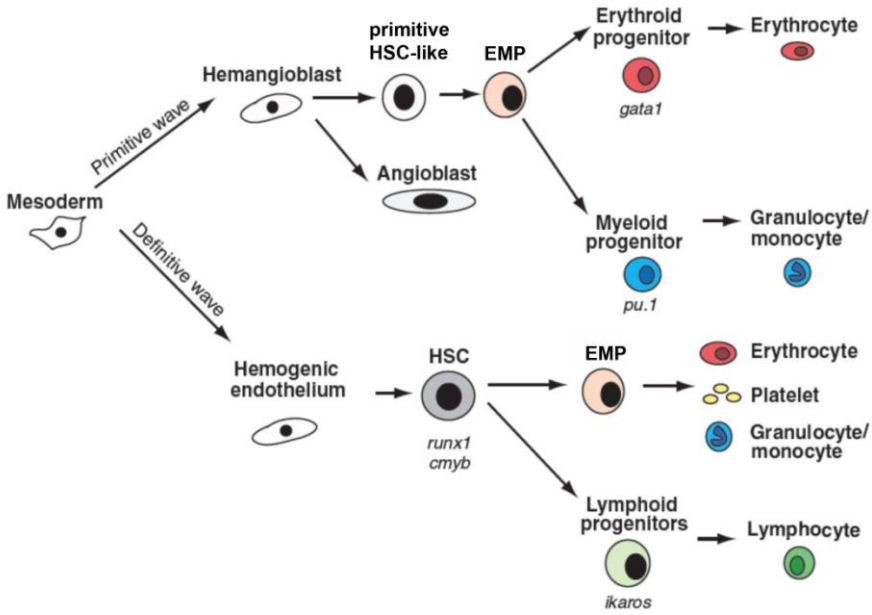

Fig. 1.8: Primitive and definitive waves in zebrafish. EMP: erythroid-myeloid progenitor, HSC: hematopoietic stem cell (modified from Jing and Zon, 2011).

1.2.1 Primitive wave

In mammals and avians, primitive hematopoiesis occurs in the blood islands in the extra-embryonic yolk sac (Palis et al., 2001). In zebrafish, on

the contrary, primitive blood cells originate in intra-embryonic structures (Detrich et al., 1995). Early erythroid precursors originate from two bilateral stripes in the posterior lateral plate mesoderm (PLM; Fig. 1.9) around 5 ss. Later in development, around 18 ss, these precursors migrate towards the midline to give rise to the equivalent of the mammalian blood islands, the intermediate cell mass (ICM; Fig. 1.9). Within the ICM, erythroid progenitors differentiate in proerytrhroblasts that enter the circulation at 24-26 hpf (Detrich et al., 1995). On the other hand, myelopoieis occurs in the rostral portion of the embryo, the anterior lateral plate mesoderm (ALM; Fig. 1.9), and mainly produces macrophages (Herbomel et al., 1999).

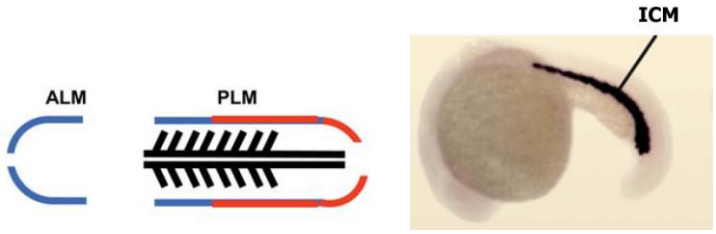

Fig. 1.9: Anatomical districts of primitive hematopoieis. Anterior lateral plate mesoderm (ALM) and posterior lateral plate mesoderm (PLM; left panel) (Ciau-Uitz et al., 2010). Intermediate cell mass (ICM) (modified from Orkin and Zon, 2008).

In zebrafish, all erythrocytes are nucleated (Al-Adhami, 1977). Erythrocytes differentiation consists in changes in cell size, in nuclear shape and in cytoplasm staining. The most immature cells are big round-shaped, have a large and open nucleus and a more basophilic cytoplasm (Ransom et al., 1996). Mature erythrocyte are rugby-ball shaped and smaller than controls, the nucleus is more condensed and the cytoplasm is acidophilic (Ransom et al., 1996). From 30 hpf to 5 dpf four main stages can be identified: stage I, basophilic erythroblast; stage II, polychromatophilic erythroblast; stage III, orthochromatophilic

erythroblast; and stage IV, mature erythrocyte (Qian et al., 2007) (Fig. 1.10).

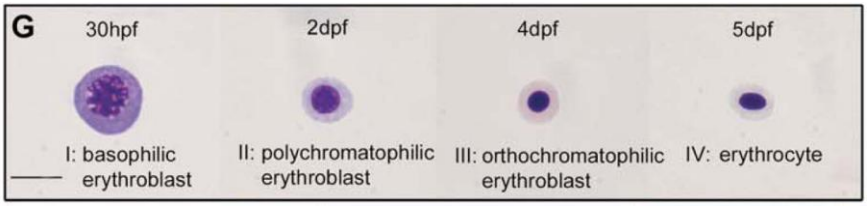

Fig. 1.10: Erythrocytes at different stages of maturation from 30 hpf to 5 dpf. May-Grunwald Giemsa staining (modified from Qian et al., 2007).

Primitive hematopoieis is largely regulated by Gata1, the master regulator of erythrocyte development, and Pu.1, crucial for myeloid fate acquisition (Scott et al., 1994; Cantor et al., 2002). These two transcription factors exhibit a cross-inhibitory relationship to regulate erythrocyte and myeloid fates.

1.2.2 Definitive wave

Definitive hematopoieis provides long-term hematopoietic stem cells (HSC) with self-renewal property, which are able to differentiate in erythroid, myeloid and lymphoid lineages. In mammals and frog HSCs originate from the aorta-gonad-mesonephros region (AGM) (Cumano and Godin, 2007; Taoudi and Medvinsky, 2007). In zebrafish, the ventral wall of the dorsal aorta has been identified as the analogous of this structure (Murayama et al., 2006; Kissa et al., 2008).

The transcription factor *Runx1* is expressed in mouse embryos by those cells of arterial vessels that will become HSCs and so it is essential for their emergence from the AGM (North et al., 2002). In zebrafish, HSCs bud from the aortic floor, they enter circulation through the axial vein, and

accumulate in the region of the caudal hematopoietic tissue (CHT) (Kissa and Herbomel, 2010). Around 4-5 dpf, cells leave the CHT to colonize the organs that will be the sites of adult hematopoiesis where precursors of these cells will proliferate and differentiate: the thymus for the T cells and the kidney marrow for erythrocytes (Murayama et al., 2006; Jin et al., 2007; Kissa et al., 2008).

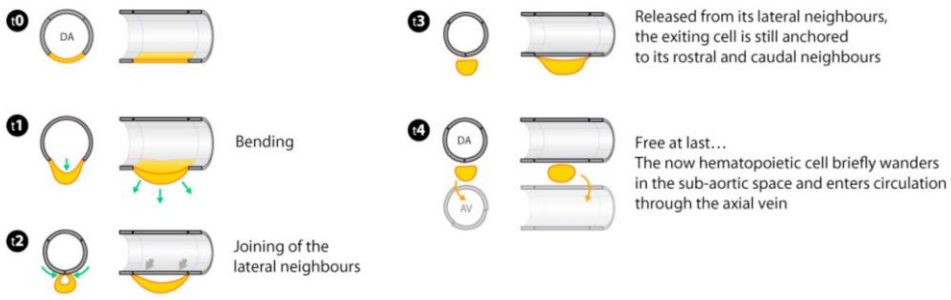

Fig. 1.11: Endothelial cells bud from the ventral wall of the dorsal aorta and transform into hematopoietic cells. Transverse and sagittal views of the successive steps of the endothelial to hematopoietic transition (modified from Kissa and Herbomel, 2010).

1.3 The SOX family

Members of the Sry-related HMG box (SOX) family of transcription factors are found throughout the animal kingdom. They have been implicated in cell fate decisions in several developmental processes and they have diverse tissue-specific expression patterns during early development (Pevny and Lovell-Badge, 1997; Wegner, 1999; Bowles et al., 2000).

SOX proteins are characterized by the presence of a DNA-binding high mobility group (HMG) box domain (Bowles et al., 2000). The HMG box is 79 aa long and consists of three alfa-helices which can bind the

minor groove of the DNA to ATTGTT or related sequences motifs. This binding widens the minor groove and causes DNA to bend towards the major groove (reviewed in Kamachi and Kondoh, 2013). In 1990, this family of transcription factors was first identified in mammals based on the conservation of the HMG box of the gene for the mammalian testis determining factor SRY (Gubbay et al., 1990). By convention, HMG box domains of SOX proteins are at least 50% identical to the HMG box domain of SRY. However, over the years, new SOX genes, which do not confirm this rule, have been identified. Recent studies allow classifying SOX proteins on the base of the conservation of a key motif within the HMG box: the sequence RPMNAFMVW (position 5-13) appears to be conserved in all SOX proteins but not in the most closely related outgroups (Bowles et al., 2000).

In mice and humans the SOX family comprises 20 genes (Schepers et al., 2002) which have been divided into 8 groups (A-G) on the basis of sequence similarity and genomic organization (Bowles et al., 2000) (Fig. 1.12). It is not unusual that members of the same groups, when expressed in the same developing tissue, share equivalent function, and many redundant roles between SOX proteins that co-regulate the same targets has been observed (well reviewed in Kamachi and Kondoh, 2013). The transcriptional activity of a SOX protein is strictly related to the propensity to form a complex with other partner transcription factors, thus, a Sox binding site in the DNA is accompanied by a second binding site for its partner (Kondoh and Kamachi, 2010).

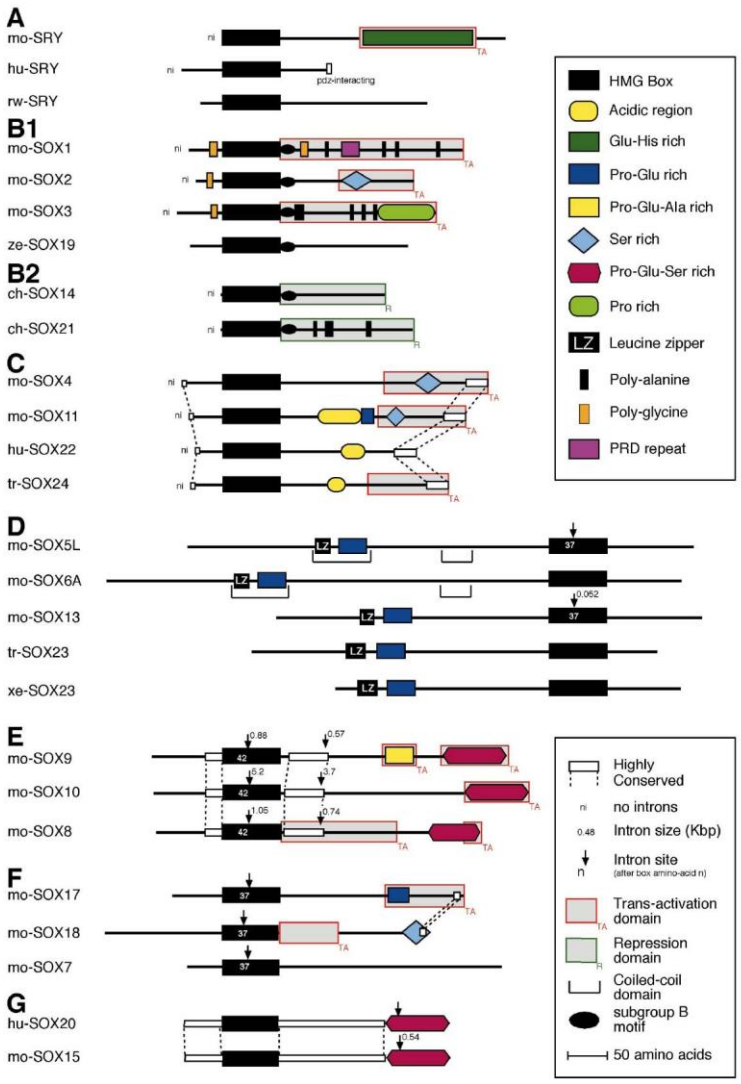

Fig.1.12: Schematic representation of SOX proteins highlighting conserved region and domain within SOX family groups. Proteins are arranged in groups as defined by HMG domain sequence. Various structural features, motifs, and functional regions are shown along with intron positions and sizes where known (Bowles et al., 2000).

1.3.1 SOX13

SOX13 belongs with its closely related SOX proteins, SOX5 and SOX6, to the SoxD group. SoxD proteins differ from the other SOX proteins because they have their HMG-box domain in the C-terminus and do not present a trans-activation nor a trans-repression domain. In the N-terminus, SOXD proteins present a coiled-coil domain, which is important to reinforce protein–protein interactions (Lefebvre, 2010). This domain is constituted by a leucine zipper and a neighboring glutamine-rich sequence stretch, which was named Q box (Kido et al., 1998) .

Sox13 expression pattern in mouse tissues during embryogenesis was firstly analyzed by Roose and colleagues by *in situ* hybridization on histological sections (Roose et al., 1998). *Sox13* was first detected in the wall of the great arteries at E13.5 (Fig. 1.13 A), while the vein walls did not express *Sox13*. A *Sox13* signal was also found in the saccular component of the inner ear. In E16.5 embryos, the intensity of *Sox13* expression in the arteries is similar to that at E13.5 (Fig. 1.13 B). In the inner ear, a signal was seen in the saccular and utricular components and in the ampullae of the semicircular canals. A small number of strongly staining cells were observed in the thymus. Just before birth (E18.5), staining in the arteries had strongly increased and appeared confined to the media and intima layers (Fig. 1.13 C). In addition to the great vessels, *Sox13* expression included other smaller vessels. The wall of the veins remained negative for *Sox13* staining. *Sox13* was expressed also in the tracheal epithelium below the vocal cord and by the hair follicles in the skin. In neonates of 1 day old, expression of *Sox13* in the wall of most arteries further increased in intensity (Fig. 1.13D) (Roose et al., 1998).

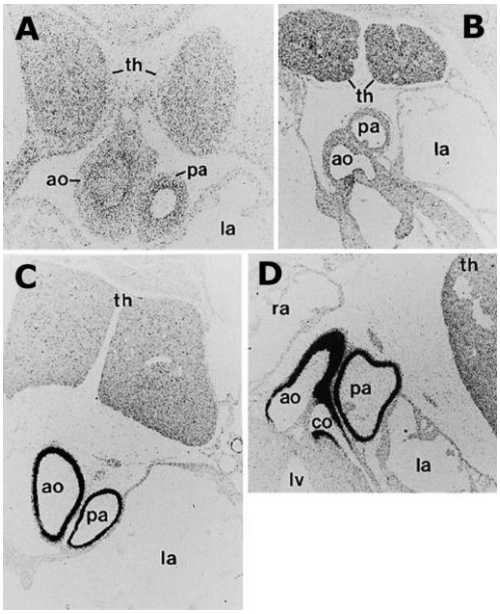

Fig. 1.13: Sox13 expression in arterial walls during embryonic development in mice. *In situ* hybridization on histological sections at E13.5 (A), E16.5 (B), E18.5 (C) and neonates day one (D). ao: aorta , pa: pulmonary artery. Positive signals have been detected also in thymus (th) (modified from Roose et al., 1998).

Sox13 is expressed also in developing central nervous system in mouse and its spatial distribution has been well characterized by immunohistochemistry on mice embryos and histological sections (Wang et al., 2005; Wang et al., 2006). At E12.5, SOX13 expression was detected in the brain and with a lower expression level in the spinal cord. From E13.5 to E15.5, SOX13 was strongly expressed in the forebrain, midbrain, and hindbrain and in the developing spinal cord (Wang et al., 2005; Wang et al., 2006). SOX13 expression was predominantly detected in the differentiating zone of these structures and, in particular, it identifies a sub-population of post-mitotic differentiating neuronal cells (Wang et al., 2005). SOX13 was also expressed in the condensing mesenchyme and cartilage progenitor cells during endochondral bone formation in the limb as well as the somite sclerotome and its derivatives (Wang et al., 2006).

Finally, SOX13 was detected in the developing kidney, pancreas, and liver as well as in the visceral mesoderm of the extra-embryonic yolk sac and spongiotrophoblast layer of the placenta (Wang et al., 2006). *SOX13* expression was also investigated in human adult tissues by Northern blot analysis. *SOX13* mRNA was detected in multiple tissues, including heart, brain, placenta, lung, liver, kidney, and pancreas, suggesting that SOX13 may be involved in a variety of cellular processes (Kasimiotis et al., 2000).

Sox13 is known to be involved in the regulation of T-cell differentiation by promoting gammadelta T-cell development while opposing alphabeta T-cell differentiation (Melichar et al., 2007; Gray et al., 2013; Ouyang et al., 2014). In addition, Sox13 may enhance IL-7 responsiveness for the survival of such thymocytes, and one effect of *Sox13* deficiency on gammadelta T cells is to diminish progenitor survival (Turchinovich and Hayday, 2011). During T cell differentiation, SOX13 acts by directly binding and presumably sequestering TCF1 and/or modifying its activity. The activity of TCF1 is induced by canonical Wnt signaling by its association with the coactivator beta-catenin, thus SOX13 has been proposed as an inhibitor of the Wnt signaling in T-cell differentiation (Melichar et al., 2007). The ability of SOX13 to modulate Wnt activity has been further demonstrated (Marfil et al., 2010). The binary interactions between Hhex, SOX13 and TCF to regulate Wnt activity have been shown both *in vitro* and *in vivo*. Sox13 can bind TCF1 to disrupt the beta-catenin-TCF complex. However, the addition of Hhex results in the formation of the Hhex·SOX13 complex that can restore the TCF1-beta catenin interaction and results in restoration/elevation of the Wnt activity levels (Marfil et al., 2010).

1.3.2 SOX18

SOX18 belongs to the SoxF group with Sox7 and Sox17. Sox18 protein is characterized by the HMG-box, at the N-terminus, and a central trans-activation domain (Hosking et al., 1995). The C-terminus region comprises a beta-catenin interaction motif and it is involved in the transactivation activity too, (Sinner et al., 2004; Sandholzer et al., 2007).

Sox18 is transiently expressed in endothelial cells of the nascent blood vessels during embryonic development and adult neo-vascularization (Downes and Koopman, 2001). Whole-mount *in situ* hybridization (WISH) analysis performed in our laboratory, revealed that this is true also in zebrafish embryo (Cermenati et al., 2008). *sox18* expression is detectable at 6-8 somite stage in bilateral stripes corresponding to the posterior lateral plate mesoderm (PLM; Fig. 1.14 D and F) and, at a lower level, in the anterior lateral plate mesoderm (ALM; Fig. 1.14 F), where the presumptive common precursors of blood and endothelial cells reside (Gering et al., 1998; Brown et al., 2000). Moreover, *sox18* is expressed in the innermost PLM *fli1*-positive cells, corresponding to endothelial cell precursors, as revealed by double ISH (Fig. 1.14 F). Later in development, *sox18* marks the developing axial and intersomitic vessels (ISVs), the intermediate cell mass (ICM), where endothelial and blood cell precursors reside, and the developing head vasculature (Fig. 1.14 J-K-L-M) (Cermenati et al., 2008). *sox18* is also expressed in the rostral region of the embryo from early somitogenesis. At around 24 hpf, a *sox18* signal is detectable in rostral parts of the central nervous system, notably in the eye region (Fig. 1.14L) (Cermenati et al., 2008).

Fig. 1.14: *sox18* expression pattern during zebrafish embryogenesis from 8 somites stage to 36 hpf by WISH. Double ISH with *fli1a* endothelial cell precursors marker (F; in red) modified from (Cermenati et al., 2008).

During zebrafish development *sox7* expression is largely overlapping with that of *sox18*. The *sox7* signal is detectable a little bit earlier in the LPM during somitogenesis (4 somites), but at the following stages, up to 29 hpf, they share the expression in the same vascular districts (Cermenati et al., 2008). However, *sox7* expression in the PCV goes down earlier and at 36 hpf only *sox18* is detectable in the venous trunk vessel (Cermenati et al., 2013).

Sox18 is known to be involved in vascular and lymphatic development in different species (Irrthum et al., 2003; Francois et al., 2008). Mutations in SOX18 are associated with the Hypotrichosis-Lymphedema-Telangiectasia (HLT) syndrome, combining defects in hair, blood vessels and lymphatic development (Slee, 1957; Irrthum et al., 2003). Very recently it has been reported for the first time a renal failure

associates with *SOX18* mutation (HLT-renal defect syndrome or HLTRS) (Moalem et al., 2014). The murine counterpart of the disease is represented by the *ragged* phenotype, first described in 1950s, due to the spontaneous mutations in *Sox18* (Slee, 1957). Four allelic variants of the *ragged* phenotype have been identified, altering the transactivation and C-terminal domains of the Sox18 protein, without affecting the DNA binding domain (Pennisi et al., 2000b; James et al., 2003). The most severe allele, *ragged-opossum* (*RaOp*), causes embryonic lethality before E11.0 in homozygous mutant mice (Green and Mann, 1961; Pennisi et al., 2000b). These mutations give rise to truncated SOX18 proteins which act in a dominant-negative manner and can interfere with functionally redundant SOX transcription factors (Pennisi et al., 2000a; Downes and Koopman, 2001).

On the other hand, *Sox18*-null mice were originally described as viable and presented only a mild coat defect (Pennisi et al., 2000a). Some years later, in another study, *Sox18*-null mice showed gross subcutaneous edema at E13.5 and died after E14.5 (Fig. 1.15) (Francois et al., 2008).

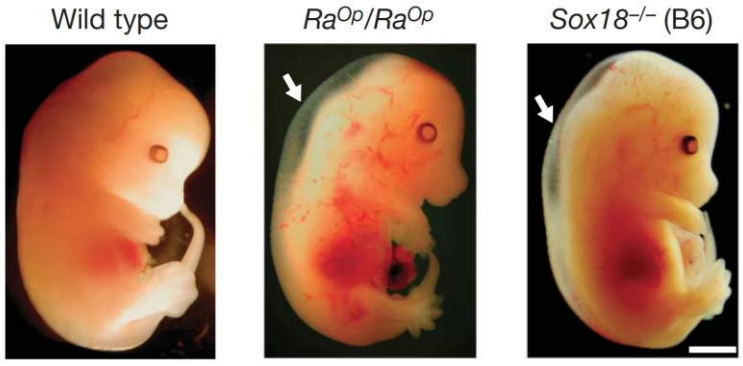

Fig. 1.15: $Sox18^{-/-}$ (B6) and Ra^{Op}/Ra^{Op} mutant embryos show edema at E13.5 (white arrows) (Francois et al., 2008).

The difference between the two studies was that the first one was carried out using a mixed 129-CD1 background, and the second one in a pure C57BL/6 (B6) background. Another study demonstrated that Sox7 and Sox17 could act as strain specific modifiers of the lymphangiogenic defects caused by *Sox18* dysfunction in mice (Hosking et al., 2009). Although these genes could act redundantly with *Sox18*, their action in this context is not one of simple redundancy, because these genes are not normally expressed during lymphangiogenesis. However, these genes were upregulated in the absence of *Sox18* function, and specifically on a mixed background but not on the B6, indicating that they act as strain-specific modifiers of the *Sox18* lymphatic phenotype (Hosking et al., 2009).

In mice, Sox18 can act as a molecular switch to induce differentiation of lymphatic endothelial cells (LECs) (Francois et al., 2008). *Sox18* is expressed in a subset of cardinal vein cells that later co-express the transcription factor prospero-related homeobox 1 (*Prox1)* and migrate to form lymphatic vessels, under the control of a VegfC signal (Fig. 1.16). Sox18 directly activates *Prox1* transcription by binding to its proximal promoter. Over-expression of Sox18 in blood vascular endothelial cells induces them to express Prox1 and other lymphatic endothelial markers, while *Sox18*-null embryos in the B6 background show a complete blockage of lymphatic endothelial cell differentiation from the cardinal vein (Francois et al., 2008). Sox18 acts at the nexus of differentiation of lymphatic endothelial progenitor cells from blood endothelial cells (BECs) in the embryo.

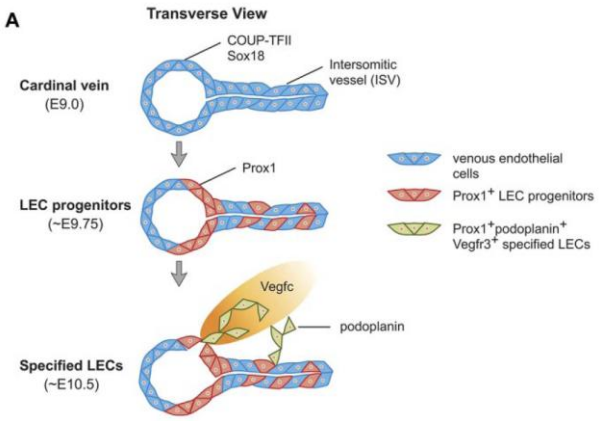

Fig. 1.16: **Development of the mammalian lymph sacs.** (Yang et al., 2012).

2. Aim of the project

The focus of our laboratory is to investigate the role of Sox genes in vascular development, using zebrafish as model system. In 2008, a paper that well elucidates the redundant role of Sox7 and Sox18 in arterial-venous differentiation in zebrafish was published by our laboratory (Cermenati et al., 2008). Due to the described role for Sox18 in lymphatic differentiation in mammals, and the discovery, in 2006, of a zebrafish lymphatic system, the obvious pursuit of our research line was to investigate a possible conserved activity in zebrafish. I was included in this research project to investigate some aspects of the story, such as the interplay between *sox18* and *vefgc* and the role of *sox17* in this context.

At the same time, we were interested in verifying a possible involvement of Sox13 in vascular development, as suggested by McGary and colleagues in PNAS (McGary et al., 2010). In this paper, an innovative method that quantitatively and systematically identifies nonobvious equivalences between mutant phenotypes in different species was proposed, based on overlapping sets of orthologs genes from human, mouse, yeast, worm, and plants. Using this method an association between a reduction in yeast growth rate and abnormal angiogenesis in mouse was found. The researchers tried to validate their hypothesis by the knockdown of human *SOX13* by siRNA, that disrupts tube formation in HUVECs, and showing that *Xenopus sox13* morpholino-knocked down embryos presented defects in vascular tree formation (McGary et al., 2010).

Sox13 is poorly studied compared with other Sox protein and in zebrafish it is completely uncharacterized. We identified a *bona fide Sox13* in zebrafish and I have analyzed its detailed expression pattern. To investigate its role during zebrafish embryo development, I performed

morpholino-mediated knockdown. *sox13* morphants (embryos injected with morpholino) phenotype has been characterized using different approach and, finally, I tried to shed light on the potential molecular pathways that required Sox13 action.

3. Main results and conclusions

3.1 Sox18 genetically interacts with VegfC to regulate lymphangiogenesis in zebrafish

In our lab a strong genetic interaction between Sox18 and VegfC has been demonstrated in the early phases of lymphatic development in zebrafish (Cermenati et al., 2013). Knockdown of *sox18* selectively impaired lymphatic sprouting leading to a defective TD formation and the combined partial knockdown of *sox18* and *vegfc*, using subcritical doses of specific morpholinos, revealed a synergistic interaction in this process and suggests a crosstalk between Sox18 and Vegfc pathways in zebrafish lymphatic development.

A cross-regulation at transcripts level between *sox18* and *vegfc* is excluded because *vegfc* expression is not altered in *sox18* morphants and *vegfc* knockdown does not affect *sox18* expression. In cultured mouse Lymphatic Endothelial Cells (LECs) stimulation with VEGF-C modulates the transcriptional activity of SOX18 protein (Francois et al., 2008). It can be hypothesized that VEGF-C/VEGFR3 signaling is implicated in modulating Sox18 transcriptional activity by inducing a post-translational modification.

To better characterize the molecular interplay between VegfC and Sox18, we analyzed TD formation at 5 dpf in both *sox18* morphants injected with *vegfc* mRNA and *vegfc* morphants injected with *sox18* mRNA. *vegfc* knockdown is not rescued by the injection of *sox18* mRNA. However the injection of *vegfc* mRNA partially rescues defects in thoracic duct formation in *sox18* morphants. These data suggest that the Sox18 transcriptional activity could be modulated by VEGFR3/VEGFC signaling in an evolutionarily conserved manner.

We decided to check for background dependent effects, like compensatory up-regulation of the other *SoxF* genes (Hosking et al., 2009). In zebrafish, *sox18* and *sox7* have largely overlapping expression in the developing vasculature and, as I mentioned previously, play a redundant role in the establishment of proper arterial-venous identity (Cermenati et al., 2008). *sox17* expression in endodermal districts is well characterized, however nothing was reported in literature about a possible expression in vascular districts. I observed *sox17* expression in the region of the ventral wall of the dorsal aorta at 29 hpf. I performed WISH assays for *sox17* on *sox18* and *sox18*/*vegfc* morphants at 29 hpf and no difference of its expression levels were detectable in both type of morphants compared to controls (unpublished data, included in the answers to the referees). The expression levels of *sox7* in *sox18* morphants and *sox18*/*vegfc* morphants were analysed by WISH before or around early stages of lymphatic development, and no significant change was observed. In conclusion, we excluded a compensatory upregulation of *sox7* and *sox17* in vascular districts as a consequence of *sox18* knockdown.

3.2 Sox13 is involved in ISV angiogensis, as a modulator of the Notch signaling

Characterization of *sox13* expression by RT-PCR revealed that *sox13* transcripts are present from very early developmental stages up to 5 days post fertilization (dpf), which was the last stage I analyzed. WISH analysis revealed that *sox13* is widely expressed in the developing Central Nervous System (CNS), as described in mice (Wang et al., 2005; Wang et al., 2006). During somitogenesis, initially *sox13* is weakly expressed by

angioblasts and later it is clearly detectable in the forming axial vessels. At 22 hours post fertilization (hpf) I detected *sox13* expression in the endothelium of the dorsal aorta and in the intermediate cell mass (ICM), where cells of the erythroid lineage develop. *sox13* expression in zebrafish adult organs has been detected in ovary, kidney, gills, gut and, at a very low level, also in liver, heart and muscle.

We decided to characterize *sox13* functional roles during embryonic development via morpholino-induced knockdown. We report here that in *sox13* morphants the formation of blood vessels by angiogenesis is largely disrupted in different vascular beds. We focused our attention on primary intersomitic vessels (ISVs) migration and dorsal longitudinal anastomotic vessels (DLAVs) formation. A range of ISV defects are observed in *sox13* morphants with increasingly severe phenotypes, leading to partially formed or completely absent DLAVs. These defects could be rescued by *sox13* RNA injection. Notch pathway hyper-activation inhibits normal angiogenesis, similarly to *sox13* knockdown. Furthermore, the expression of the Notch-controlled gene *ephrinB2a* is slightly upregulated in *sox13* morphants. We were able to rescue ISVs migration and DLAVs formation by treating *sox13* morphants with DAPT, a Notch pathway inhibitor. Our results suggest an involvement of Sox13 in angiogenesis in zebrafish as a modulator of the Notch signaling pathway.

3.3 Sox13 is involved in primitive erythropoieis

Sox13 expression has not been reported until now in erythropoietic tissues in mouse and a role in erythropoiesis was so far excluded (Dumitriu

et al., 2006). Up to now, the SoxD-group gene Sox6 has been demonstrated to be an important enhancer of definitive erythropoiesis in mouse and in human erythroid cultures (Dumitriu et al., 2006; Cantu et al., 2011). We report here for the first time *sox13* expression in erythropoietic tissues and its involvement in erythrocyte differentiation in zebrafish.

In vivo analyses do not evidence gross circulatory defects in *sox13* morphants compared to controls. Simultaneously, o-dianisidine staining, which detects hemoglobin activity, is remarkably reduced in *sox13* morphants, pointing to a reduction of differentiated primitive erythrocytes. By ISH analysis, we observed in *sox13* morphants at 2 dpf the persistent or increased signal of some early erythroid markers that are normally absent or less expressed at this stage in controls embryos. Cytological analysis showed that in *sox13* morphants erythroid cells maintain a morphology which is more similar to the aspect of an immature cell. Preliminary flow cytometry analyses show that erythroid cells in *sox13* morphants have a different distribution in FACS plots with respect to control embryos, again supporting the hypotesis that these cells have not reached the same degree of differentiation.

We conclude that *sox13* morphants present defects in primitive erythrocyte differentiation; in particular progenitors are formed but their maturation is affected.

References

Al-Adhami MA, and Kunz, Y.W. 1977. Ontogenesis of hematopoietic sites in *Brachydanio rerio*. *Develop. Growth. Differ* 19:171-179.

Alitalo K. 2011. The lymphatic vasculature in disease. Nat Med 17:1371-1380.

Bowles J, Schepers G, Koopman P. 2000. Phylogeny of the SOX family of developmental transcription factors based on sequence and structural indicators. Dev Biol 227:239-255.

Brown LA, Rodaway AR, Schilling TF, Jowett T, Ingham PW, Patient RK, Sharrocks AD. 2000. Insights into early vasculogenesis revealed by expression of the ETS-domain transcription factor Fli-1 in wild-type and mutant zebrafish embryos. Mech Dev 90:237-252.

Bussmann J, Bos FL, Urasaki A, Kawakami K, Duckers HJ, Schulte-Merker S. 2010. Arteries provide essential guidance cues for lymphatic endothelial cells in the zebrafish trunk. Development 137:2653-2657.

Cantor AB, Katz SG, Orkin SH. 2002. Distinct domains of the GATA-1 cofactor FOG-1 differentially influence erythroid versus megakaryocytic maturation. Mol Cell Biol 22:4268-4279.

Cantu C, Ierardi R, Alborelli I, Fugazza C, Cassinelli L, Piconese S, Bose F, Ottolenghi S, Ferrari G, Ronchi A. 2011. Sox6 enhances erythroid differentiation in human erythroid progenitors. Blood 117:3669-3679.

Carmeliet P. 2005. Angiogenesis in life, disease and medicine. Nature 438:932-936.

Cermenati S, Moleri S, Cimbro S, Corti P, Del Giacco L, Amodeo R, Dejana E, Koopman P, Cotelli F, Beltrame M. 2008. Sox18 and Sox7 play redundant roles in vascular development. Blood 111:2657-2666.

Cermenati S, Moleri S, Neyt C, Bresciani E, Carra S, Grassini DR, Omini A, Goi M, Cotelli F, Francois M, Hogan BM, Beltrame M. 2013. Sox18 genetically interacts with VegfC to regulate lymphangiogenesis in zebrafish. Arterioscler Thromb Vasc Biol 33:1238-1247.

Ciau-Uitz A, Liu F, Patient R. 2010. Genetic control of hematopoietic development in Xenopus and zebrafish. Int J Dev Biol 54:1139-1149.

Cumano A, Godin I. 2007. Ontogeny of the hematopoietic system. Annu Rev Immunol 25:745-785.

Davidson AJ, Zon LI. 2004. The 'definitive' (and 'primitive') guide to zebrafish hematopoiesis. Oncogene 23:7233-7246.

Detrich HW, 3rd, Kieran MW, Chan FY, Barone LM, Yee K, Rundstadler JA, Pratt S, Ransom D, Zon LI. 1995. Intraembryonic hematopoietic cell migration during vertebrate development. Proc Natl Acad Sci U S A 92:10713-10717.

Downes M, Koopman P. 2001. SOX18 and the transcriptional regulation of blood vessel development. Trends Cardiovasc Med 11:318-324.

Dumitriu B, Patrick MR, Petschek JP, Cherukuri S, Klingmuller U, Fox PL, Lefebvre V. 2006. Sox6 cell-autonomously stimulates erythroid cell survival, proliferation, and terminal maturation and is thereby an important enhancer of definitive erythropoiesis during mouse development. Blood 108:1198-1207.

Ellertsdottir E, Lenard A, Blum Y, Krudewig A, Herwig L, Affolter M, Belting HG. 2010. Vascular morphogenesis in the zebrafish embryo. Dev Biol 341:56-65.

Folkman J. 1995. Angiogenesis in cancer, vascular, rheumatoid and other disease. Nat Med 1:27-31.

Fouquet B, Weinstein BM, Serluca FC, Fishman MC. 1997. Vessel patterning in the embryo of the zebrafish: guidance by notochord. Dev Biol 183:37-48.

Francois M, Caprini A, Hosking B, Orsenigo F, Wilhelm D, Browne C, Paavonen K, Karnezis T, Shayan R, Downes M, Davidson T, Tutt D, Cheah KS, Stacker SA, Muscat GE, Achen MG, Dejana E, Koopman P. 2008. Sox18 induces development of the lymphatic vasculature in mice. Nature 456:643-647.

Francois M, Short K, Secker GA, Combes A, Schwarz Q, Davidson TL, Smyth I, Hong YK, Harvey NL, Koopman P. 2012. Segmental territories along the cardinal veins generate lymph sacs via a ballooning mechanism during embryonic lymphangiogenesis in mice. Dev Biol 364:89-98.

Galloway JL, Zon LI. 2003. Ontogeny of hematopoiesis: examining the emergence of hematopoietic cells in the vertebrate embryo. Curr Top Dev Biol 53:139-158.

Gerhardt H, Golding M, Fruttiger M, Ruhrberg C, Lundkvist A, Abramsson A, Jeltsch M, Mitchell C, Alitalo K, Shima D, Betsholtz C. 2003. VEGF guides angiogenic sprouting utilizing endothelial tip cell filopodia. J Cell Biol 161:1163-1177.

Gering M, Rodaway AR, Gottgens B, Patient RK, Green AR. 1998. The SCL gene specifies haemangioblast development from early mesoderm. EMBO J 17:4029-4045.

Gray EE, Ramirez-Valle F, Xu Y, Wu S, Wu Z, Karjalainen KE, Cyster JG. 2013. Deficiency in IL-17-committed Vgamma4(+) gammadelta T cells in a spontaneous Sox13-mutant CD45.1(+) congenic mouse substrain provides protection from dermatitis. Nat Immunol 14:584-592.

Green E, Mann S. 1961. Opossum, a semi-dominant lethal mutation affecting hair and other characteristics of mice. J Hered 52:223-227.

Gubbay J, Collignon J, Koopman P, Capel B, Economou A, Munsterberg A, Vivian N, Goodfellow P, Lovell-Badge R. 1990. A gene mapping to the sex-determining region of the mouse Y chromosome is a member of a novel family of embryonically expressed genes. Nature 346:245-250.

Hagerling R, Pollmann C, Andreas M, Schmidt C, Nurmi H, Adams RH, Alitalo K, Andresen V, Schulte-Merker S, Kiefer F. 2013. A novel multistep mechanism for initial lymphangiogenesis in mouse embryos based on ultramicroscopy. EMBO J 32:629-644.

Herbert SP, Huisken J, Kim TN, Feldman ME, Houseman BT, Wang RA, Shokat KM, Stainier DY. 2009. Arterial-venous segregation by selective cell sprouting: an alternative mode of blood vessel formation. Science 326:294-298.

Herbert SP, Stainier DY. 2011. Molecular control of endothelial cell behaviour during blood vessel morphogenesis. Nat Rev Mol Cell Biol 12:551-564.

Herbomel P, Thisse B, Thisse C. 1999. Ontogeny and behaviour of early macrophages in the zebrafish embryo. Development 126:3735-3745.

Hogan BM, Herpers R, Witte M, Helotera H, Alitalo K, Duckers HJ, Schulte-Merker S. 2009. Vegfc/Flt4 signalling is suppressed by Dll4 in developing zebrafish intersegmental arteries. Development 136:4001-4009.

Hosking B, Francois M, Wilhelm D, Orsenigo F, Caprini A, Svingen T, Tutt D, Davidson T, Browne C, Dejana E, Koopman P. 2009. Sox7 and Sox17 are strain-specific modifiers of the lymphangiogenic defects caused by Sox18 dysfunction in mice. Development 136:2385-2391.

Hosking BM, Muscat GE, Koopman PA, Dowhan DH, Dunn TL. 1995. Trans-activation and DNA-binding properties of the transcription factor, Sox-18. Nucleic Acids Res 23:2626-2628.

Irrthum A, Devriendt K, Chitayat D, Matthijs G, Glade C, Steijlen PM, Fryns JP, Van Steensel MA, Vikkula M. 2003. Mutations in the

transcription factor gene SOX18 underlie recessive and dominant forms of hypotrichosis-lymphedema-telangiectasia. Am J Hum Genet 72:1470-1478.

Isogai S, Horiguchi M, Weinstein BM. 2001. The vascular anatomy of the developing zebrafish: an atlas of embryonic and early larval development. Dev Biol 230:278-301.

Isogai S, Lawson ND, Torrealday S, Horiguchi M, Weinstein BM. 2003. Angiogenic network formation in the developing vertebrate trunk. Development 130:5281-5290.

Jakobsson L, Franco CA, Bentley K, Collins RT, Ponsioen B, Aspalter IM, Rosewell I, Busse M, Thurston G, Medvinsky A, Schulte-Merker S, Gerhardt H. 2010. Endothelial cells dynamically compete for the tip cell position during angiogenic sprouting. Nat Cell Biol 12:943-953.

James K, Hosking B, Gardner J, Muscat GE, Koopman P. 2003. Sox18 mutations in the ragged mouse alleles ragged-like and opossum. Genesis 36:1-6.

Jeltsch M, Kaipainen A, Joukov V, Meng X, Lakso M, Rauvala H, Swartz M, Fukumura D, Jain RK, Alitalo K. 1997. Hyperplasia of lymphatic vessels in VEGF-C transgenic mice. Science 276:1423-1425.

Jin H, Xu J, Wen Z. 2007. Migratory path of definitive hematopoietic stem/progenitor cells during zebrafish development. Blood 109:5208-5214.

Jing L, Zon LI. 2011. Zebrafish as a model for normal and malignant hematopoiesis. Dis Model Mech 4:433-438.

Kabrun N, Buhring HJ, Choi K, Ullrich A, Risau W, Keller G. 1997. Flk-1 expression defines a population of early embryonic hematopoietic precursors. Development 124:2039-2048.

Kallianpur AR, Jordan JE, Brandt SJ. 1994. The SCL/TAL-1 gene is expressed in progenitors of both the hematopoietic and vascular systems during embryogenesis. Blood 83:1200-1208.

Kamachi Y, Kondoh H. 2013. Sox proteins: regulators of cell fate specification and differentiation. Development 140:4129-4144.

Kasimiotis H, Myers MA, Argentaro A, Mertin S, Fida S, Ferraro T, Olsson J, Rowley MJ, Harley VR. 2000. Sex-determining region Y-related protein SOX13 is a diabetes autoantigen expressed in pancreatic islets. Diabetes 49:555-561.

Kido S, Hiraoka Y, Ogawa M, Sakai Y, Yoshimura Y, Aiso S. 1998. Cloning and characterization of mouse mSox13 cDNA. Gene 208:201-206.

Kissa K, Herbomel P. 2010. Blood stem cells emerge from aortic endothelium by a novel type of cell transition. Nature 464:112-115.

Kissa K, Murayama E, Zapata A, Cortes A, Perret E, Machu C, Herbomel P. 2008. Live imaging of emerging hematopoietic stem cells and early thymus colonization. Blood 111:1147-1156.

Kohli V, Schumacher JA, Desai SP, Rehn K, Sumanas S. 2013. Arterial and venous progenitors of the major axial vessels originate at distinct locations. Dev Cell 25:196-206.

Koltowska K, Betterman KL, Harvey NL, Hogan BM. 2013. Getting out and about: the emergence and morphogenesis of the vertebrate lymphatic vasculature. Development 140:1857-1870.

Kondoh H, Kamachi Y. 2010. SOX-partner code for cell specification: Regulatory target selection and underlying molecular mechanisms. Int J Biochem Cell Biol 42:391-399.

Kuchler AM, Gjini E, Peterson-Maduro J, Cancilla B, Wolburg H, Schulte-Merker S. 2006. Development of the zebrafish lymphatic system requires VEGFC signaling. Curr Biol 16:1244-1248.

Lawson ND, Scheer N, Pham VN, Kim CH, Chitnis AB, Campos-Ortega JA, Weinstein BM. 2001. Notch signaling is required for arterial-venous differentiation during embryonic vascular development. Development 128:3675-3683.

Lawson ND, Weinstein BM. 2002. Arteries and veins: making a difference with zebrafish. Nat Rev Genet 3:674-682.

Lefebvre V. 2010. The SoxD transcription factors--Sox5, Sox6, and Sox13--are key cell fate modulators. Int J Biochem Cell Biol 42:429-432.

Lelievre E, Lionneton F, Soncin F, Vandenbunder B. 2001. The Ets family contains transcriptional activators and repressors involved in angiogenesis. Int J Biochem Cell Biol 33:391-407.

Leslie JD, Ariza-McNaughton L, Bermange AL, McAdow R, Johnson SL, Lewis J. 2007. Endothelial signalling by the Notch ligand Delta-like 4 restricts angiogenesis. Development 134:839-844.

Liao EC, Paw BH, Oates AC, Pratt SJ, Postlethwait JH, Zon LI. 1998. SCL/Tal-1 transcription factor acts downstream of cloche to specify hematopoietic and vascular progenitors in zebrafish. Genes Dev 12:621-626.

Marfil V, Moya M, Pierreux CE, Castell JV, Lemaigre FP, Real FX, Bort R. 2010. Interaction between Hhex and SOX13 modulates Wnt/TCF activity. J Biol Chem 285:5726-5737.

McGary KL, Park TJ, Woods JO, Cha HJ, Wallingford JB, Marcotte EM. 2010. Systematic discovery of nonobvious human disease models

through orthologous phenotypes. Proc Natl Acad Sci U S A 107:6544-6549.

Melichar HJ, Narayan K, Der SD, Hiraoka Y, Gardiol N, Jeannet G, Held W, Chambers CA, Kang J. 2007. Regulation of gammadelta versus alphabeta T lymphocyte differentiation by the transcription factor SOX13. Science 315:230-233.

Moalem S, Brouillard P, Kuypers D, Legius E, Harvey E, Taylor G, Francois M, Vikkula M, Chitayat D. 2014. Hypotrichosis-lymphedema-telangiectasia-renal defect associated with a truncating mutation in the SOX18 gene. Clin Genet.

Murayama E, Kissa K, Zapata A, Mordelet E, Briolat V, Lin HF, Handin RI, Herbomel P. 2006. Tracing hematopoietic precursor migration to successive hematopoietic organs during zebrafish development. Immunity 25:963-975.

Nicoli S, Presta M. 2007. The zebrafish/tumor xenograft angiogenesis assay. Nat Protoc 2:2918-2923.

North TE, de Bruijn MF, Stacy T, Talebian L, Lind E, Robin C, Binder M, Dzierzak E, Speck NA. 2002. Runx1 expression marks long-term repopulating hematopoietic stem cells in the midgestation mouse embryo. Immunity 16:661-672.

Oliver G, Srinivasan RS. 2010. Endothelial cell plasticity: how to become and remain a lymphatic endothelial cell. Development 137:363-372.

Orkin SH, Zon LI. 2008. Hematopoiesis: an evolving paradigm for stem cell biology. Cell 132:631-644.

Ouyang K, Leandro Gomez-Amaro R, Stachura DL, Tang H, Peng X, Fang X, Traver D, Evans SM, Chen J. 2014. Loss of IP3R-dependent Ca(2+) signalling in thymocytes leads to aberrant development and acute lymphoblastic leukemia. Nat Commun 5:4814.

Palis J, Chan RJ, Koniski A, Patel R, Starr M, Yoder MC. 2001. Spatial and temporal emergence of high proliferative potential hematopoietic precursors during murine embryogenesis. Proc Natl Acad Sci U S A 98:4528-4533.

Pennisi D, Bowles J, Nagy A, Muscat G, Koopman P. 2000a. Mice null for sox18 are viable and display a mild coat defect. Mol Cell Biol 20:9331-9336.

Pennisi D, Gardner J, Chambers D, Hosking B, Peters J, Muscat G, Abbott C, Koopman P. 2000b. Mutations in Sox18 underlie cardiovascular and hair follicle defects in ragged mice. Nat Genet 24:434-437.

Pevny LH, Lovell-Badge R. 1997. Sox genes find their feet. Curr Opin Genet Dev 7:338-344.

Pham VN, Lawson ND, Mugford JW, Dye L, Castranova D, Lo B, Weinstein BM. 2007. Combinatorial function of ETS transcription factors in the developing vasculature. Dev Biol 303:772-783.

Qian F, Zhen F, Xu J, Huang M, Li W, Wen Z. 2007. Distinct functions for different scl isoforms in zebrafish primitive and definitive hematopoiesis. PLoS Biol 5:e132.

Ransom DG, Haffter P, Odenthal J, Brownlie A, Vogelsang E, Kelsh RN, Brand M, van Eeden FJ, Furutani-Seiki M, Granato M, Hammerschmidt M, Heisenberg CP, Jiang YJ, Kane DA, Mullins MC, Nusslein-Volhard C. 1996. Characterization of zebrafish mutants with defects in embryonic hematopoiesis. Development 123:311-319.

Risau W. 1997. Mechanisms of angiogenesis. Nature 386:671-674.

Risau W, Flamme I. 1995. Vasculogenesis. Annu Rev Cell Dev Biol 11:73-91.

Rissone A, Foglia E, Sangiorgio L, Cermenati S, Nicoli S, Cimbro S, Beltrame M, Bussolino F, Cotelli F, Arese M. 2012. The synaptic proteins beta-neurexin and neuroligin synergize with extracellular matrix-binding vascular endothelial growth factor a during zebrafish vascular development. Arterioscler Thromb Vasc Biol 32:1563-1572.

Roose J, Korver W, Oving E, Wilson A, Wagenaar G, Markman M, Lamers W, Clevers H. 1998. High expression of the HMG box factor sox-13 in arterial walls during embryonic development. Nucleic Acids Res 26:469-476.

Saaristo A, Veikkola T, Tammela T, Enholm B, Karkkainen MJ, Pajusola K, Bueler H, Yla-Herttuala S, Alitalo K. 2002. Lymphangiogenic gene therapy with minimal blood vascular side effects. J Exp Med 196:719-730.

Sabin FR. 1902. On the origin of the lymphatic system from the veins and the development of the lymph hearts and thoracic ducts in the pig. Am J Anat 1:367-389.

Sandholzer J, Hoeth M, Piskacek M, Mayer H, de Martin R. 2007. A novel 9-amino-acid transactivation domain in the C-terminal part of Sox18. Biochem Biophys Res Commun 360:370-374.

Schepers GE, Teasdale RD, Koopman P. 2002. Twenty pairs of sox: extent, homology, and nomenclature of the mouse and human sox transcription factor gene families. Dev Cell 3:167-170.

Scott EW, Simon MC, Anastasi J, Singh H. 1994. Requirement of transcription factor PU.1 in the development of multiple hematopoietic lineages. Science 265:1573-1577.

Siekmann AF, Lawson ND. 2007a. Notch signalling and the regulation of angiogenesis. Cell Adh Migr 1:104-106.

Siekmann AF, Lawson ND. 2007b. Notch signalling limits angiogenic cell behaviour in developing zebrafish arteries. Nature 445:781-784.

Sinner D, Rankin S, Lee M, Zorn AM. 2004. Sox17 and beta-catenin cooperate to regulate the transcription of endodermal genes. Development 131:3069-3080.

Slee. 1957. The morphology and development of Ragged-a mutant affecting the skin and hair of the house mouse. J. Genet. 55:570-584.

Stainier DY, Weinstein BM, Detrich HW, 3rd, Zon LI, Fishman MC. 1995. Cloche, an early acting zebrafish gene, is required by both the endothelial and hematopoietic lineages. Development 121:3141-3150.

Sumanas S, Lin S. 2006. Ets1-related protein is a key regulator of vasculogenesis in zebrafish. PLoS Biol 4:e10.

Tammela T, Alitalo K. 2010. Lymphangiogenesis: Molecular mechanisms and future promise. Cell 140:460-476.

Tammela T, Zarkada G, Wallgard E, Murtomaki A, Suchting S, Wirzenius M, Waltari M, Hellstrom M, Schomber T, Peltonen R, Freitas C, Duarte A, Isoniemi H, Laakkonen P, Christofori G, Yla-Herttuala S, Shibuya M, Pytowski B, Eichmann A, Betsholtz C, Alitalo K. 2008. Blocking VEGFR-3 suppresses angiogenic sprouting and vascular network formation. Nature 454:656-660.

Taoudi S, Medvinsky A. 2007. Functional identification of the hematopoietic stem cell niche in the ventral domain of the embryonic dorsal aorta. Proc Natl Acad Sci U S A 104:9399-9403.

Turchinovich G, Hayday AC. 2011. Skint-1 identifies a common molecular mechanism for the development of interferon-gamma-secreting versus interleukin-17-secreting gammadelta T cells. Immunity 35:59-68.

Wang HU, Chen ZF, Anderson DJ. 1998. Molecular distinction and angiogenic interaction between embryonic arteries and veins revealed by ephrin-B2 and its receptor Eph-B4. Cell 93:741-753.

Wang Y, Bagheri-Fam S, Harley VR. 2005. SOX13 is up-regulated in the developing mouse neuroepithelium and identifies a sub-population of differentiating neurons. Brain Res Dev Brain Res 157:201-208.

Wang Y, Ristevski S, Harley VR. 2006. SOX13 exhibits a distinct spatial and temporal expression pattern during chondrogenesis, neurogenesis, and limb development. J Histochem Cytochem 54:1327-1333.

Wegner M. 1999. From head to toes: the multiple facets of Sox proteins. Nucleic Acids Res 27:1409-1420.

Wiley DM, Kim JD, Hao J, Hong CC, Bautch VL, Jin SW. 2011. Distinct signalling pathways regulate sprouting angiogenesis from the dorsal aorta and the axial vein. Nat Cell Biol 13:686-692.

Yang Y, Garcia-Verdugo JM, Soriano-Navarro M, Srinivasan RS, Scallan JP, Singh MK, Epstein JA, Oliver G. 2012. Lymphatic endothelial progenitors bud from the cardinal vein and intersomitic vessels in mammalian embryos. Blood 120:2340-2348.

Yaniv K, Isogai S, Castranova D, Dye L, Hitomi J, Weinstein BM. 2006. Live imaging of lymphatic development in the zebrafish. Nat Med 12:711-716.

You LR, Lin FJ, Lee CT, DeMayo FJ, Tsai MJ, Tsai SY. 2005. Suppression of Notch signalling by the COUP-TFII transcription factor regulates vein identity. Nature 435:98-104.

Part II

Arteriosclerosis, Thrombosis, and Vascular Biology

JOURNAL OF THE AMERICAN HEART ASSOCIATION

Sox18 Genetically Interacts With VegfC to Regulate Lymphangiogenesis in Zebrafish

Solei Cermenati, Silvia Moleri, Christine Neyt, Erica Bresciani, Silvia Carra, Daniela R. Grassini, Alice Omini, Michela Goi, Franco Cotelli, Mathias François, Benjamin M. Hogan and Monica Beltrame

Arterioscler Thromb Vasc Biol. 2013;33:1238-1247; originally published online March 21, 2013;
doi: 10.1161/ATVBAHA.112.300254
Arteriosclerosis, Thrombosis, and Vascular Biology is published by the American Heart Association, 7272 Greenville Avenue, Dallas, TX 75231

Print ISSN: 1079-5642. Online ISSN: 1524-4636

Sox18 Genetically Interacts With VegfC to Regulate Lymphangiogenesis in Zebrafish

Solei Cermenati,* Silvia Moleri,* Christine Neyt, Erica Bresciani, Silvia Carra, Daniela R. Grassini, Alice Omini, Michela Goi, Franco Cotelli, Mathias François, Benjamin M. Hogan, Monica Beltrame

Objective—Lymphangiogenesis is regulated by transcription factors and by growth factor pathways, but their interplay has not been extensively studied so far. We addressed this issue in zebrafish.

Approach and Results—Mutations in the transcription factor–coding gene *SOX18* and in *VEGFR3* cause lymphedema, and the VEGFR3/Flt4 ligand VEGFC plays an evolutionarily conserved role in lymphangiogenesis. Here, we report a strong genetic interaction between Sox18 and VegfC in the early phases of lymphatic development in zebrafish. Knockdown of *sox18* selectively impaired lymphatic sprouting from the cardinal vein and resulted in defective lymphatic thoracic duct formation. Sox18 and the related protein Sox7 play redundant roles in arteriovenous differentiation. We used a novel transgenic line that enables inducible expression of a dominant-negative mutant form of mouse Sox18 protein. Our data led us to conclude that Sox18 is crucially involved in lymphangiogenesis after arteriovenous differentiation. Combined partial knockdown of *sox18* and *vegfc*, using subcritical doses of specific morpholinos, revealed a synergistic interaction in both venous and lymphatic sprouting from the cardinal vein and greatly impaired thoracic duct formation.

Conclusions—This interaction suggests a previously unappreciated crosstalk between the growth factor and transcription factor pathways that regulate lymphangiogenesis in development and disease. **(*Arterioscler Thromb Vasc Biol*. 2013;33:1238-1247.)**

Key Words: lymphangiogenesis ■ lymphedema ■ Sox transcription factors ■ vascular development ■ zebrafish

The lymphatic system is a major component of the vertebrate vasculature and plays key roles in tissue fluid homeostasis, fat absorption, and the immune response.[1] Lymphatic vessel function and dysfunction contribute to the progression of several pathological conditions, such as tumor metastasis, lymphedema, obesity, and inflammation.[2] Despite its relevance for human health and disease, lymphangiogenesis has been far less studied than blood vessel angiogenesis. Hereditary (primary) lymphedema is a rare genetic disorder commonly caused by inherited mutations in genes that regulate crucial pathways during the development of the lymphovascular system. Several genes have been identified in lymphedema, including *VEGFR3* (Milroy disease),[3,4] *FOXC2* (lymphedema distichiasis syndrome),[5] *HGF/MET*,[6] *GJC2*,[7] *PTPN14*,[8] *GATA2*,[9] and *KIF11*.[10]

Hypotrichosis–lymphedema–telangiectasia is a human syndrome displaying mutations in the transcription factor SOX18 and is characterized by the association of heritable alopecia, lymphedema, and vascular malformations.[11] The spontaneous ragged (*Ra*) mutant mice represent the murine counterpart of the hypotrichosis–lymphedema–telangiectasia syndrome.[12,13] The most severe *Ra* mutation, ragged-opossum (*RaOp*), and the *Sox18* null mice, in a pure C57BL/6 (B6) background, showed gross subcutaneous edema at 13.5 days after coitum and died after 14.5 days after coitum, precluding study of lymphatic physiology beyond that stage.[14] Recent findings in mice demonstrated that Sox18 directly activates the transcription of *Prox1*, a master regulator of lymphatic endothelial cells (LECs) specification, by binding to its proximal promoter.[14]

In mammals, according to the currently widely accepted model, lymphatic vessels arise by direct sprouting of precursors from the cardinal veins to give rise to the early lymph sacs, which remodel and sprout to give rise to the entire lymphatic vasculature.[15,16] Very recently, it has been shown that a combination of cellular processes that involve ballooning from the cardinal vein and migration as single cells are necessary to establish the lymphatic vascular plexus.[17,18] A venous origin has been shown also for the recently discovered zebrafish lymphatic system,[19,20] that shares key molecular regulators (including the vascular endothelial growth factor VEGFC and its receptor VEGFR3/Flt4) with the mammalian system. Recently Ccbe1 (Collagen and calcium-binding EGF domains-1), identified in zebrafish as an important regulator of lymphangioblast budding,[21] has been found to be mutated

Received on: August 3, 2012; final version accepted on: March 5, 2013.

From the Dipartimento di Scienze Biomolecolari e Biotecnologie (S. Cermenati, S.M., D.R.G., M.G., M.B.), Dipartimento di Bioscienze (S. Cermenati, S.M., S. Carra, A.O., F.C., M.B.), and Dipartimento di Biologia (E.B., S. Carra, F.C.), Universita' degli Studi di Milano, Milan, Italy; and Institute for Molecular Bioscience, The University of Queensland, Brisbane, Australia (C.N., M.F., B.M.H.).

*These authors contributed equally to this study.

The online-only Data Supplement is available with this article at http://atvb.ahajournals.org/lookup/suppl/doi: 10.1161/ATVBAHA.112.300254/-/DC1.

Correspondence to Monica Beltrame, Dipartimento di Bioscienze, Universita' degli Studi di Milano, Via Celoria 26, 20133 Milano, Italy. E-mail monica.beltrame@unimi.it

Arterioscler Thromb Vasc Biol **is available at http://atvb.ahajournals.org** **DOI: 10.1161/ATVBAHA.112.300254**

in human patients affected by Hennekam Lymphangiectasia Lymphedema syndrome,[22,23] clearly demonstrating that the zebrafish model system could directly aid in defining the molecular basis of human lymphangiopathies.

In zebrafish, developmental angiogenesis occurs in 2 different waves: during the first wave, primary sprouts from the dorsal aorta (DA) give rise to intersomitic vessels (ISVs) from ≈22 hours postfertilization (hpf); during the second wave, half of the sprouts from the vein will convert arterial ISVs into venous ISVs (vISVs), whereas the other half gives rise to a pool of lymphatic precursors at the horizontal myoseptum (HMS),[19,24] the parachordal lymphangioblasts (PLs), from ≈32 hpf.[21,25] The lymphatic thoracic duct (TD), the main lymphatic vessel described in zebrafish,[19,20] is then generated by the ventral migration of these PLs.

We decided to specifically address the role played by *sox18* in zebrafish lymphatic development and the interplay between *sox18* and the central lymphatic growth factor *vegfc*. We have previously shown that *sox18* and the closely related *sox7* gene play redundant roles in arteriovenous differentiation: their simultaneous partial knockdown impairs particularly the acquisition of a full venous identity, thus pointing to a potential role in lymphatic differentiation.[26] We now show that the 2 genes are differentially expressed in the posterior cardinal vein (PCV): at stages crucial for early lymphatic development, only *sox18* expression is clearly detectable in the PCV. The knockdown of *sox18* specifically affects lymphatic development: the number of sprouts from the vein and of PLs at the myoseptum are significantly impaired, however the number of vISVs is largely unaffected. The inducible expression of a dominant-negative Sox18–*RaOp* mutant protein in zebrafish embryos causes impairment of lymphatic precursor sprouting from the vein at stages after arteriovenous differentiation, dissociating the phenotype from earlier potential arteriovenous defects.

Significantly, TD defects are synergistically induced by the coinjection of subcritical doses of *sox18* and *vegfc* morpholinos. The simultaneous partial knockdown of *sox18* and *vegfc* reduces the number of PLs, but also vISVs, thus suggesting that both venous and lymphatic sprouting are coregulated by *vegfc* and *sox18*. These data support the key importance of Sox18 in early phases of lymphatic development and, for the first time, indicate that a strong genetic interaction exists between Sox18 and VegfC in this process.

Materials and Methods

Materials and Methods are available in the online-only Supplement.

Results

sox18, but not *sox7*, Is Expressed in the Cardinal Vein During Lymphatic Precursor Sprouting

Sox18 and Sox7 play redundant roles in arteriovenous differentiation of endothelial cells in zebrafish.[26–28] Simultaneous partial knockdown of both genes, but not single partial knockdowns, causes multiple fusions between the major axial vessels (the DA and the PCV) because of an incomplete acquisition of arteriovenous identity by endothelial cells. In particular, venous endothelial cell differentiation is more impaired than arterial differentiation in *sox18/sox7* double morphants.[26]

We found that both *sox18* and *sox7* are expressed in the developing axial and ISVs, and in the developing head vasculature at 29 hpf (Figure 1Aa, 1Aa', 1Ab, and 1Ab'). However, at later stages of development, the 2 genes are differentially expressed in the PCV: at 36 hpf, only *sox18* expression is clearly detectable in the PCV by in situ hybridization (ISH), whereas both *sox18* and *sox7* are expressed in the DA (Figure 1Ac, 1Ac', 1Ad and 1Ad'). Given the venous origin of LECs, we decided to evaluate the role played by Sox18 and Sox7 in the early phases of lymphatic development.

Knockdown of *sox18* Affects TD Formation

The analysis of TD formation is commonly used to study lymphatic development in zebrafish (Materials and Methods in the online-only Data Supplement). To knockdown *sox18* or *sox7*, we injected splice-blocking morpholinos (*sox18*-MO2 and *sox7*-MO2) and translation-blocking morpholinos (*sox18*-MO1 and *sox7*-MO1)[26] into tg(*fli1a*:EGFP)^{y1} embryos, where both blood and lymphatic vessels are labeled.[19] Larvae were subdivided into phenotypic classes of increasing severity, ranging from fully formed to completely absent TD, to account for the variability of the lymphatic defects (Materials and Methods in the online-only Data Supplement).

We optimized the dose of *sox18*-MOs to produce relevant defects in TD formation, while minimizing morphological or circulatory defects that would interfere with TD analysis (data not shown). The injection of *sox18*-MO2 at 1pmol/embryo specifically impairs TD formation at 5 dpf (Figure 1B and 1C; Table I and Figure I in the online-only Data Supplement). In contrast, most control larvae showed fully formed TD (Figure 1C; Table I and Figure I in the online-only Data Supplement). Similar defects in TD formation resulted from the injection of an independent morpholino targeting *sox18* (*sox18*-MO1) although with lower penetrance (Figure IIA and IIB in the online-only Data Supplement). Moreover, *sox18* RNA rescues the lymphatic phenotype of *sox18* morphants in a dose-dependent manner (Figure 1B and 1C; Table I in the online-only Data Supplement), supporting the specificity of these phenotypes (Figure 1C; Table I in the online-only Data Supplement).

We next analyzed the effects of *sox7* knockdown on lymphatic development. Using 2 different morpholinos at the maximal doses allowing robust blood circulation, we found that the knockdown of *sox7* caused only minor defects in TD formation (Figure IIC and IID in the online-only Data Supplement and data not shown). The coinjection of even low doses of *sox18*- and *sox7*-MOs blocks blood circulation in the trunk, due to impaired arteriovenous differentiation and arteriovenous shunt formation[26]; therefore, we could not fully investigate whether knocking down *sox7* exacerbates the lymphatic phenotype of *sox18* morphants.

When dealing with a subfamily of SOX genes, it is important to check for background-dependent effects, like strain-specific compensatory upregulation of other Sox family members when one is knocked down or out.[14,29] We analyzed the expression

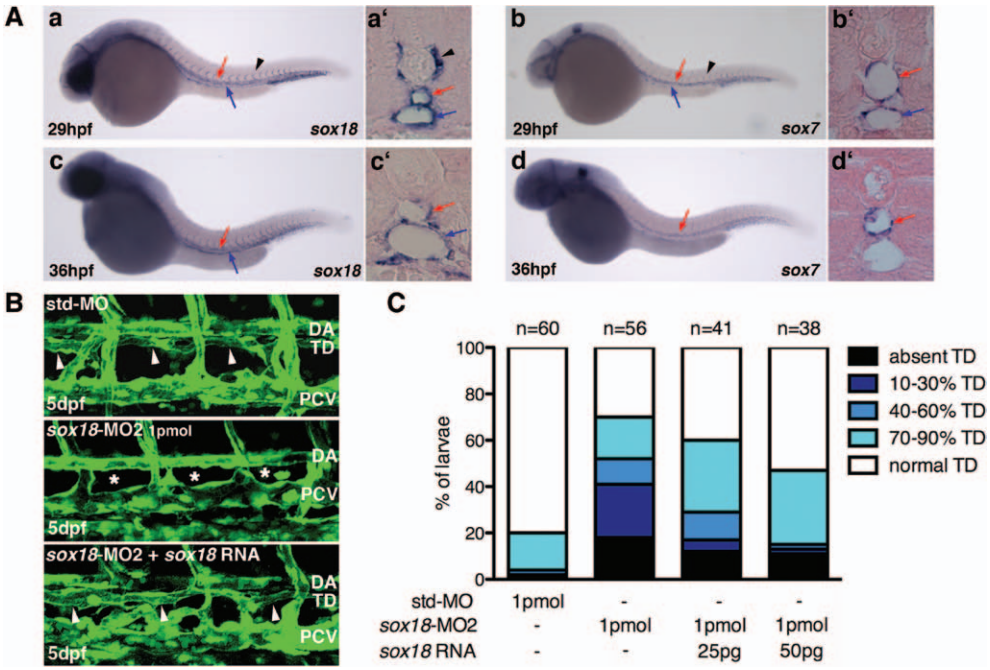

Figure 1. *sox18* is expressed longer than *sox7* in the posterior cardinal vein (PCV), and it plays a role in zebrafish lymphatic development. **A**, The expression of *sox18* and *sox7* was analyzed by in situ hybridization (ISH) at 29 hpf (**a** and **b**, respectively) and 36 hpf (**c** and **d**, respectively), and cross-sections were made (**a'**–**d'**). At 29 hpf, *sox18* and *sox7* mark the developing axial vessels (dorsal aorta [DA] and PCV, red and blue arrows, respectively, in **a**, **a'**, **b**, **b'**), and the intersomitic vessels (black arrowhead in **a**, **a'**, **b**); *sox7* staining in intersomitic vessel is visible in other sections of the same embryo (data not shown). At 36 hpf, *sox18* staining is still clearly detectable in both DA and PCV (red and blue arrows, respectively, in **c**, **c'**), whereas *sox7* is expressed in the DA (red arrows in **d**, **d'**) but not in the PCV. ISH images (**a**–**d**) were taken at ×40 magnification, lateral views anterior to the left; cross-sections images (**a'**–**d'**) were taken at ×350 magnification. **B** and **C**, We analyzed thoracic duct (TD) formation in control larvae (std-MO) and in larvae injected with *sox18*-MO2 or coinjected with *sox18*-MO2 and *sox18* RNA, at 5 dpf using the tg(*fli1a*:EGFP)^{y1} line. **B**, Representative confocal images of trunk regions are shown (lateral views, anterior to the left). Presence or absence of TD is marked with a white arrowhead or asterisk, respectively. **C**, Circulating larvae were analyzed by scoring the presence/absence of TD within 10 consecutive intersomitic segments along the trunk and subdivided into phenotypic classes. The injection of *sox18*-MO2 at 1 pmol/embryo specifically impairs TD formation: >60% of *sox18* morphants showed defects in TD formation and half of these larvae belonged to the most severe classes. In contrast, control larvae showed only mild TD formation defects: the TD developed as a continuous vessel in >80% of the std-MO injected larvae. *sox18* RNA rescues the lymphatic phenotype of *sox18* morphants in a dose-dependent way: when increasing doses of *sox18*-RNA were coinjected with *sox18*-MO2, the number of larvae with a fully formed TD increased, and the number of larvae belonging to the most severe classes was drastically reduced. The number and percentage of larvae belonging to each phenotypic class are reported in Table I (online-only Data Supplement).

levels of *sox7* in *sox18* morphants at various developmental stages (18–20 somites, 24 hpf and 36 hpf), before or around early lymphatic development, and we did not observe any significant changes (Figure IIIa–IIIf in the online-only Data Supplement).

Our data thus point to an important role of Sox18 in lymphatic development, whereas Sox7 does not seem to play such a prominent role in this process and has not been analyzed any further in this study.

Knockdown of *sox18* Impairs the Sprouting of Lymphatic Precursors From the Vein, but Does Not Alter vISV Angiogenesis

We next sought to better characterize early steps of lymphatic development in *sox18* morphants. In the secondary wave of zebrafish angiogenesis, half of the sprouts from the vein anastomose with and convert arterial derived ISVs into vISVs, whereas the other half gives rise to a pool of lymphatic precursors at the myoseptum, the PLs (also called lymphangioblasts or parachordal chain cells).[19,21,24,25,30] This process involves several molecular players and is known to be controlled by VEGF-C/VEGFR3 signaling.[24,25,31]

Knockdown of *sox18* caused a reduction of ≈40% in the total number of sprouts from the vein scored at 1.5 dpf, which is compatible with an effect limited to lymphangiogenic sprouting (Figure 2A). Knockdown of *vegfc* caused, instead, a much more drastic reduction (Figure 2A), pointing to an overall impairment of secondary sprouting, as already reported in literature.[31] These data indicate considerably more specificity to the *sox18* morphants phenotype we observe here.

Lymphatic precursors, originating from the PCV, are transiently residing at the HMS before migrating ventrally or dorsally to give rise to TD and other trunk lymphatic vessels.[19,21] We directly scored PLs at the HMS in circulating *sox18* morphants and found a significant decrease at 56 hpf (5.1+0.5 versus 8.3+0.2 in controls, Figure 2B).

We next scored vISVs in circulating control embryos and *sox18* morphants at 2.5 dpf. In 3 independent experiments, we found that *sox18* knockdown did not significantly alter vISV numbers (Figure 2C). Additionally, in separate experiments, we scored for a/v ISVs at 2.5 dpf and kept morphants for further TD scoring at 5 dpf. This enabled us to calculate,

a posteriori, the number of a/v ISVs at 2.5 dpf in *sox18* morphants showing different degrees of lymphatic defects at 5 dpf. We found that *sox18* morphants with more severe TD defects and those either unaffected or with minor TD defects showed comparable vISV numbers (Figure IVA and IVB in the online-only Data Supplement).

These analyses confirm that *sox18* knockdown, at the morpholino dose we chose to avoid circulatory defects, impairs lymphatic development, without significantly altering the venous component of the secondary angiogenic wave.

Heat-Shock Inducible Overexpression of Mouse Sox18 Ragged Opossum Inhibits Zebrafish PL Development Postarteriovenous Segregation

Sox18 plays a role in early arteriovenous differentiation and, theoretically, a ubiquitous knockdown across all developmental stages (morpholino approach) could induce PL and TD defects secondarily to a mild arteriovenous defect that we might not be able to score at a basic morphological level.

To inhibit Sox18 activity at stages subsequent to arteriovenous differentiation, we generated a transgenic line for the temporally inducible inhibition of its transcriptional activity. *RaOp* is the strongest of the 4 known ragged mutant alleles, all coding for Sox18 mutant proteins with an intact DNA–binding domain but compromised transactivation ability.[32–34] Ragged mutant proteins act in a dominant-negative fashion, preventing the binding of redundant SoxF factors (ie, Sox7 and Sox17) to Sox18 target genes.

Sox18^{RaOp} dominantly interferes with Sox18-, 7-, and 17-regulated transcription in mouse embryonic lymphangiogenesis.[14,29] We took advantage of this mutant allele and cloned the mouse *Sox18*^{RaOp} cDNA, fused in frame with the mCherry coding sequence, under the control of the *hsp70l* promoter (Figure 3A). We used Tol2-mediated transgenesis[35] to generate a stable zebrafish tg(*hsp70l:Sox18*^{RaOp} mCherry) line.

We performed staged heat shocks and observed the nuclear accumulation of mCherry protein by 3 to 4 hours (but not 2 hours) after heat-shock treatment (data not shown) using confocal microscopy. The tg(*hsp70l:Sox18*^{RaOp} mCherry) line was crossed to tg(*fli1a*:EGFP)^{y1} or tg(*fli1a*:EGFP)^{y1};tg(*flt1*^{enh}:RFP). Therefore, half of the GFP+ progeny carries the inducible transgene, and the other half of the GFP+ progeny serves as nontransgenic controls, alongside non-heat-shocked transgenic controls. Heat shock was performed at 24, 29, 36, 48, and 72 hpf, and embryos were separated based on mCherry expression at 3 to 4 hours after heat shock.

Heat-shock induction of Sox18^{RaOp} at 24 hpf led to significant cardiovascular defects and a general (not lymph-) edema phenotype by 5 dpf (Figure VA in the online-only Data Supplement), attributable to circulatory defects, thus further

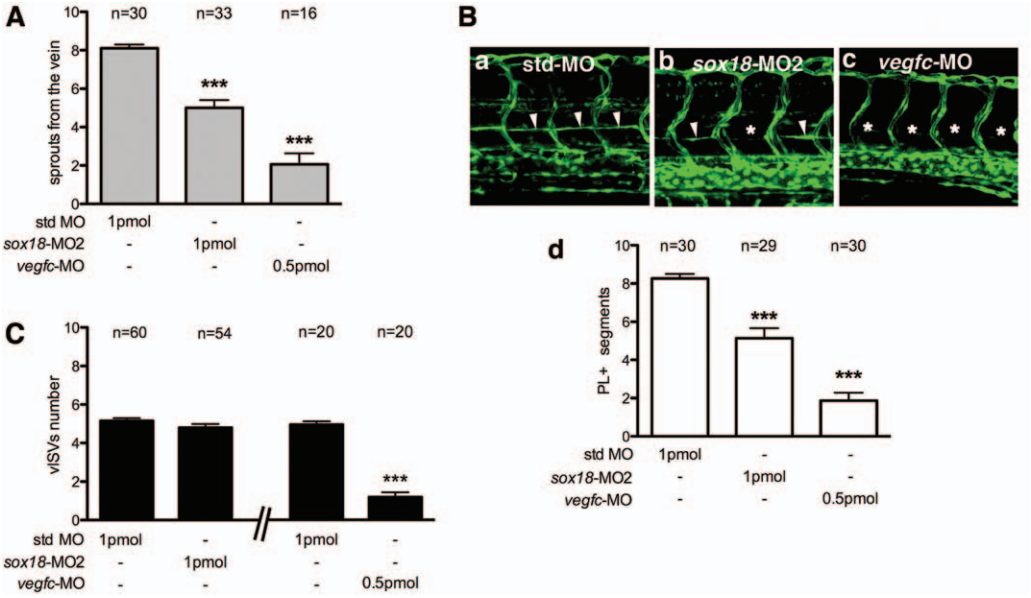

Figure 2. Knockdown of *sox18* impairs sprouts from the vein and reduces the number of lymphatic precursors, but it does not affect the number of arterial and venous intersomitic vessels (ISVs). **A**, We scored the number of sprouts from the vein on one side of tg(*fli1a*:EGFP)^{y1} circulating embryos at 1.5 dpf, in 10 consecutive segments of the trunk region. *sox18* and *vegfc* single morphants (injected with high doses of morpholinos, ie, 1 pmol and 0.5 pmol, respectively) display a statistically highly significant decrease in the number of sprouts from the vein if compared with control embryos (***P<0.001 vs std-MO): the number of sprouts from the vein was reduced of ≈40% in *sox18* morphants and of 75% in *vegfc* morphants (see Table IIA in the online-only Data Supplement). **B**, Confocal analysis of circulating tg(*fli1a*:EGFP)^{y1} embryos at 2.5 dpf shows that the number of parachordal lymphangioblast (PL)+ segments at the horizontal myoseptum is reduced in *sox18* (**b**) and *vegfc* (**c**) single morphants if compared with control embryos (**a**). PL+ segments are marked with an arrowhead, segments devoid of PLs at the horizontal myoseptum (HMS) with an asterisk. **d**, We scored the number of PL+ segments only on one side of the embryos in the trunk region and plotted here mean values considering 10 segments/embryo. All reductions are highly significant (***P<0.001 vs std-MO; see Table IIB in the online-only Data Supplement). The PL phenotype is more pronounced in *vegfc* morphants than in *sox18* morphants. PLs indicates parachordal lymphangioblasts. **C**, The number of venous ISVs was scored in 10 consecutive segments of the trunk region, in 2.5 dpf tg(*fli1a*:EGFP)^{y1} circulating embryos. The single knockdown of *sox18* with high doses of *sox18*-MO2 does not significantly affect the number of venous ISVs (vISVs; left bar chart); on the contrary, the single knockdown of *vegfc* with high doses of *vegfc*-MO results in a much more pronounced decrease in the mean number of vISVs (right bar chart; ***P<0.001 vs std-MO; see Table IIC in the online-only Data Supplement).

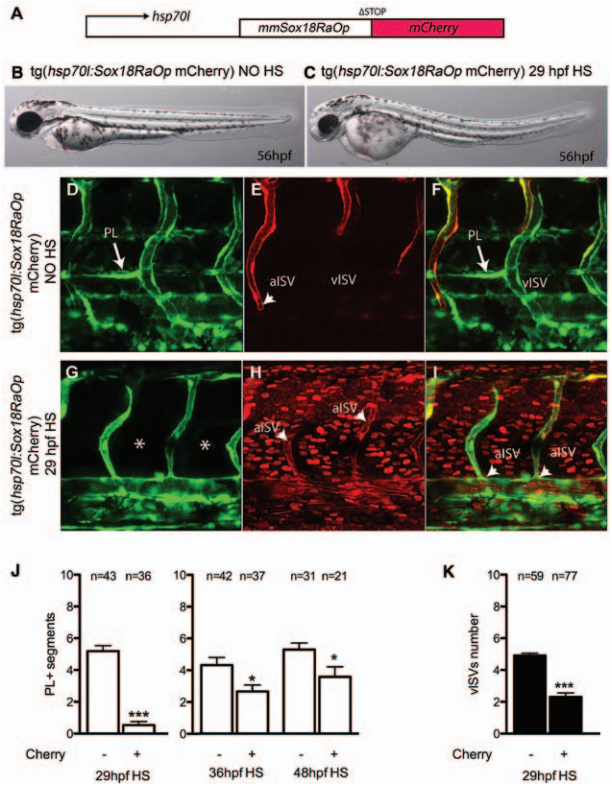

Figure 3. Heat-shock–induced expression of murine *Sox18*^{RaOp} inhibits parachordal lymphangioblast (PL) development and venous intersomitic vessel (vISV) formation in zebrafish. **A**, Schematic representation of the Gateway-generated construct used in transgenesis. An *hsp70l* promoter drives the expression of the mouse *Sox18*^{RaOp} variant with the stop codon removed and fused in frame to the mCherry coding sequence. **B** and **C**, Representative bright-field images of 56 hpf tg(*hsp70l:Sox18*^{RaOp} mCherry) transgenic embryos without heat shock (**B**) and after 29 hpf heat shock (**C**). Overall morphology is not greatly affected by heat-shock–induced expression of murine *Sox18*^{RaOp}. Overall trunk vascular tree development visualized by tg(*fli1a*:EGFP)^{y1} expression is shown in Figure V B (online-only Data Supplement). **D–I**, PL development and a/vISV scoring in a double transgenic tg(*fli1a*:EGFP)^{y1};tg(*flt1*^{enh}:RFP) background at 56 hpf. **D** and **G**, Representative images of PL development visualized by tg(*fli1a*:EGFP)^{y1} expression in tg(*hsp70l:Sox18*^{RaOp} mCherry) transgenic embryos without heat shock (**D**) and after 29 hpf heat shock (**G**). Arrows indicate the presence of PLs, and asterisk indicates the absence of PLs at the horizontal myoseptum. **E** and **H**, arterial ISVs (aISVs; white arrowheads) analyzed in tg(*hsp70l:Sox18*^{RaOp} mCherry) transgenic embryos without heat shock (**E**) and after 29 hpf heat shock (**H**) by tg(*flt1*^{enh}:RFP) expression. Nuclear accumulation of mCherry is still evident at 56 hpf on heat shock at 29 hpf (**H**). **F** and **I**, merge of images shown in **D**, **E** and **G**, **H**, respectively. vISVs are only visible without heat-shock. **J** and **K**, Quantification of PL development and vISVs after heat shock at 29, 36, and 48 hpf. Cherry positive embryos are transgenic induced animals, sorted based on visual scoring 3 to 4 hours after heat shock. Cherry negative embryos, that is, either non-heat-shocked transgenic or heat-shocked nontransgenic embryos, serve as controls. Analyses after 29 hpf heat shock were performed in a double transgenic tg(*fli1a*:EGFP)^{y1};tg(*flt1*^{enh}:RFP) background, after 36 and 48 hpf heat shocks in a tg(*fli1a*:EGFP)^{y1} background. ***P<0.001 vs control embryos; *P<0.05 vs control embryos. Raw data are reported in Table IV (online-only Data Supplement).

revealing an ongoing role of SoxF proteins in cardiovascular development, as reported in the literature for other organisms.[36] Heat shock at 29 hpf did not cause cardiac edema (Figure 3C) and did not interfere with major axial blood circulation through the DA and PCV, however the circulation through ISVs was abnormal at 2.5 dpf. Embryos heat shocked at later time points showed normal circulation.

Heat shock at 29 hpf led to a near complete loss of PLs at the HMS at 56 hpf, whereas 36 and 48 hpf heat shocks led to milder reductions in PL numbers (Figure 3G and 3J; Table IV in the online-only Data Supplement). Later heat shock at 72 hpf had no effect on later TD formation (data not shown). Non-heat-shocked transgenic animals and heat-shocked non-transgenic controls showed no phenotype (Figure 3B, 3D–3F, and data not shown).

Heat shock at 29 hpf also led to a highly significant reduction in the number of vISVs with respect to control embryos (Figure 3E, 3F, 3H, 3I, and 3K). Such a reduction was not detectable in *sox18* morphants (Figure 2C, and Figure IVA and IVB in the online-only Data Supplement). This prompted us to analyze the expression level of *vegfc* in the Sox18^{RaOp} induced transgenic embryos, because Vegfc/Vegfr3 signaling is crucial for venous and lymphatic sprouting.[21,31] Heat shock at 29 hpf resulted in a reduction of *vegfc* expression in these embryos (Figure VC in the online-only Data Supplement). This reduction may contribute to the severe phenotypes observed on overexpression of the dominant-negative Sox18 mutant protein, but these may also be due to a more generally impaired input of SoxF proteins.

These experiments show that dramatic PL defects were observed when Sox18^{RaOp} mCherry overexpression was induced at 29 hpf, which leads to the expression of nuclear mCherry protein by 32 to 33 hpf. The milder phenotype with 36 hpf heat shocks suggests a critical period for SoxF activity in lymphatic development between 32 and 40 hpf, during the period of PL sprouting from the cardinal vein.

sox18 and *vegfc* Genetically Interact in Zebrafish TD Formation

To gain insight into the molecular events governing the early phases of lymphatic development, we decided to analyze the interplay between *sox18* and *vegfc*, a growth factor crucial for this process.[19,20,31]

We reproduced the lymphatic phenotype associated with knockdown of *vegfc* and then constructed a dose–response curve by injecting several doses of *vegfc*-MO to identify a critical range (Figure VI in the online-only Data Supplement). This led us to define a subcritical dose of *vegfc*-MO (0.06 pmoles/embryo) to be used in coinjection experiments along with a subcritical dose of *sox18*-MO2 (0.5 pmoles/embryo).

The single injection of these low doses of *sox18* and *vegfc* morpholinos caused no gross morphological or lymphatic abnormalities (Figure 4; Figure VII in the online-only Data Supplement). On the contrary, coinjection of subcritical doses led to severe defects in TD development (Figure 4): almost 70% of coinjected larvae showed a total absence of TD or the presence of only 10% to 30% TD+ segments (Figure 4B; Figure VII in the online-only Data Supplement). The synergistic effect of the coinjection can also be obtained even when cutting by half the subcritical doses of *sox18*-MO2 and *vegfc*-MO (0.25 and 0.03 pmoles/embryo, respectively; Figure VIIIA and VIIIC in the online-only Data Supplement), and TD formation is drastically affected also by coinjecting

a low dose of *vegfc*-MO (0.06 pmoles/embryo, Figure 4) with a subcritical dose of an independent *sox18* morpholino (*sox18*-MO1, 0.5 pmoles/embryo), that does not largely affect TD formation when injected on its own (Figure VIIIB in the online-only Data Supplement).

Moreover, synergistic defects in TD formation were also obtained by simultaneous partial knockdown of *sox18* and of the VegfC receptor gene *flt4* (Figure IX in the online-only Data Supplement), coinjecting low doses of *sox18*-MO2 (0.5 pmoles/embryo) and *flt4*-MO (0.06 pmoles/embryo).

To determine whether Sox18 and VegfC cross-regulate at the mRNA level, we analyzed by ISH whether the mRNA levels of *sox18* or *vegfc* are perturbed by the knockdown of *vegfc* or *sox18*, respectively. *sox18* transcripts did not show any significant reduction in *vegfc* morphants nor did *vegfc* expression show changes in *sox18* morphants (Figure X in the online-only Data Supplement). In addition, we found that the simultaneous partial knockdown of *sox18* and *vegfc* does not alter *sox7* expression (Figure III in the online-only Data Supplement). These data suggest that the interactions observed here are not occurring at the level of embryonic transcription of these genes.

The overexpression of a dominant-negative Sox18 mutant protein resulted in a reduction of *vegfc* expression, whereas the knockdown of *sox18* did not produce detectable changes in the *vegfc* ISH signal. These data might imply other SoxF proteins in the regulation of *vegfc*. Alternatively, they might imply that a more pronounced reduction in Sox18 than the one caused by knockdown is needed to produce an alteration in *vegfc* levels.

To further address the molecular basis of the Sox18/VegfC interplay, we coinjected *vegfc* RNA while knocking down *sox18* by morpholino injection: overexpression of *vegfc* partially rescued TD formation defects in *sox18* morphants (Figure XIA in the online-only Data Supplement). The reverse experiment, namely *sox18* RNA injection in *vegfc* morphants, did not cause any amelioration of the TD phenotype (Figure XIB in the online-only Data Supplement).

Taken together, our data for the first time suggest a relationship between the growth factor pathways that specifically regulate lymphangiogenesis (VegfC/Vegfr3 signaling) and the transcriptional pathways that modulate lymphangiogenesis.

Sox18 and VegfC Cooperate in Both PL and vISV Sprouting From the Cardinal Vein

We next investigated the specific population of venous-derived cells impaired in these double morphants. In full knockdown scenarios, Sox18 primarily regulates PL sprouting, but VegfC regulates both PL and vISV sprouting.

We scored total sprouts from the vein, PLs, and vISVs in embryos coinjected with subcritical doses of *sox18* and *vegfc* MOs. Combined partial knockdown caused a reduction of >50% in the total number of sprouts from the vein at 1.5 dpf (Figure 5A) and a marked loss of PLs at the HMS at 56 hpf (Figure 5B). Furthermore, we scored vISVs at 2.5 dpf and found a synergistic interaction in vISV development: the subcritical doses of *sox18*- and *vegfc*-MOs caused a statistically significant reduction in vISVs only when coinjected (Figure 5C; Figure IVC in the online-only Data Supplement).

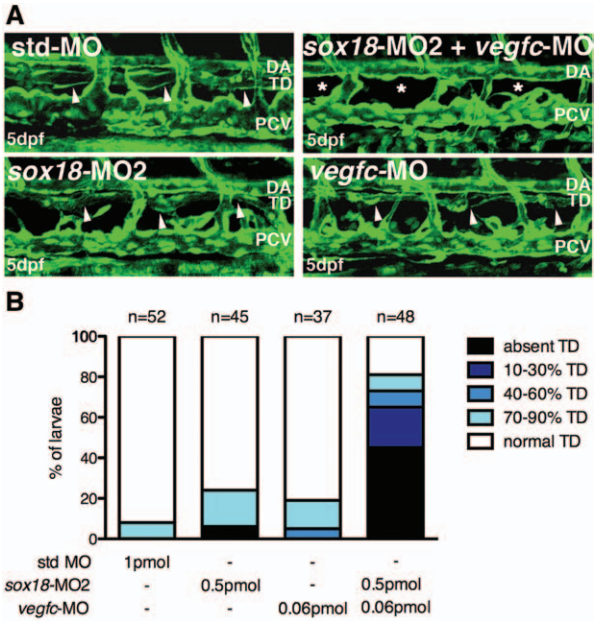

Figure 4. The simultaneous partial knockdown of *sox18* and *vegfc* severely affects thoracic duct (TD) formation. **A**, Confocal analysis of circulating larvae at 5 dpf revealed that partial knockdown of *sox18* or *vegfc* with subcritical doses of either *sox18*- or *vegfc*-MOs (0.5 pmol and 0.06 pmol, respectively) does not affect TD formation, as observed in tg(*fli1a*:EGFP)^{y1} control larvae injected with std-MO (white arrowheads). On the contrary, TD formation is largely impaired by the coinjection of the same subcritical doses of both MOs (*sox18+vegfc* double partial morphants; white asterisks). **B**, The bar chart shows the percentage of larvae grouped in phenotypic classes with increasing TD defects. TD formation defects observed in *sox18+vegfc* double partial morphants are greater than the mere sum of the defects observed in single partial morphants, indicating a synergistic effect of MOs on coinjection. The number and percentage of embryos belonging to each class are reported in Table V (online-only Data Supplement); statistical analysis is shown in Figure VII (online-only Data Supplement). DA indicates dorsal aorta; PCV, posterior cardinal vein; and TD, thoracic duct.

To test how robust these observations are, we decided to examine the interaction with independent molecular markers of the vasculature. We performed ISHs with the pan-endothelial marker *cdh5* and some venous specific markers, such as *dab2*, *ephB4*, and *flt4* around 29 hpf. Hybridization signals for these molecular probes were comparable in *sox18* morphants and in combined partial *sox18* and *vegfc* morphants with respect to controls, suggesting that blood endothelial cells were largely unaffected (Figure 6A; Figure XIIA in the online-only Data Supplement).

Next, we examined venous and lymphatic precursor sprouting using the *lyve1* marker[21,37] in ISHs at 2 dpf. *lyve1*+ sprouts from the PCV were clearly visible in controls (Figure 6Bb, white arrows) but severely reduced or absent in *sox18* morphants and in combined partial *sox18* and *vegfc* morphants (Figure 6Bd, 6Be, and 6Bg). We subdivided morphants to better describe their phenotypes in terms of presence/absence and length of *lyve1*+ sprouts (Figure 6B). Normal *lyve1*+ sprouts were detectable in most control embryos, but in only ≈10% of *sox18* morphants and 5% of combined partial *sox18-vegfc* morphants (Figure 6Bh). Interestingly, among *sox18* morphants, the prevalent phenotype was that of embryos with

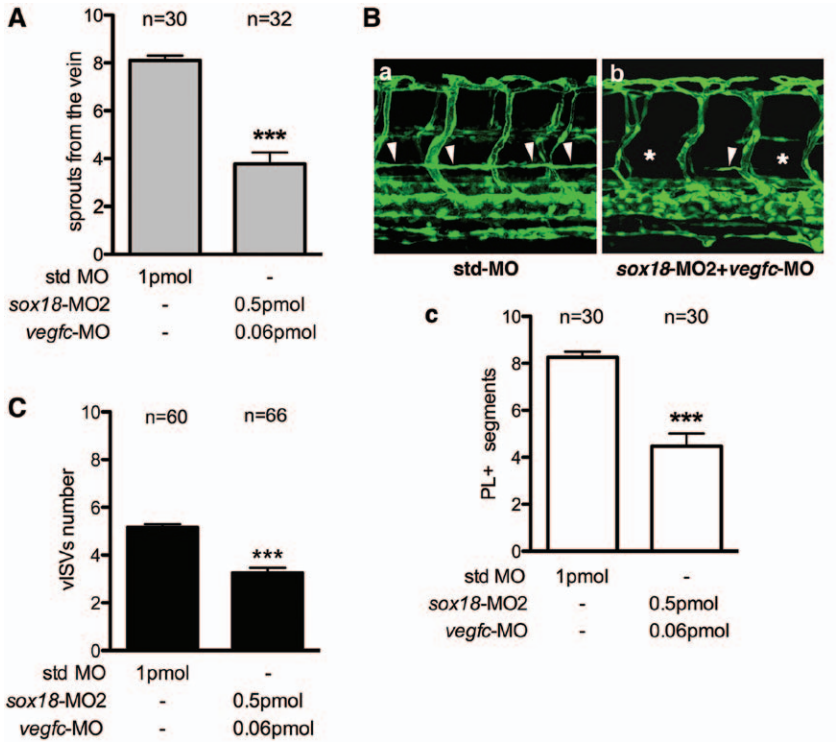

Figure 5. The simultaneous partial knockdown of *sox18* and *vegfc* impairs sprouts from the vein and reduces parachordal lymphangioblast (PL) and venous intersomitic vessel (vISV) numbers. **A**, We scored the number of sprouts from the vein on one side of *sox18+vegfc* double partial morphants (injected with 0.5 pmol *sox18*-MO2+0.06 pmol *vegfc*MO) and plotted here mean values considering 10 segments/embryo of circulating tg(*fli1a*:EGFP)^{y1} embryos at 1.5 dpf. When subcritical doses of *sox18* and *vegfc*-MOs were coinjected, we scored slightly less than half of the total number of venous-derived sprouts present in controls (***P<0.001 vs std-MO; see Table IIA in the online-only Data Supplement). **B**, We next scored the presence/absence of PLs at the horizontal myoseptum: we analyzed 10 consecutive trunk segments of circulating tg(*fli1a*:EGFP)^{y1} embryos at 2.5 dpf, only on one side. PL+ segments are marked with an arrowhead, segments devoid of PLs with an asterisk. Confocal analysis shows that the number of PL+ segments at the horizontal myoseptum is reduced in *sox18+vegfc* double partial morphants (**b**) if compared with control embryos (**a**). **c**, Mean values are plotted in the bar chart (see Table IIB in the online-only Data Supplement). All reductions are highly significant (***P<0.001 vs std-MO).**C**, We also scored the number of vISV in 10 consecutive trunk segments of 2.5 dpf tg(*fli1a*:EGFP)^{y1} embryos. Only circulating embryos were analyzed. The simultaneous partial knockdown of *sox18+vegfc* with low doses of MOs (0.5+0.06 pmol) causes a statistically significant decrease in the number of vISVs (***P<0.001 vs std-MO; see Table IIC in the online-only Data Supplement). We show here the same control embryos data present in Figure 2, because we performed a unique set of 3 experiments to analyze single *sox18* morphants and double partial *sox18-vegfc* morphants.

reduced numbers of *lyve1*+ sprouts, accounting for almost 40% (Figure 6Bd and 6Bh), but in combined partial *sox18-vegfc* morphants, the complete absence of *lyve1*+ sprouts (asterisk) prevailed, characterizing ≈40% of the embryos (Figure 6Bg and 6Bh). These data give an alternative confirmation of the genetic interaction and could be considered indicative of a combined impairment in lymphatic differentiation and in secondary sprouting in the combined partial *sox18-vegfc* knockdown but not in single *sox18* knockdown scenarios.

Discussion

In the past few years, zebrafish has emerged as a very potent system to study lymphangiogenesis.[38,39] Overall, the zebrafish lymphatic system shares several morphological, functional, and molecular characteristics with mammals. Since the initial description of the zebrafish lymphatic system in 2006,[19,20] a handful of molecular players have been shown to be evolutionarily conserved, but much remains to be elucidated and we are far from a complete picture of the degree of conservation of molecular pathways from zebrafish to human lymphangiogenesis. This prompted us to study the role of *sox18* in zebrafish lymphatic development, because *SOX18* mutations are associated with lymphedema in patients affected by the hypotrichosis–lymphedema–telangiectasia syndrome, and studies in mouse placed Sox18 very high in the hierarchy of transcription factors governing LEC differentiation.[40]

Sox18 belongs to the Sox F group of Sry-related high mobility group box transcription factors, also comprising the closely related Sox7 and Sox17 proteins. Sox proteins of the same subfamily tend to be biochemically interchangeable in vitro, and the relevance of individual *Sox* genes for a specific process is often linked to their differential expression in vivo.[14,29]

Ours and other groups have reported that *sox7* and *sox18* are coexpressed in angioblasts and endothelial cells of the forming vasculature, and that they play redundant roles in arteriovenous differentiation.[26–28] We show here that *sox7* stops being expressed earlier than *sox18* in the axial vein, whereas both genes are still expressed in the DA, and that Sox18 specifically regulates lymphatic development.

In mice, Sox18 acts in concert with CoupTFII to drive the transcription of *Prox1*.[14,41] The polarized expression of Sox18 precedes that of Prox1 in a subset of cells along the dorsolateral aspect of the cardinal vein at 9 days after coitum,[14] whereas no polarized expression of CoupTFII has been reported so far. Remarkably, we have no evidence of a polarized expression of *sox18* within the PCV, when secondary sprouts are arising from the dorsal aspect of the axial vein in zebrafish.

Although quite prominent and statistically highly significant, the degree of impairment in TD formation we observe in *sox18* morphants versus control embryos is less striking than that observable when *vegfc* is fully knocked down. Our analysis is limited to circulating morphants without gross morphological abnormalities, and this sets an upper limit to the dose of *sox18* morpholino we use. Hence, the strong but not full impairment in TD formation in *sox18* morphants could be the result of a submaximal dose of MO in these experiments.

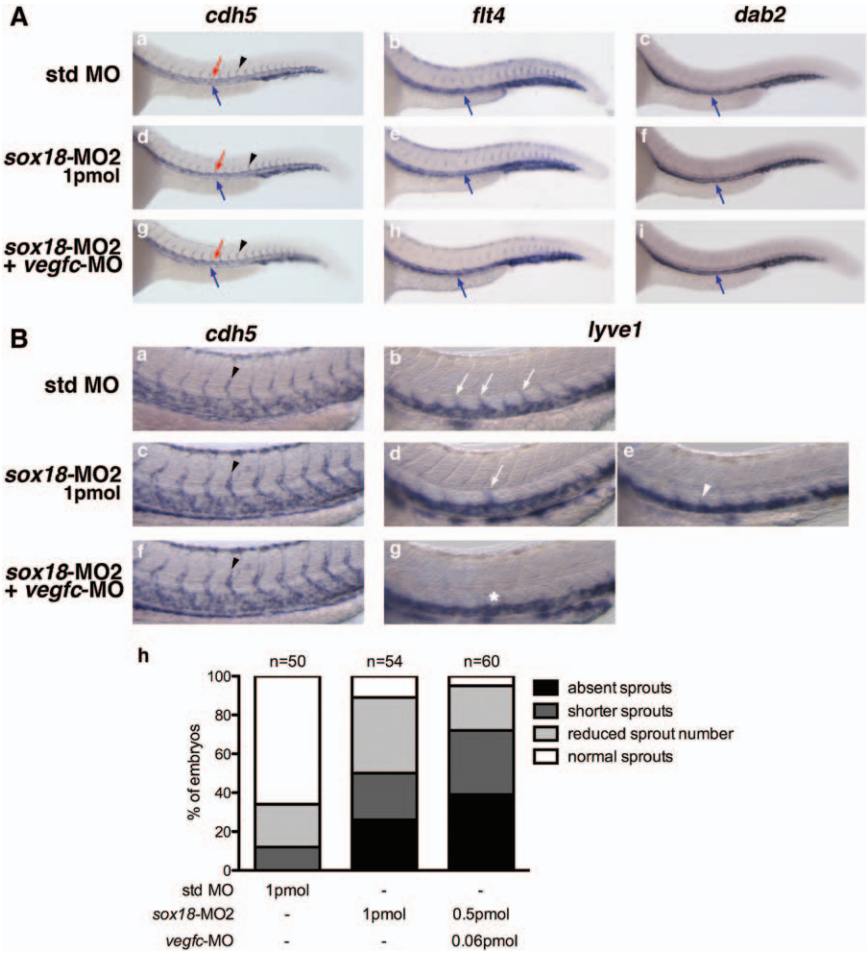

Figure 6. *sox18-vegfc* double partial knockdown specifically impairs *lyve1*+ sprouts without generally altering endothelial markers. **A**, In situ hybridizations were carried out with the pan-endothelial marker *cdh5* (**a**, **d**, **g**) and the venous markers *flt4* (**b**, **e**, **h**), *dab2* (**c**, **f**, **i**), and *ephB4* (Figure XII in the online-only Data Supplement), on *sox18* single morphants and *sox18-vegfc* double partial morphants of the tg(*fli1a*:EGFP)^{y1} line. Around 29 hpf, their expression is largely unaffected. Images were taken at ×63 magnification, lateral views anterior to the left. Red arrows: dorsal aorta; blue arrows: posterior cardinal vein; black arrowheads: intersomitic vessels (ISVs). **B**, We analyzed the expression of the pan-endothelial marker *cdh5* (**a**, **c**, **f**) and the zebrafish ortholog of the mammalian lymphatic marker *LYVE1* (**b**, **d**, **e**, **g**) on 2 dpf morphants of the tg(*fli1a*:EGFP)^{y1} line: *cdh5* staining of ISVs in *sox18* morphants and *sox18-vegfc* double partial morphants (black arrowheads in **c** and **f**, respectively) is similar to that of standard control embryos (**a**). On the contrary, *lyve1*+ sprouts are reduced in number (white arrow in **d**) and in length (white arrowhead in **e**) or totally absent (white asterisk in **g**) in *sox18* single morphants and *sox18-vegfc* double partial morphants if compared with control embryos (white arrows in **b**). Images were taken at ×63 magnification, lateral views anterior to the left. **h**, The bar chart shows the percentage of embryos with absent (black bars), shorter (gray bars), diminished (light gray bars), or normal (white bars) *lyve1*+ sprouts in controls, *sox18* morphants and *sox18-vegfc* double partial morphants. The number and percentage of embryos belonging to each class are reported in Table VII (online-only Data Supplement). Lower magnification embryos are shown in Figure XIIB (online-only Data Supplement).

Lymphatic precursors sprout from the vein at ≈1.5 dpf and account for approximately half of the total sprouts,[19,25,31] the other half consisting of venous sprouts that will connect to arterial ISVs and convert them into venous ISVs. Our results point to a specific impairment of lymphangiogenic sprouting from the cardinal vein in *sox18* morphants, whereas secondary venous angiogenic sprouting is not substantially perturbed. Importantly, several pan-endothelial (*cdh5*) or venous markers (*dab2*, *ephB4*, *flt4/vegfr3*) are unaffected in *sox18* morphants, whereas the venous/lymphatic endothelial marker *lyve1* is altered: *lyve1*+ sprouts are either shorter or reduced in number, up to totally absent in the most severely affected *sox18* morphants, providing an independent molecular assay for our morphological observations. Notably, PL defects in *sox18* morphants do not seem to be secondary to overt venous differentiation problems. These data together imply a specific role of Sox18 in the early phases of lymphatic differentiation and sprouting in zebrafish.

Injection of an uncaged morpholino at very early stages of embryo development leads to a constitutive knockdown of gene function. We used a complementary approach, based on an inducible overexpression of a dominant-negative mutant form of mouse Sox18 in a newly developed stable transgenic line, to interfere with zebrafish SoxF proteins function in a temporally regulated way. A series of heat shocks enabled us to conclude that Sox18 and, possibly, other SoxF proteins function at the time of lymphatic precursor emergence from the PCV and regulate PL sprouting post-arteriovenous differentiation.

Although many signaling pathways have been implicated in lymphangiogenesis,[2,42] it has been pointed out that most of

their effects may be secondary to the induction of VEGF-C/D in a variety of cell types.[1] VEGF-C/VEGFR3 signaling has an established and evolutionarily conserved role in lymphatic development.[3,19,20,31,43] The current literature holds that the specification of LEC fate and the sprouting of LECs from the PCV are regulated independently.[1,44,45] Our findings that Sox18 and VegfC show strong genetic interaction in zebrafish lymphatic development challenge this model and mandate a careful mechanistic analysis of this interaction in vertebrate model systems. Specifically, we show that embryos coinjected with subcritical doses of morpholinos against *sox18* and *vegfc*, which produce little or no effect when injected separately, display severe PL and TD defects. This observation seems to be highly specific because the trunk vascular tree does not show abnormalities at the morphological or molecular marker levels. Interestingly, whereas the single knockdown of *sox18* does not perturb venous sprouts but only PLs, double partial knockdown of *sox18* and *vegfc* impacts more generally on all secondary angiogenesis from the vein, thus possibly revealing a combined role of both genes in endothelial cell migration. Notably, cell culture data revealed a role for Sox18 in controlling cell migration.[46]

The molecular mechanisms underlying the Sox18–VEGF-C crosstalk remain to be elucidated. Our data exclude a simple cross-regulation at transcripts level between *sox18* and *vegfc*. Knockdown of *sox18* does not alter *vegfc* (nor *flt4/vegfr3*) ISH signals, and *sox18* hybridization signals are not affected in *vegfc* morphants. A possibility exists that VEGF-C/VEGFR3 signaling is implicated in modulating Sox18 transcriptional activity by inducing a post-translational modification. Sox18 has been shown to bind to and activate its target genes in vitro only on stimulation with VEGF-C (M.F., personal communication).[14] In cultured mouse LECs, stimulation with VEGF-C does not alter *Sox18* mRNA level or the activity of a 5-kb fragment of *Sox18* promoter (M.F., personal communication), whereas modulating the transcriptional activity of SOX18 protein. These observations may point to a post-translational modification mechanism, which remains to be studied. Interestingly, *vegfc* overexpression ameliorates TD formation in embryos where *sox18* is knocked down, possibly suggesting that the transcriptional activity of the residual Sox18 protein is positively modulated by enhanced VegfC/Vegfr3 signaling. Whatever the mechanism may be, it is clear from the data presented here that the strong Sox18–VEGF-C interplay in lymphangiogenesis is evolutionarily conserved and points to a novel molecular mechanism in lymphangiogenesis that remains to be further investigated.

Sox18 expression is not required for the maintenance of the lymphatic identity in mammals, whereas under pathological conditions, such as tumor growth, Sox18 is critical for tumor-induced angiogenesis and lymphangiogenesis.[46,47] Both Sox18 and VEGF-C/VEGFR3 are promising targets for inhibition of tumor lymphangiogenesis.[47,48] Our findings uncover a novel interplay between a key transcription factor and one of the most potent lymphangiogenic growth factors, hence opening new potential therapeutic avenues.

Note added in proof: A mutation in *VEGFC* has just been reported in a patient affected by Milroy-like primary lymphedema.[49]

Acknowledgments

We thank Maria V. Flores for sending a *lyve1* plasmid; Neil Bower and Giuseppina Caretti for their help in quantitative reverse transcriptase-polymerase chain reaction primer design and data analysis; and Giuseppe Brunetti for his help in fish husbandry. Imaging at Institute for Molecular Bioscience was performed through the Dynamic Biology Imaging Facility of the Australian Cancer Research Foundation.

Sources of Funding

We acknowledge financial support by Regione Lombardia (grant SAL-01 to M. Beltrame) and by Fondazione Cariplo (grant 2011-0555 to M. Beltrame). B.M. Hogan was supported by an Australian Research Council Future Fellowship (FT100100165).

Disclosures

None.

References

1. Tammela T, Alitalo K. Lymphangiogenesis: molecular mechanisms and future promise. *Cell*. 2010;140:460–476.
2. Alitalo K. The lymphatic vasculature in disease. *Nat Med*. 2011;17:1371–1380.
3. Karkkainen MJ, Haiko P, Sainio K, Partanen J, Taipale J, Petrova TV, Jeltsch M, Jackson DG, Talikka M, Rauvala H, Betsholtz C, Alitalo K. Vascular endothelial growth factor C is required for sprouting of the first lymphatic vessels from embryonic veins. *Nat Immunol*. 2004;5:74–80.
4. Mellor RH, Hubert CE, Stanton AW, Tate N, Akhras V, Smith A, Burnand KG, Jeffery S, Mäkinen T, Levick JR, Mortimer PS. Lymphatic dysfunction, not aplasia, underlies Milroy disease. *Microcirculation*. 2010;17:281–296.
5. Fang J, Dagenais SL, Erickson RP, Arlt MF, Glynn MW, Gorski JL, Seaver LH, Glover TW. Mutations in *FOXC2 (MFH-1)*, a forkhead family transcription factor, are responsible for the hereditary lymphedema-distichiasis syndrome. *Am J Hum Genet*. 2000;67:1382–1388.
6. Finegold DN, Schacht V, Kimak MA, Lawrence EC, Foeldi E, Karlsson JM, Baty CJ, Ferrell RE. HGF and MET mutations in primary and secondary lymphedema. *Lymphat Res Biol*. 2008;6:65–68.
7. Ferrell RE, Baty CJ, Kimak MA, Karlsson JM, Lawrence EC, Franke-Snyder M, Meriney SD, Feingold E, Finegold DN. *GJC2* missense mutations cause human lymphedema. *Am J Hum Genet*. 2010;86:943–948.
8. Au AC, Hernandez PA, Lieber E, Nadroo AM, Shen YM, Kelley KA, Gelb BD, Diaz GA. Protein tyrosine phosphatase PTPN14 is a regulator of lymphatic function and choanal development in humans. *Am J Hum Genet*. 2010;87:436–444.
9. Kazenwadel J, Secker GA, Liu YJ, et al. Loss-of-function germline *GATA2* mutations in patients with MDS/AML or MonoMAC syndrome and primary lymphedema reveal a key role for GATA2 in the lymphatic vasculature. *Blood*. 2012;119:1283–1291.
10. Ostergaard P, Simpson MA, Mendola A, et al. Mutations in *KIF11* cause autosomal-dominant microcephaly variably associated with congenital lymphedema and chorioretinopathy. *Am J Hum Genet*. 2012;90:356–362.
11. Irrthum A, Devriendt K, Chitayat D, Matthijs G, Glade C, Steijlen PM, Fryns JP, Van Steensel MA, Vikkula M. Mutations in the transcription factor gene *SOX18* underlie recessive and dominant forms of hypotrichosis-lymphedema-telangiectasia. *Am J Hum Genet*. 2003;72:1470–1478.
12. Carter TC, Phillips RJS. *Ragged*, a semidominant coat texture mutant in the house mouse. *J Hered*. 1954;45:151–154.
13. Slee J. The morphology and development of *ragged*-a mutant affecting the skin and hair of the house mouse. II Genetics, embriology and gross juvenile morphology. *J Genet*. 1957;55:570–584.
14. François M, Caprini A, Hosking B, et al. Sox18 induces development of the lymphatic vasculature in mice. *Nature*. 2008;456:643–647.
15. Sabin FR. On the origin of the lymphatic system from the veins, and the development of the lymph hearts and thoracic duct in the pig. *Am J Anat*. 1902;1:367–389.
16. Oliver G, Srinivasan RS. Endothelial cell plasticity: how to become and remain a lymphatic endothelial cell. *Development*. 2010;137:363–372.

17. François M, Short K, Secker GA, Combes A, Schwarz Q, Davidson TL, Smyth I, Hong YK, Harvey NL, Koopman P. Segmental territories along the cardinal veins generate lymph sacs via a ballooning mechanism during embryonic lymphangiogenesis in mice. *Dev Biol*. 2012;364:89–98.
18. Hägerling R, Pollmann C, Andreas M, Schmidt C, Nurmi H, Adams RH, Alitalo K, Andresen V, Schulte-Merker S, Kiefer F. A novel multistep mechanism for initial lymphangiogenesis in mouse embryos based on ultramicroscopy. *EMBO J*. 2013;32:629–644.
19. Yaniv K, Isogai S, Castranova D, Dye L, Hitomi J, Weinstein BM. Live imaging of lymphatic development in the zebrafish. *Nat Med*. 2006;12:711–716.
20. Küchler AM, Gjini E, Peterson-Maduro J, Cancilla B, Wolburg H, Schulte-Merker S. Development of the zebrafish lymphatic system requires VEGFC signaling. *Curr Biol*. 2006;16:1244–1248.
21. Hogan BM, Bos FL, Bussmann J, Witte M, Chi NC, Duckers HJ, Schulte-Merker S. ccbe1 is required for embryonic lymphangiogenesis and venous sprouting. *Nat Genet*. 2009;41:396–398.
22. Alders M, Hogan BM, Gjini E, et al. Mutations in *CCBE1* cause generalized lymph vessel dysplasia in humans. *Nat Genet*. 2009;41:1272–1274.
23. Connell F, Kalidas K, Ostergaard P, Brice G, Homfray T, Roberts L, Bunyan DJ, Mitton S, Mansour S, Mortimer P, Jeffery S; Lymphoedema Consortium. Linkage and sequence analysis indicate that *CCBE1* is mutated in recessively inherited generalised lymphatic dysplasia. *Hum Genet*. 2010;127:231–241.
24. Isogai S, Lawson ND, Torrealday S, Horiguchi M, Weinstein BM. Angiogenic network formation in the developing vertebrate trunk. *Development*. 2003;130:5281–5290.
25. Bussmann J, Bos FL, Urasaki A, Kawakami K, Duckers HJ, Schulte-Merker S. Arteries provide essential guidance cues for lymphatic endothelial cells in the zebrafish trunk. *Development*. 2010;137:2653–2657.
26. Cermenati S, Moleri S, Cimbro S, Corti P, Del Giacco L, Amodeo R, Dejana E, Koopman P, Cotelli F, Beltrame M. Sox18 and Sox7 play redundant roles in vascular development. *Blood*. 2008;111:2657–2666.
27. Herpers R, van de Kamp E, Duckers HJ, Schulte-Merker S. Redundant roles for sox7 and sox18 in arteriovenous specification in zebrafish. *Circ Res*. 2008;102:12–15.
28. Pendeville H, Winandy M, Manfroid I, Nivelles O, Motte P, Pasque V, Peers B, Struman I, Martial JA, Voz ML. Zebrafish Sox7 and Sox18 function together to control arterial-venous identity. *Dev Biol*. 2008;317:405–416.
29. Hosking B, François M, Wilhelm D, Orsenigo F, Caprini A, Svingen T, Tutt D, Davidson T, Browne C, Dejana E, Koopman P. *Sox7* and *Sox17* are strain-specific modifiers of the lymphangiogenic defects caused by *Sox18* dysfunction in mice. *Development*. 2009;136:2385–2391.
30. Lim AH, Suli A, Yaniv K, Weinstein B, Li DY, Chien CB. Motoneurons are essential for vascular pathfinding. *Development*. 2011;138:3847–3857.
31. Hogan BM, Herpers R, Witte M, Heloterä H, Alitalo K, Duckers HJ, Schulte-Merker S. Vegfc/Flt4 signalling is suppressed by Dll4 in developing zebrafish intersegmental arteries. *Development*. 2009;136:4001–4009.
32. Pennisi D, Gardner J, Chambers D, Hosking B, Peters J, Muscat G, Abbott C, Koopman P. Mutations in *Sox18* underlie cardiovascular and hair follicle defects in *ragged* mice. *Nat Genet*. 2000;24:434–437.
33. James K, Hosking B, Gardner J, Muscat GE, Koopman P. *Sox18* mutations in the *ragged* mouse alleles *ragged-like* and *opossum*. *Genesis*. 2003;36:1–6.
34. Hosking BM, Wang SC, Downes M, Koopman P, Muscat GE. The *VCAM-1* gene that encodes the vascular cell adhesion molecule is a target of the Sry-related high mobility group box gene, *Sox18*. *J Biol Chem*. 2004;279:5314–5322.
35. Villefranc JA, Amigo J, Lawson ND. Gateway compatible vectors for analysis of gene function in the zebrafish. *Dev Dyn*. 2007;236:3077–3087.
36. Francois M, Koopman P, Beltrame M. SoxF genes: key players in the development of the cardio-vascular system. *Int J Biochem Cell Biol*. 2010;42:445–448.
37. Flores MV, Hall CJ, Crosier KE, Crosier PS. Visualization of embryonic lymphangiogenesis advances the use of the zebrafish model for research in cancer and lymphatic pathologies. *Dev Dyn*. 2010;239:2128–2135.
38. Isogai S, Hitomi J, Yaniv K, Weinstein BM. Zebrafish as a new animal model to study lymphangiogenesis. *Anat Sci Int*. 2009;84:102–111.
39. Karpanen T, Schulte-Merker S. Zebrafish provides a novel model for lymphatic vascular research. *Methods Cell Biol*. 2011;105:223–238.
40. Francois M, Harvey NL, Hogan BM. The transcriptional control of lymphatic vascular development. *Physiology (Bethesda)*. 2011;26:146–155.
41. Srinivasan RS, Geng X, Yang Y, Wang Y, Mukatira S, Studer M, Porto MP, Lagutin O, Oliver G. The nuclear hormone receptor Coup-TFII is required for the initiation and early maintenance of *Prox1* expression in lymphatic endothelial cells. *Genes Dev*. 2010;24:696–707.
42. Christiansen A, Detmar M. Lymphangiogenesis and cancer. *Genes Cancer*. 2011;2:1146–1158.
43. Karkkainen MJ, Ferrell RE, Lawrence EC, Kimak MA, Levinson KL, McTigue MA, Alitalo K, Finegold DN. Missense mutations interfere with VEGFR-3 signalling in primary lymphoedema. *Nat Genet*. 2000;25:153–159.
44. Oliver G, Alitalo K. The lymphatic vasculature: recent progress and paradigms. *Annu Rev Cell Dev Biol*. 2005;21:457–483.
45. Oliver G, Srinivasan RS. Lymphatic vasculature development: current concepts. *Ann N Y Acad Sci*. 2008;1131:75–81.
46. Young N, Hahn CN, Poh A, Dong C, Wilhelm D, Olsson J, Muscat GE, Parsons P, Gamble JR, Koopman P. Effect of disrupted SOX18 transcription factor function on tumor growth, vascularization, and endothelial development. *J Natl Cancer Inst*. 2006;98:1060–1067.
47. Duong T, Proulx ST, Luciani P, Leroux JC, Detmar M, Koopman P, Francois M. Genetic ablation of SOX18 function suppresses tumor lymphangiogenesis and metastasis of melanoma in mice. *Cancer Res*. 2012;72:3105–3114.
48. Alitalo A, Detmar M. Interaction of tumor cells and lymphatic vessels in cancer progression. *Oncogene*. 2012;31:4499–4508.
49. Gordon K, Schulte D, Brice G, Simpson MA, Roukens MG, van I, mpel A, Connell F, Kalidas K, Jeffery S, Mortimer PS, Mansour S, Schulte-Merker S, Ostergaard P. Mutation in vascular endothelial growth factor-C, a ligand for vascular endothelial growth factor receptor-3, is associated with autosomal dominant milroy-like primary lymphedema. *Circ Res*. 2013;112:956–960.

Significance

This work reveals for the first time a conserved role for the transcription factor Sox18 in lymphatic development in a non-mammalian organism, thus strengthening the use of zebrafish as a potent system to study the molecular network at the basis of lymphangiogenesis. Our data reinforce the notion that Sox18 controls the early phases of lymphangiogenesis.

Transcription factors and growth factor pathways have been implicated in lymphangiogenesis, but their interplay has not yet been extensively studied. The genetic interaction we observe points to a so far poorly characterized role of the VEGFC growth factor pathway in the modulation of the activity of a key transcription factor that regulates lymphangiogenesis.

"Sox18 genetically interacts with VegfC to regulate lymphangiogenesis in zebrafish"

Cermenati *et al.*

Materials and Methods

Zebrafish lines and maintenance

Zebrafish were raised and maintained according to established techniques [1]. The following strains were used: AB (from the Wilson lab, UCL, London, UK), tg(*fli1a*:EGFP)^{y1} [2](from the Lawson lab, University of Massachusetts Medical School, MA), tg(*flt1*^{enh}:RFP) line [3].

MO/RNA microinjections

Antisense morpholinos (MOs; Gene Tools, Philomath, OR) used in this study were already described: *sox18*-MO1, *sox18*-MO2, *sox7*-MO1, *sox7*-MO2, [4]; *vegfc*-MO [5]; *flt4*-MO [6]. MOs, diluted in Danieau buffer [7], were injected at 1- to 2-cell stage. Escalating doses of each MO were tested for phenotypic effects; as control for unspecific effects, each experiment was performed in parallel with a std-MO (standard control oligo) with no target in zebrafish embryos. We usually injected 1 pmol/embryo of *sox18*-MO2, 0.5 pmol/embryo of *vegfc*-MO, and 0.8 pmol/embryo of *sox18*-MO1, *sox7*-MO1 and *sox7*-MO2. For combined knockdown experiments, we injected *sox18*-MO2 and *vegfc*-MO at 0.5 and 0.06 pmol/embryo or 0.25 and 0.03 pmol/embryo, respectively; *sox18*-MO2 and *flt4*-MO at 0.5 and 0.06 pmol/embryo, respectively.

For *sox18* RNA, a *Sma*I-*Xba*I fragment from pBSKS^{+}*sox18* [4], containing zebrafish *sox18* cDNA, was subcloned into pCS2^{+}; the resulting plasmid was digested with *Not*I and transcribed with Sp6 RNA Polymerase (Roche). Rescue experiments were performed with the coinjection, into 1-cell stage embryos, of 1pmol/embryo *sox18*-MO2 and 25 or 50pg/embryo *sox18* RNA diluted in Danieau buffer.

For *vegfc* RNA injections, plasmid pCS2+*vegfc* [8] was digested with *Not*I and transcribed with Sp6 RNA polymerase. As an internal control, we wanted to check if *vegfc* RNA could rescue the severe lymphatic phenotype in *vegfc* morphants. Given the full complementarity of *vegfc*-MO to *vegfc* RNA, all injections with *vegfc* RNA were carried out using two independent needles: the same 1-cell stage embryos were injected first with 1 nl of *vegfc* RNA (50 pg) and then with 1 nl of *vegfc*-MO or *sox18*-MO2 (0.5 or 1 pmol, respectively).

Specificity of *sox18/sox7*-MOs

All *sox18/sox7*-MOs used in this study had been previously described[4]. Specificity of the splicing morpholinos (*sox18*-MO2, *sox7*-MO2) had been addressed by checking through RT-PCR that each splicing morpholino was altering processing of its target pre-mRNA, without affecting the splicing of the other *sox* transcripts (as shown in Figure S4 of the above mentioned paper). The efficacy of the translation blocking MOs (targeting the AUG region or the 5'UTR) could not be directly tested due to lack of specific antibodies. However, we could show that three independent sets of MOs (*sox18*-MO1+*sox7*-MO1, *sox18*-MO2+*sox7*-MO2, *sox18*-MO4+*sox7*-MO4) when coinjected at low doses, but not when injected separately, were producing the same circulatory phenotype in the trunk region. Taken together, these observations strongly support the notion that all *sox18/sox7*-MOs presented in Cermenati *et al.*, 2008[4] are specific for their targets.

The sequences of the *sox18/sox7*-MOs used in this study are reported below. For splicing MOs, sequences complementary to the intron sequence of the pre-mRNA target are shown in lowercase letters:

sox18-MO1 5'-TATTCATTCCAGCAAGACCAACACG-3',
sox18-MO2 5'-gtgagtgtcttacCCAGCATTTTAC-3',
sox7-MO1 5'-ACGCACTTATCAGAGCCGCCATGTG-3',
sox7-MO2 5'-gttaaaatcttacCAAGCATCTTGC-3'.

Phenotypic analysis

The analysis of TD formation is commonly used to study lymphatic development in zebrafish. We analyzed TD formation by scoring its length along 10 consecutive trunk segments, up to the anus, in tg(*fli1a*:EGFP)^{y1} larvae at 5 dpf, as previously described [5, 9]. Due to the variability of the lymphatic phenotype, the analyzed larvae were distributed into five phenotypic classes of increasing severity: fully formed TD (normal TD), TD present in 7-9 segments (70-90% TD), 4-6 segments (40-60% TD), 1-3 segments (10-30% TD) and absent TD. At 1.5 to 2.5 dpf, we scored 10 segments in the same region also to analyze the number of sprouts from the vein, PLs and a/v ISVs. All larvae analyzed in this study were circulating to avoid secondary defects that would interfere with TD phenotypes.

Production of tg(*hsp70l:Sox18*^{RaOp} mCherry) transgenic line

The inducible construct consisting of an in frame fusion of the *Sox18*^{RaOp} cDNA with mCherry, under the control of the *hsp70l* promoter, was generated with Gateway system (see below for detailed description). The construct is sketched in Figure 3A. The pDestTol2CG-*Ragged* plasmid was injected with Tol2 transposase RNA (25ng/µl) to generate tg(*hsp70l:Sox18*^{RaOp} mCherry) lines. Founders, crossed with tg(*fli1a*:EGFP)^{y1} or tg(*fli1a*:EGFP)^{y1};tg(*flt1*^{enh}:RFP), were heat shocked at 37-38°C for 1 hour and embryos sorted for mCherry expression 3-4 h post-heat shock to confirm induction of construct expression. PLs and a/vISVs were counted at 54-56 hpf and the presence of TD was scored at 5 dpf.

Construct for tg(*hsp70l:Sox18*^{RaOp} mCherry) transgenic line

The *RaOp* mutation was introduced into a mouse *Sox18* cDNA using site-directed mutagenesis (Quickchange Lightning Site-Directed Mutagenesis Kit, Stratagene) with the primers Sox18ragmut f (5'-GAGCCTGGCGAGGCTCCTTCTTCCCA-3') and Sox18ragmut r (5'-TGGGAAGAAGGAGCCTCGCCAGGCTC-3'). This cDNA sequence was amplified using the primers attB1kozacsox18F (5'-GGGGACAAGTTTGTACAAAAAAGCAGGCTGACCATGCAGAGATCGCCGCCCGGC-3') and sox18ragged-nostop-attB2R (5'-GGGGACCACTTTGTACAAGAAAGCTGGGTGGTTTGGCCAGTGCCACGTGGT-3') to remove the stop codon and clone into a Gateway entry vector. The amplified insert was cloned into DONR211 donor using Gateway technology to generate a pME-*Sox18*^{RaOp} middle entry vector [10, 11].

p5E-*hsp70l* 5'entry clone, p3E mCherry-pA 3' entry clone, pME-*ragged* middle entry vector and pDestTol2CG were combined to generate pDestTol2CG-*ragged* where Sox18^{RaOp} is fused with mCherry and under the control of the *hsp70l* promoter.

***In situ* hybridization and imaging**

Whole-mount *in situ* hybridizations (ISHs) were carried out essentially as described [4]. For ISHs on AB embryos, we synthesized probes as described in the following papers: *sox18* and *sox7* [4], *cdh5* [12] and *vegfc* [8]. *ephB4* was kindly provided by R. Patient.

For ISHs on tg(*fli1a*:EGFP)^{y1} embryos, to avoid background problems as reported on the dedicated web page at zfin.org and recently published [13], we generated probes using the following primers and templates:

probe	primer sequence	template	Ref
sox18	5′-GGAGCCAGGAGTTACAAAACAC-3′ 5′-CTAATACGACTCACTATAGGGCTCCATATGTGCACCAGACTTC-3′	Image clone 6790334	4
sox7	5′-CCCGCTTGATAAAGATGACG-3′ 5′-CTAATACGACTCACTATAGGGCTTGGAAGAGACCAGCCTCAC-3′	Image clone 7045912	4
flt4	5′-CAAGTGCGACGGATGATAGA-3′ 5′-CTAATACGACTCACTATAGGGGTAATGGTGCCACCCAGTG-3′	pBS*flt4*	14
dab2	5′-GCTCTTGCTGTCTCGTTCCT-3′ 5′-CTAATACGACTCACTATAGGGCATCTGCAAGAGCAGCATTC-3′	pBK-CMV*dab2*	15
lyve1	5′-AAGGTTTTGGTGGCATGTTC-3′ 5′-CTAATACGACTCACTATAGGGGATGATGTTGCTGCATGTCC-3′	Image clone 679881	16

Images were taken with a Leica MZFLIII epifluorescence stereomicroscope equipped with a DFC 480-R2 digital camera and the LAS imaging software (Leica, Wetzlar, Germany). Confocal microscopy was performed on a Leica TCS SP2 AOBS microscope, equipped with an argon laser, or a Zeiss 510 microscope. Images were processed using the Adobe Photoshop software (Adobe, San Jose, CA) or Imaris software packages.

Histological sections

For histological analysis after ISH, embryos were re-fixed in 4% PFA, dehydrated, wax embedded, sectioned (8 μm) with a microtome (Leitz 1516) and stained with eosin. Images were taken with a Leica microscope equipped with a Leica 480 digital camera and the LAS software (Leica, Germany).

Statistical analysis

Statistical analyses were performed with Student's *t*-test or one-way ANOVA followed by Dunnett's Multiple Comparison post-test, when needed, using GraphPad PRISM version 5.0 (GraphPad, San Diego, CA). In the graphs, * and ** mark statistically significant data with a p value <0.05 and <0.01, respectively. Statistically highly significant data, with a p value <0.001, are marked by ***.

Quantitative RT-PCR analysis

Quantitative Real Time reverse-transcriptase (qRT) polymerase chain reaction (PCR) analysis was performed on RNA extracted at 32.5 hpf from pools of around 30 Cherry+ embryos of the tg(*hsp70l:Sox18*^{RaOp} mCherry) line heat-shocked at 29 hpf or the same number of Cherry- non heat-shocked controls. Total RNA was isolated with the RNAeasy Minikit (Qiagen) and reverse-trancribed with the Superscript III kit (Invitrogen). Quantitative PCR was performed in technical triplicates using SYBR Green PCR mastemix (Applied Biosystem) according to manufacturer's instructions. Gene expression was normalized to *hprt1*; relative fold-changes were calculated by the comparative Ct or ΔΔCt method, where Ct stands for threshold cycle.

Primers were as follows: *vegfc*-qF 5'-ACCCTACCTACCGGATCATG-3', *vegfc*-qR 5'-TCAAACAACGTCTTGCTGATG-3'; *cdh5*-qF 5'-AAGCCCAATGGTGACCTAAT-3', *cdh5*-qR 5'-ATGGTAACAACGGTAGTGGC-3'; *hprt1*-qF1 5'-ATCATGGACCGAACTGAACG-3', *hprt1*-qR1 5'-AGCGATCACTGTTGCGATTA-3'.

References for Materials and Methods

1. Westerfield M. *The zebrafish book*. Eugene, OR: University of Oregon Press; 1993.
2. Lawson ND, Weinstein BM. In vivo imaging of embryonic vascular development using transgenic zebrafish. *Dev Biol.* 2002;248:307-318.
3. Bussmann J, Bos FL, Urasaki A, Kawakami K, Duckers HJ, Schulte-Merker S. Arteries provide essential guidance cues for lymphatic endothelial cells in the zebrafish trunk. *Development.* 2010;137:2653-2657.
4. Cermenati S, Moleri S, Cimbro S, Corti P, Del Giacco L, Amodeo R, Dejana E, Koopman P, Cotelli F, Beltrame M. Sox18 and Sox7 play redundant roles in vascular development. *Blood.* 2008;111:2657-2666.
5. Yaniv K, Isogai S, Castranova D, Dye L, Hitomi J, Weinstein BM. Live imaging of lymphatic development in the zebrafish. *Nat Med.* 2006;12:711-716.
6. Hogan BM, Herpers R, Witte M, Helotera H, Alitalo K, Duckers HJ, Schulte-Merker S. Vegfc/Flt4 signalling is suppressed by Dll4 in developing zebrafish intersegmental arteries. *Development.* 2009;136:4001-4009.
7. Nasevicius A, Ekker SC. Effective targeted gene 'knockdown' in zebrafish. *Nat Genet.* 2000;26:216-220.
8. Hogan BM, Bos FL, Bussmann J, Witte M, Chi NC, Duckers HJ, Schulte-Merker S. *ccbe1* is required for embryonic lymphangiogenesis and venous sprouting. *Nat Genet.* 2009;41:396-398.
9. Lee SJ, Chan TH, Chen TC, Liao BK, Hwang PP, Lee H. LPA1 is essential for lymphatic vessel development in zebrafish. *Faseb J.* 2008;22:3706-3715.
10. Kwan KM, Fujimoto E, Grabher C, Mangum BD, Hardy ME, Campbell DS, Parant JM, Yost HJ, Kanki JP, Chien CB. The Tol2kit: a multisite gateway-based construction kit for *Tol2* transposon transgenesis constructs. *Dev Dyn.* 2007;236:3088-3099.
11. Villefranc JA, Amigo J, Lawson ND. Gateway compatible vectors for analysis of gene function in the zebrafish. *Dev Dyn.* 2007;236:3077-3087.
12. Larson JD, Wadman SA, Chen E, Kerley L, Clark KJ, Eide M, Lippert S, Nasevicius A, Ekker SC, Hackett PB, Essner JJ. Expression of *VE-cadherin* in zebrafish embryos: a new tool to evaluate vascular development. *Dev Dyn.* 2004;231:204-213.
13. Cha YR, Weinstein BM. Use of PCR template-derived probes prevents off-target whole mount in situ hybridization in transgenic zebrafish. *Zebrafish.* 2012;9:85-89.
14. Thompson MA, Ransom DG, Pratt SJ*, et al.* The *cloche* and *spadetail* genes differentially affect hematopoiesis and vasculogenesis. *Dev Biol.* 1998;197:248-269.
15. Song HD, Sun XJ, Deng M*, et al.* Hematopoietic gene expression profile in zebrafish kidney marrow. *Proc Natl Acad Sci U S A.* 2004;101:16240-16245.
16. Flores MV, Hall CJ, Crosier KE, Crosier PS. Visualization of embryonic lymphangiogenesis advances the use of the zebrafish model for research in cancer and lymphatic pathologies. *Dev Dyn.* 2010;239:2128-2135.

Supplemental material
Cermenati *et al.*

Figure I

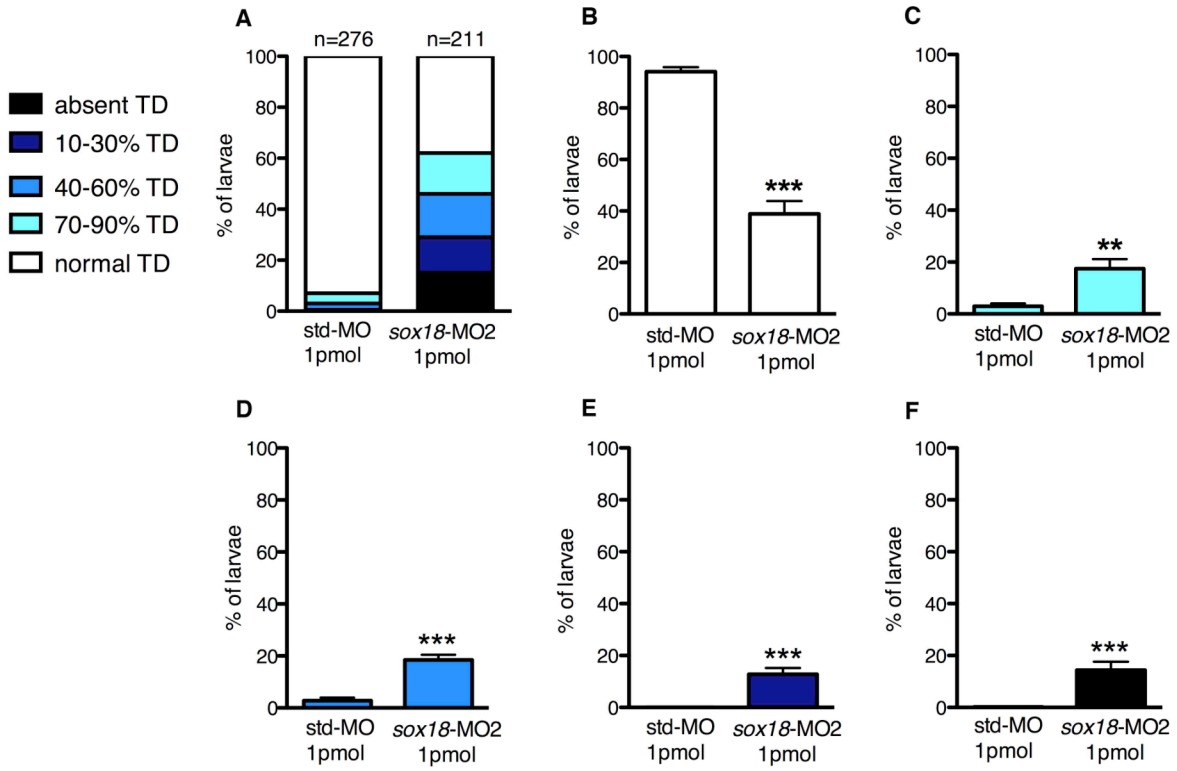

Figure I. Knockdown of *sox18* leads to a statistically highly significant increase in TD defects. **(A)** In the bar chart, we present cumulative data from all the different experiments we performed analyzing TD formation at 5 dpf in control larvae (std-MO) and in larvae injected with 1pmol of *sox18*-MO2. All analyzed tg(*fli1a*:EGFP)^{y1} larvae (276 controls and 211 *sox18* morphants) were circulating. **(B-F)** For all phenotypic classes, based on the analysis of 10 consecutive trunk segments per larva, there is a statistically highly significant difference between *sox18* morphants and control larvae. In particular, we observed a decrease in the percentage of *sox18* morphants with fully formed TD (**B**) and an increase in the percentages of *sox18* morphants with TD present in 7-9 segments (**C**), 4-6 segments (**D**), 1-3 segments (**E**), or with no TD (**F**).

*** = $p<0.001$ *vs* std-MO, ** = $p<0.01$ *vs* std-MO.

Figure II

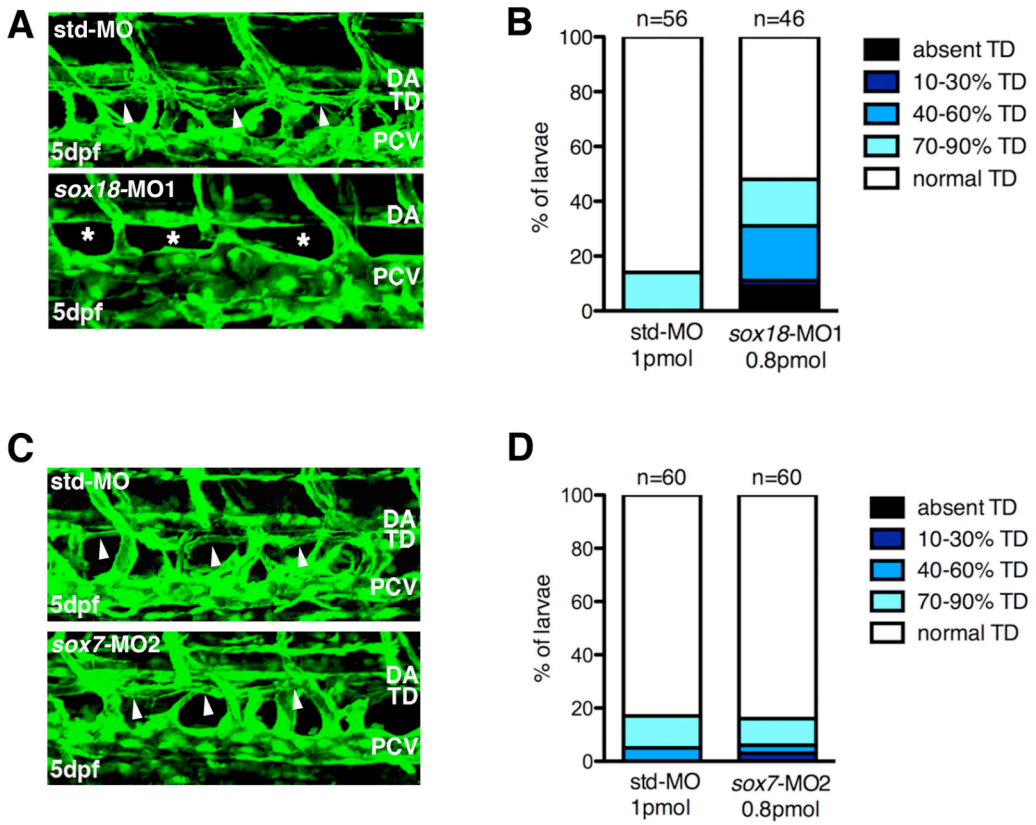

Figure II. Knockdown of *sox18* with an independent MO produces also a lymphatic phenotype, while knockdown of *sox7* causes only very minor lymphatic defects. (A,B) We analyzed TD formation in control larvae (std-MO), and in larvae injected with an independent morpholino against *sox18* (*sox18*-MO1), at 5 dpf. Circulating tg(*fli1a*:EGFP)^{y1} larvae were analyzed by scoring the presence/absence of TD within 10 consecutive intersomitic segments (bar chart **B**). Also in *sox18*-MO1 morphants TD development is defective (white asterisks in **A**) if compared with control embryos (white arrowheads in **A**), although the defects observed are less pronounced than those obtained with *sox18*-MO2. **(C,D)** We analyzed TD formation at 5 dpf in control larvae (std-MO), and in larvae injected with *sox7*-MO2. Circulating larvae were analyzed by scoring the presence/absence of TD within 10 intersomitic segments (bar chart **D**). In *sox7*-MO2 morphants TD development is similar to std control morphants (white arrowheads in **C**).

Figure III

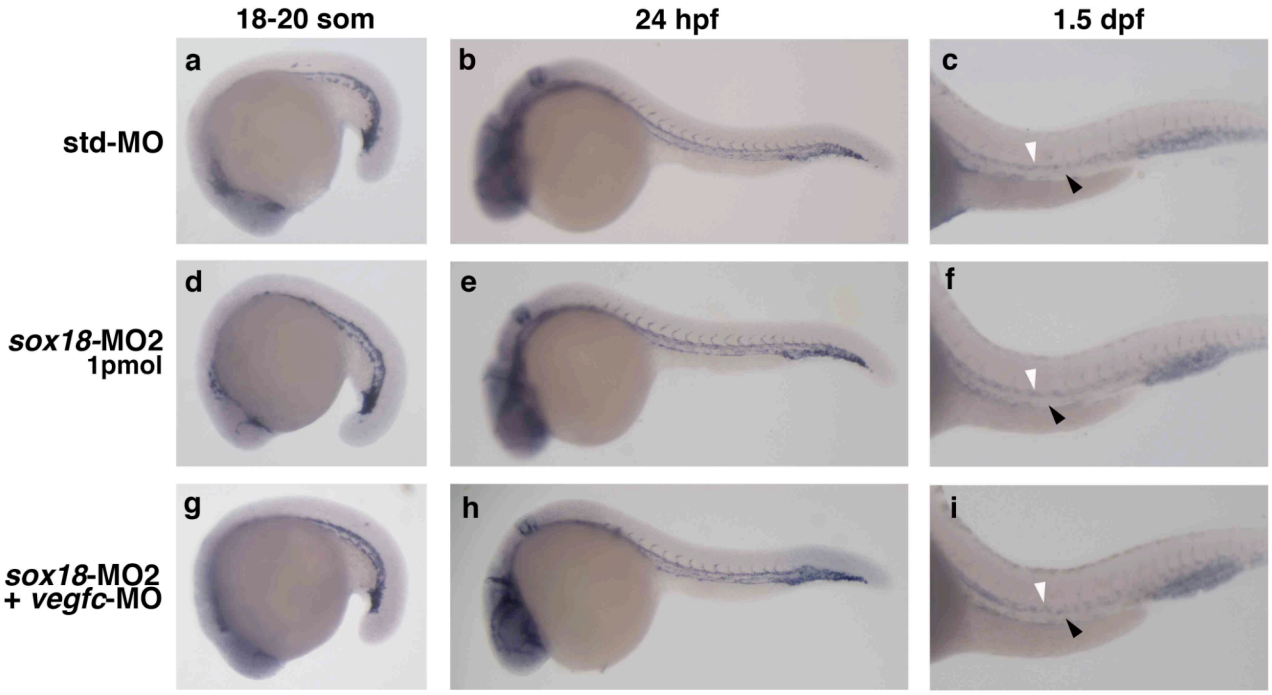

Figure III. The expression of *sox7* is largely unaffected in *sox18* morphants. The expression of *sox7* was analyzed by ISH at 18-20somites (**a,d,g**), 24 hpf (**b,e,h**) and 1.5 dpf (**c,f,i**) and we found no gross differences between control embryos (**a,b,c**), *sox18* single morphants (**d,e,f**) and *sox18-vegfc* double partial morphants (**g,h,i**). All embryos were of the tg(*fli1a*:EGFP)^{y1} line. Images were taken at 40X (a,b,d,e,g,h) or 63X magnification (c,f,i), lateral views anterior to the left. White arrowhead: DA, black arrowhead: PCV.

Figure IV

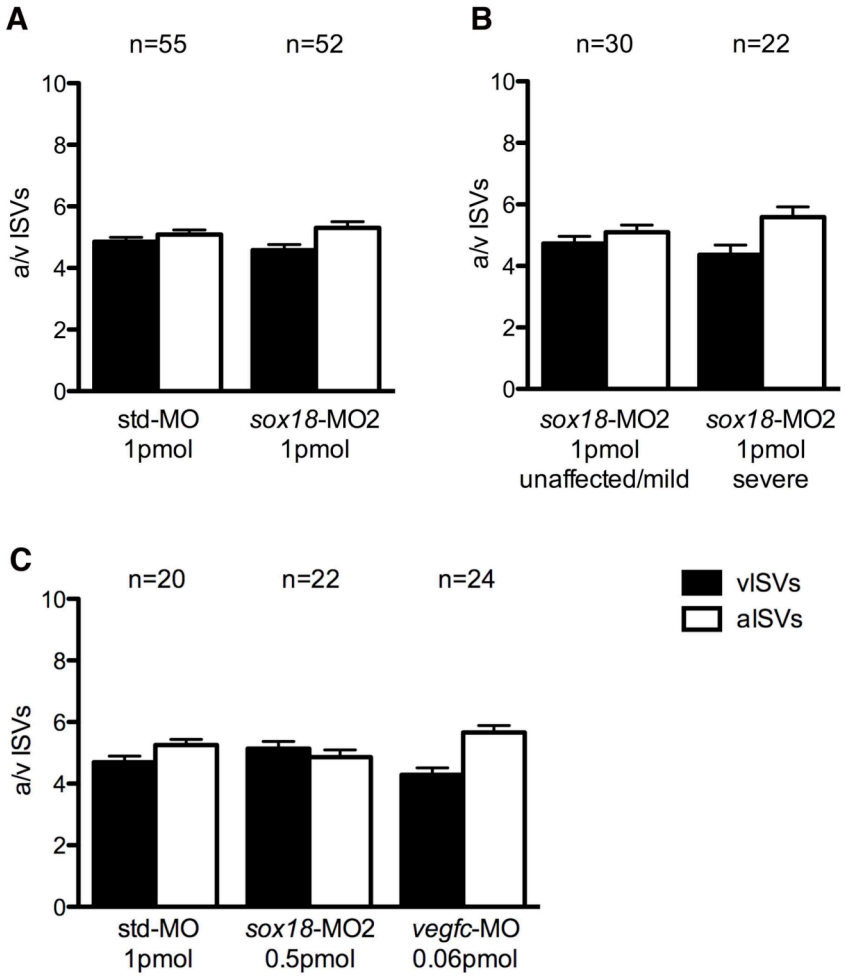

Figure IV. a/v ISV numbers are not significantly impaired even in the most severely affected *sox18* morphants and in *sox18* and *vegfc* single partial morphants. (A,B) We performed a set of three experiments counting the number of arterial and venous intersomitic vessels in circulating *sox18* morphants and controls at 2.5 dpf. The tg(*fli1a*:EGFP)^{y1} embryos were kept separate to analyze their individual TD phenotype at 5 dpf and subdivided into phenotypic classes. **(A)** t-test analysis revealed no significant variations between aggregated *sox18* morphants and controls. **(B)** The comparison of a/v ISV numbers between *sox18* morphants with mild and severe TD formation defects (TD present in 7-10 and 0-6 segments, respectively) did not highlight statistically significant differences. **(C)** We analyzed circulating *sox18* and *vegfc* single partial morphants at 2.5 dpf scoring the number of a/v ISVs in the trunk region. In *sox18*-MO2 injected embryos (0.5 pmol), no gross differences were observed if compared to controls. *vegfc* single partial morphants display a slight decrease in the number of vISVs (and consequently a small increase in the number of aISVs), but these variations are not statistically significant.

Raw data are presented in Table III.

Figure V

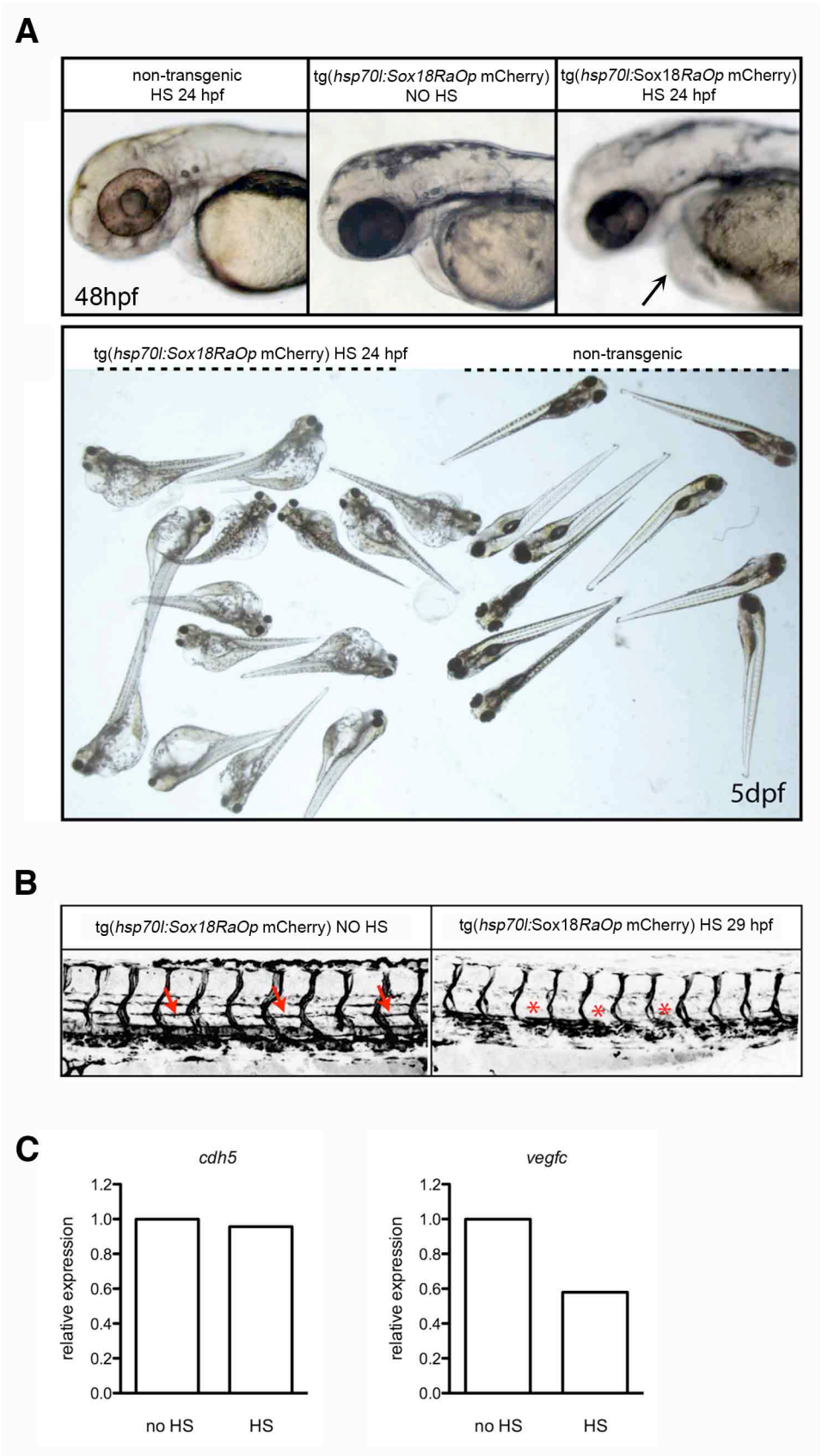
A
non-transgenic
HS 24 hpf
tg(hsp70l:Sox18RaOp mCherry)
NO HS
tg(hsp70l:Sox18RaOp mCherry)
HS 24 hpf
48hpf
tg(hsp70l:Sox18RaOp mCherry) HS 24 hpf
non-transgenic
5dpf
B
tg(hsp70l:Sox18RaOp mCherry) NO HS
tg(hsp70l:Sox18RaOp mCherry) HS 29 hpf
C
cdh5
relative expression
1.2
1.0
0.8
0.6
0.4
0.2
0.0
no HS
HS
vegfc
relative expression
1.2
1.0
0.8
0.6
0.4
0.2
0.0
no HS
HS

Figure V.

(A) tg(*hsp70l:Sox18*^{RaOp} mCherry) embryos following heat shock at 24 hpf display cardiovascular defects and generalized oedema. (A, upper panels) Gross morphology of embryos at 48 hpf following 24 hpf heat shock. Genotype and treatment indicated above in Supplementary Materials and Methods and in the main text (see Materials and Methods). Arrow indicates cardiac oedema in tg(*hsp70l:Sox18*^{RaOp} mCherry) embryos post heat shock. **(A, lower panels)** Gross morphology of tg(*hsp70l:Sox18*^{RaOp} mCherry) larvae (as indicated on the left) compared with non-transgenic larvae (right) at 5 dpf, post heat shock at 24 hpf.

(B) tg(*hsp70l:Sox18*^{RaOp} mCherry) embryos following heat shock at 29 hpf display PL defects. General trunk views of non heat-shocked controls and heat-shocked embryos at 56 hpf visualized by tg(*fli1a*:EGFP)^{y1} expression. Red arrows point to PL+ segments, asterisks mark absence of PLs.

(C) Heat-shock induced overexpression of Sox18^{RaOp} results in reduced *vegfc* expression. A representative qRT-PCR experiment is shown here (experimental details are described above in Supplementary Materials and Methods). The pan-endothelial *cdh5* gene shows no gross difference between non heat-shocked and heat-shocked embryos, while *vegfc* expression is reduced post heat shock.

Figure VI

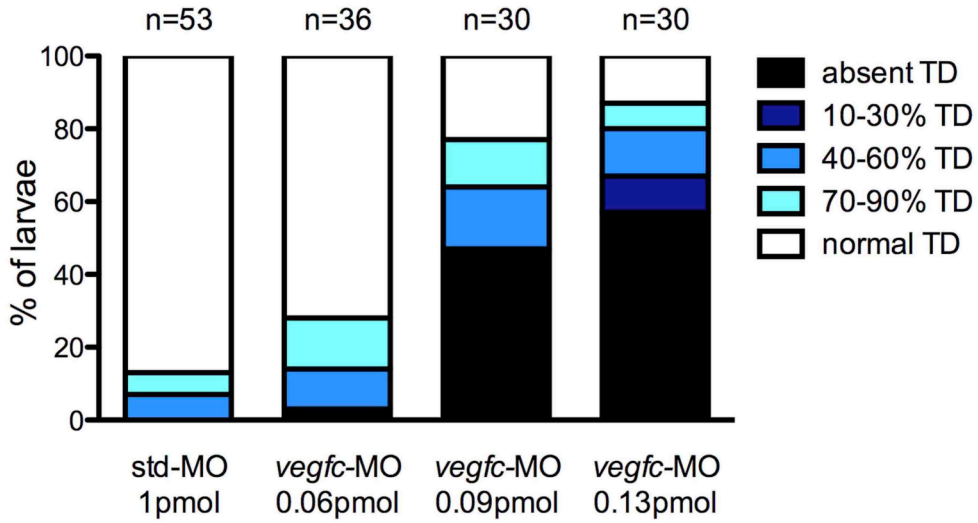

Figure VI. Injection of *vegfc* morpholino dose-dependently affects TD formation. The sub-critical dose of *vegfc*-MO that causes only mild defects in TD formation (0.06 pmol) was identified through analysis of a dose-response curve. Circulating tg(*fli1a*:EGFP)^{y1} larvae were analyzed by scoring the presence/absence of TD within 10 consecutive intersomitic segments at 5 dpf, and subdivided into phenotypic classes. The bar chart in the figure shows that raising the morpholino dose of 50% to 100% (0.09 and 0.13 pmol) the percentage of embryos with most severe TD defects is at least 10-fold greater than what observed with the sub-critical *vegfc*-MO dose (0.06 pmol).

Figure VII

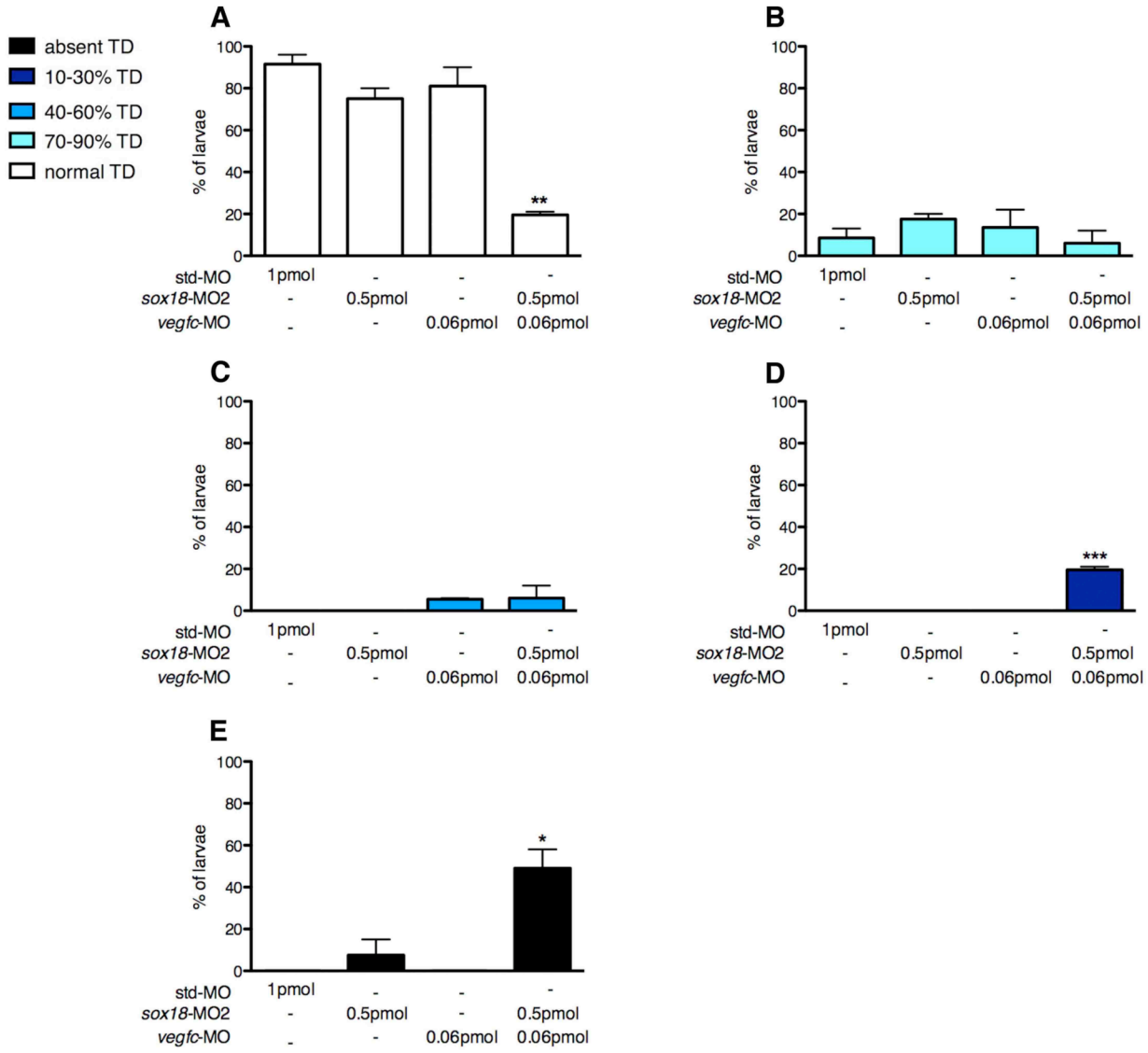

Figure VII. Combined partial knockdown of *sox18* and *vegfc* leads to a statistically significant increase of severely affected larvae. We performed statistical analysis on TD formation data of control larvae, *sox18* and *vegfc* single partial morphants and *sox18-vegfc* double partial morphants (see Figure 4). We observed a statistically significant decrease in the percentage of *sox18-vegfc*MOs double injected larvae that have a normal TD with respect to both control larvae and single partial morphants (**A**). This is linked to the statistically significant increase in the percentage of larvae belonging to the most affected classes, *i.e.* with 1-3 TD segments (**D**) or absent TD (**E**). No significant variations were found among controls and double/single partial morphants in the classes with mild TD defects, *i.e.* TD present in 7-9 (**B**) or in 4-6 segments (**C**). *** = $p<0.001$ *vs* std-MO; ** = $p<0.01$ *vs* std-MO; * = $p< 0.05$ *vs* std-MO.

Figure VIII

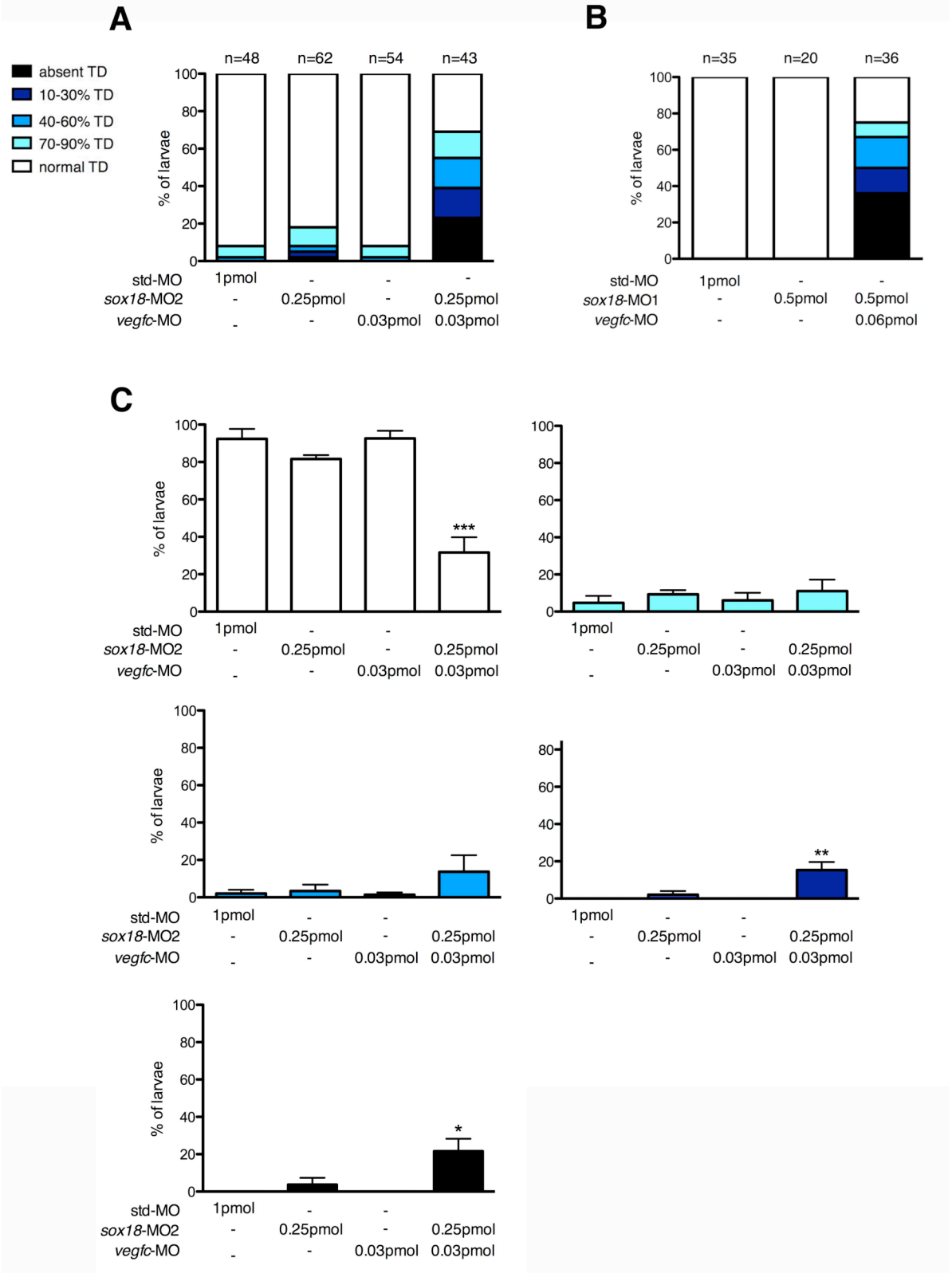
A
absent TD
10-30% TD
40-60% TD
70-90% TD
normal TD
n=48
n=62
n=54
n=43
% of larvae
std-MO 1pmol - - -
sox18-MO2 - 0.25pmol - 0.25pmol
vegfc-MO - - 0.03pmol 0.03pmol
B
n=35
n=20
n=36
% of larvae
std-MO 1pmol - -
sox18-MO1 - 0.5pmol 0.5pmol
vegfc-MO - - 0.06pmol
C
% of larvae
***
**
*
std-MO 1pmol - -
sox18-MO2 - 0.25pmol - 0.25pmol
vegfc-MO - - 0.03pmol 0.03pmol

Figure VIII. TD formation is synergistically affected even when halving the subcritical doses of *sox18*-MO2 and *vegfc*-MO or coinjecting suboptimal doses of *sox18*-MO1 and *vegfc*-MO.

(A) The subcritical doses of *sox18* and *vegfc* MOs showed in Figure 4 were reduced by 2-fold to analyze TD formation in *sox18* and *vegfc* single or double morphants at 5 dpf. Only the coinjection but not the single injection of *sox18*- and *vegfc*-MOs (0.25pmol and 0.03pmol respectively) causes noticeable TD formation defects. Statistical analysis is shown below (C).

(**B**) We also analyzed TD formation in control larvae (std-MO), and in larvae injected with a subcritical dose of *sox18*-MO1 (0.5 pmol) or coinjected with subcritical doses of *sox18*-MO1+*vegfc*-MO (0.5 + 0.06 pmol). The bar chart shows that TD formation is severely impaired only in double partial morphants.

(C) Statistical analysis of the data in bar chart A. We observed a statistically significant decrease in the percentage of *sox18*-*vegfc* double partial morphants that have a normal TD with respect to both control larvae and single partial morphants. This is linked to the statistically significant increase in the percentage of larvae belonging to the most affected classes, *i.e.* with 1-3 TD+ segments or absent TD. No significant variations were found among controls and double/single partial morphants in the classes with mild TD defects. *** = $p<0.001$, ** = $p<0.01$, * = $p< 0.05$ *vs* std-MO.

Figure IX

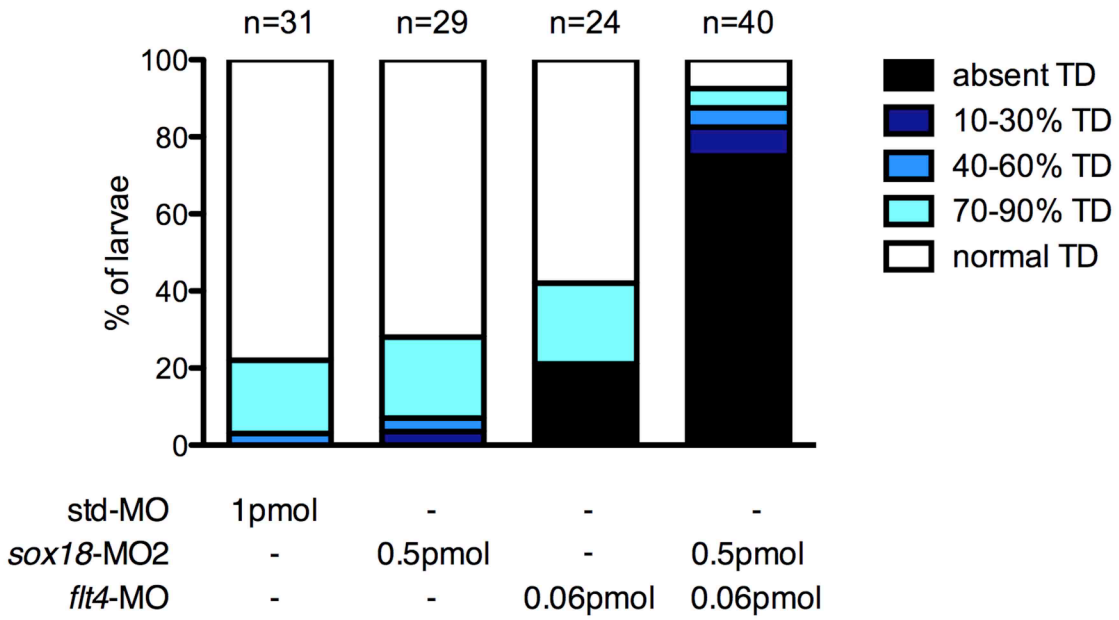

Figure IX. TD formation is synergistically affected by the coinjection of suboptimal doses of *sox18*-MO2 and *flt4*-MO. When injected separately, the subcritical dose of *sox18*-MO2 (0.5pmol) does not lead to major TD formation defects, as observed in controls, while *flt4*-MO affects TD formation in a sizeable manner even at the suboptimal dose (0.06pmol). Nevertheless, the defects observed upon coinjection of the two MOs are much more severe than the mere sum of the defects observed when they are injected separately. Circulating tg(*fli1a*:EGFP)^{y1} larvae were analyzed at 5 dpf by scoring the presence/absence of TD within 10 consecutive intersomitic segments.

Figure X

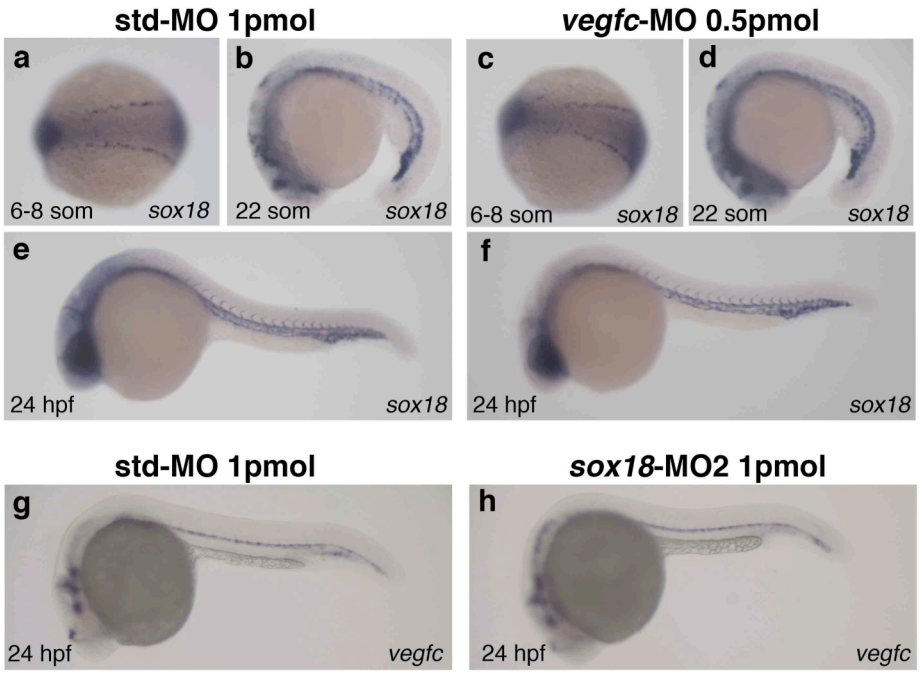

Figure X. The expression of *sox18* is not altered in *vegfc* morphants and the expression of *vegfc* appears unaffected in *sox18* morphants. Hybridizations with *sox18* probe were performed on std-MO (**a,b,e**) and *vegfc*-MO injected embryos (**c,d,f**). We also performed *vegfc* ISHs on control embryos and *sox18* morphants (**g,h**). No gross differences were found at the indicated developmental stages. Images were taken at 40X magnification, lateral views anterior to the left.

Figure XI

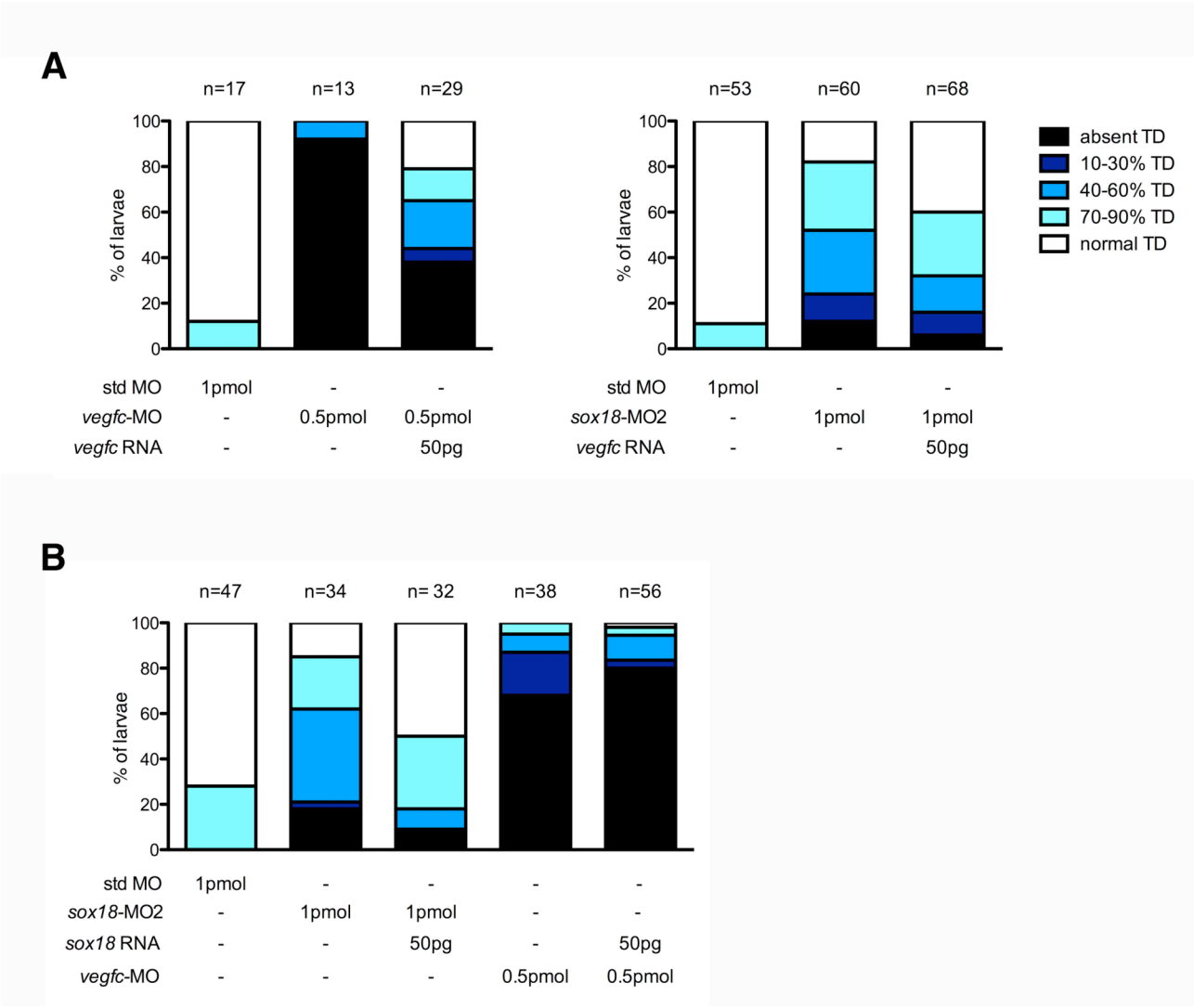

Figure XI. The injection of *vegfc* RNA partially rescues the lymphatic phenotype of *sox18* morphants. We analyzed TD formation in 5 dpf larvae of the tg(*fli1a*:EGFP)^{Y1} line. Circulating larvae were analyzed by scoring the presence/absence of TD within 10 consecutive intersomitic segments along the trunk and subdivided into phenotypic classes**.**

(A) The injection of 50 pg of *vegfc* RNA drastically reduces the severe TD formation defects of *vegfc* morphants (internal control, left bar chart) and it partially rescues TD formation defects of *sox18* morphants (right bar chart), although not as efficiently as sox18 RNA (see Figure 1).

(B) The injection of 50 pg of *sox18* RNA rescues TD formation defects of *sox18* morphants (internal control), but it does not reduce the severe TD formation defects of *vegfc* morphants.

The number and percentages of larvae belonging to each phenotypic class are reported in Table VI.

Figure XII

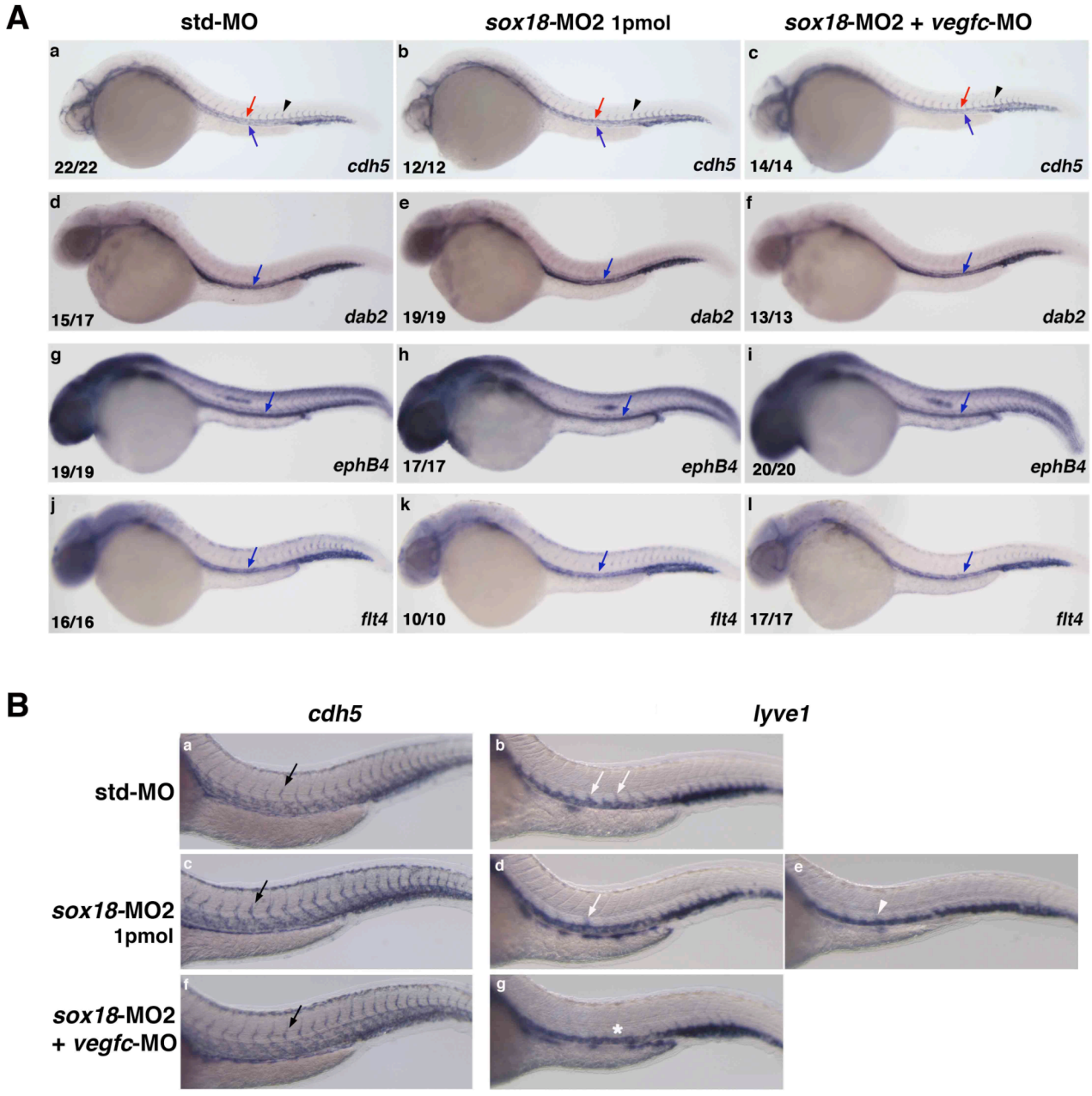

Figure XII. Analysis of *sox18* morphants and *sox18-vegfc* double partial morphants by ISHs. **(A)** ISHs were carried out with the pan-endothelial marker *cdh5* (a-c) and the venous markers *dab2* (d-f), *ephb4* (g-i) and *flt4* (j-l) in *sox18* single morphants and in *sox18+vegfc* double partial morphants of the tg(*fli1a*:EGFP)^{y1} line. Around 29 hpf, their expression is largely unaffected. Images a-c, d-f, j-l are lower magnifications of embryos showed in Figure 6A (*ephb4* ISHs are only shown here). The numbers of embryos with the pictured ISH signal among those analyzed in a typical experiment are shown in the lower left corner of each panel. Red arrows: DA; blue arrows:

PCV; black arrowheads: ISVs. **(B)** ISHs were carried out on 2 dpf tg(*fli1a*:EGFP)^{y1} morphants with the pan-endothelial marker *cdh5* (a,c,f) and the zebrafish ortholog of the mammalian lymphatic marker *LYVE1* (b,d,e,g). *lyve1*+ sprouts are reduced in single *sox18* morphants and almost absent in *sox18*-*vegfc* double partial morphants. Images are lower magnification of embryos showed in Figure 6B. Black arrows: ISVs, white arrows: *lyve1*+ sprouts, white arrowhead: *lyve1*+ sprouts reduced in length, asterisk: absence of *lyve1*+ sprouts.

Table I

	std-MO 1pmol	***sox18*-MO2 1pmol**	***sox18*-MO2 1pmol+ *sox18* RNA25 pg**	***sox18*-MO2 1pmol+ *sox18* RNA50 pg**
100% TD	48/60 (80%)	17/56 (30%)	16/41 (39%)	20/38 (53%)
70-90% TD	10/60 (16%)	10/56 (18%)	13/41 (32%)	12/38 (32%)
40-60% TD	1/60 (2%)	6/56 (10%)	5/41 (12%)	1/38 (2%)
10-30% TD	0/60 (0%)	13/56 (23%)	2/41 (5%)	1/38 (2%)
absent TD	1/60 (2%)	10/56 (18%)	5/41 (12%)	4/38 (11%)

TD analysis upon injection of *sox18*-MO2 and *sox18*-MO2 + *sox18* RNA. The number (and percentage) of larvae belonging to each phenotypic class (shown in the bar chart in Figure 1) is reported; data were gathered in three independent experiments. The number of larvae with almost completely formed TD (normal TD and 70-90% TD) is nearly doubled in *sox18*-MO2+*sox18*-RNA (50pg) coinjected embryos compared with *sox18* morphants. We also report a very strong reduction of the more affected classes (absent to 30% TD).

Data gathered in additional independent rescue experiments of *sox18* morphants with *sox18* RNA are shown in Table VI B.

Table II

A					
sprouts from the vein		**std-MO 1pmol**	***sox18*-MO2 1pmol**	***vegfc*-MO 0.5pmol**	***sox18*-MO2 0.5pmol + vegfc-MO 0.06pmol**
	MEAN	8.1000	5.0000	2.0630	3.7810
	SEM	0.2054	0.4082	0.5735	0.4746
	number	n=30	n=33	n=16	n=32
B					
PL+ segments		**std-MO 1pmol**	***sox18*-MO2 1pmol**	***vegfc*-MO 0.5pmol**	***sox18*-MO2 0.5pmol + vegfc-MO 0.06pmol**
	MEAN	8.2670	5.1380	1.8670	4.4670
	SEM	0.2346	0.5246	0.4145	0.5419
	number	n=30	n=29	n=30	n=30

C				
vISV		**std-MO 1pmol**	***sox18*-MO2 1pmol**	***sox18*-MO2 0.5pmol + vegfc-MO 0.06pmol**
	MEAN	5.1500	4.7963	3.2424
	SEM	0.1423	0.1895	0.2275
	number	n=60	n=54	n=66
vISV		**std-MO 1pmol**	***vegfc*-MO 0.5pmol**	
	MEAN	4.9500	1.1500	
	SEM	0.2348	0.3500	
	number	n=20	n=20	

Sprouts from the vein, PL+ segments and a/v ISVs scores of *sox18* and *vegfc* single morphants. Raw data used for the bar charts shown in Figure 2A and 5A **(A),** Figure 2B and 5B (**B)**, and Figure 2C and 5C **(C)** are reported here. Only circulating embryos are indicated. All data presented here were obtained in three independent experiments, except for vISV scores in *vegfc* morphants and control embryos. SEM: standard error of the mean. Statistical analysis was performed on the complete data sets.

Table III

A			
		std-MO 1pmol	***sox18*-MO2 1pmol**
vISV	**MEAN**	4.8550	4.5770
	SEM	0.1383	0.1890
	number	n=55	n=52
aISV	**MEAN**	5.0910	5.3080
	SEM	0.1428	0.1933
	number	n=55	n=52

B			
		***sox18*-MO2 1pmol unaffected/mild**	***sox18*-MO2 1pmol severe**
vISV	**MEAN**	4.7330	4.3640
	SEM	0.2296	0.3193
	number	n=30	n=22
aISV	**MEAN**	5.1000	5.5910
	SEM	0.2317	0.3267
	number	n=30	n=22

C				
		std-MO 1pmol	***sox18*-MO2 0.5pmol**	***vegfc*-MO 0.06pmol**
vISV	**MEAN**	4.7000	5.1360	4.2920
	SEM	0.1933	0.2307	0.2210
	number	n=20	n=22	n=24
aISV	**MEAN**	5.2500	4.8640	5.6670
	SEM	0.1902	0.2307	0.2225
	number	n=20	n=22	n=24

a/v ISVs counts. Raw data used for the bar chart shown in Figure IV are reported here. The data were collected in three independent experiments. SEM: standard error of the mean.

Table IV

PL+ segments		29hpf HS Cherry+	29hpf HS Cherry-	36hpf HS Cherry+	36hpf HS Cherry-	48hpf HS Cherry+	48hpf HS Cherry-
	MEAN	5.1860	0.5278	4.3100	2.6490	5.2900	3.5710
	SEM	0.3478	0.2373	0.4801	0.4123	0.4179	0.6346
	number	n=43	n=36	n=42	n=37	n=31	n=21

vISV		29hpf HS Cherry+	29hpf HS Cherry-
	MEAN	4.9150	2.6040
	SEM	0.1395	0.3060
	number	n=59	n=77

PL+ segments and vISVs counts after heat-shock induced expression of murine Sox18^{RaOp}. Raw data used for the bar chart shown in Figure 3 are indicated here.

Table V

	std-MO 1pmol	*sox18*-MO2 0.5pmol	*vegfc*-MO 0.06pmol	*sox18*-MO2 0.5pmol + vegfc-MO 0.06pmol
100% TD	48/52 (92%)	34/45 (76%)	30/37 (81%)	9/48 (19%)
70-90% TD	4/52 (8%)	8/45 (18%)	5/37 (14%)	4/48 (8%)
40-60% TD	0/52 (0%)	0/45 (0%)	2/37 (5%)	4/48 (8%)
10-30% TD	0/52 (0%)	0/45 (0%)	0/37 (0%)	9/48 (20%)
absent TD	0/52 (0%)	3/45 (6%)	0/37 (0%)	22/48 (45%)

TD formation analysis of *sox18* and *vegfc* single/double partial morphants. The number (and percentage) of larvae belonging to each phenotypic class shown in the bar chart of Figure 4 is reported here.

Table VI

A, left bar chart			
	std-MO 1pmol	***vegfc*-MO 0.5pmol**	***vegfc*-MO 0.5pmol+ *vegfc* RNA50 pg**
100% TD	15/17 (88%)	0/13 (0%)	6/29 (21%)
70-90% TD	2/17 (12%)	0/13 (0%)	4/29 (14%)
40-60% TD	0/17 (0%)	1/13 (8%)	6/29 (21%)
10-30% TD	0/17 (0%)	0/13 (0%)	2/29 (6%)
absent TD	0/17 (0%)	12/13 (92%)	11/29 (38%)
A, right bar chart			
	std-MO 1pmol	***sox18*-MO2 1pmol**	***sox18*-MO2 1pmol+ *vegfc* RNA50 pg**
100% TD	47/53 (89%)	11/60 (18%)	27/68 (40%)
70-90% TD	6/53 (11%)	18/60 (30%)	19/68 (28%)
40-60% TD	0/53 (0%)	17/60 (28%)	11/68 (16%)
10-30% TD	0/53 (0%)	7/60 (12%)	7/68 (10%)
absent TD	0/53 (0%)	7/60 (12%)	4/68 (6%)

B					
	std-MO 1pmol	***sox18*-MO2 1pmol**	***sox18*-MO2 1pmol+ *sox18* RNA50 pg**	***vegfc*-MO 0.5pmol**	***vegfc*-MO 0.5pmol+ *sox18* RNA50 pg**
100% TD	34/47 (78%)	5/34 (15%)	16/32 (50%)	0/38 (0%)	1/56 (2%)
70-90% TD	13/47 (28%)	8/34 (23%)	10/32 (32%)	2/38 (5%)	2/56 (3.5%)
40-60% TD	0/47 (0%)	14/34 (41%)	3/32 (9%)	3/38 (8%)	6/56 (11%)
10-30% TD	0/47 (0%)	1/34 (3%)	0/32 (0%)	7/38 (19%)	2/56 (3.5%)
absent TD	0/47 (0%)	6/34 (18%)	3/32 (9%)	26/38 (68%)	45/56 (80%)

TD analysis upon injection of *vegfc* RNA in *vegfc* and *sox18* morphants (A) and of *sox18* RNA in *sox18* and *vegfc* morphants (B). The number (and percentage) of larvae belonging to each phenotypic class (shown in the bar charts in Figure XI) is reported here.

Table VII

***lyve1*+ sprouts**	**std-MO 1pmol**	***sox18*-MO2 1pmol**	***sox18*-MO2 0.5pmol + vegfc-MO 0.06pmol**
normal sprouts	33/50 (66%)	6/54 (11%)	3/60 (5%)
reduced sprouts number	11/50 (22%)	21/54 (39%)	14/60 (23%)
shorter sprouts	6/50 (12%)	13/54 (24%)	20/60 (33%)
absent sprouts	0	14/54 (26%)	23/60 (39%)

Analysis of lyve1+ sprouts in *sox18* morphants and *sox18-vegfc* double partial morphants. Numbers (and percentages) of embryos shown in Figure 6B are reported here. These are cumulative data gathered in three independent experiments.

Among controls, the vast majority of embryos showed normal *lyve1*+ sprouts (33/50 std-MO injected embryos). On the contrary, normal *lyve1*+ sprouts were detectable in only about 10% of *sox18* morphants and 5% of combined partial *sox18-vegfc* morphants (6/54 and 3/60, respectively), while the remaining morphants were variably affected. Among *sox18* morphants, the prevalent phenotype we observed is the reduction of *lyve1*+ sprout number, accounting for almost 40% (21/54 vs 11/50 in controls), followed by embryos characterized by *lyve1*+ sprouts of reduced length (13/54 vs 6/50 in controls) and embryos devoid of *lyve1*+ sprouts (14/54; this class is not represented in controls). Among combined partial *sox18-vegfc* morphants, the absence of *lyve1*+ sprouts in the trunk characterized about 40% of the embryos (23/60), about 30% of them showed *lyve1*+ sprouts of reduced length (20/60 vs 6/50 in controls), while the percentage of embryos with a reduced number of *lyve1*+ sprouts was comparable to controls (14/60 vs 11/50)

Sox13 is involved in ISV angiogenesis in zebrafish, as a modulator of the Notch signaling

Alice Omini[a], Solei Cermenati[a] and Monica Beltrame[a*]

[a] Dipartimento di Bioscienze, Università degli Studi di Milano, Milano, Italy

Dipartimento di BioScienze, Università degli Studi di Milano, Via Celoria 26, 20133, Milano, Italy

alice.omini@unimi.it

solei.cermenati@unimi.it

monica.beltrame@unimi.it

*Corresponding author:

Monica Beltrame
Dipartimento di Bioscienze
Universita' degli Studi di Milano
Via Celoria 26
20133 Milano
Italy
e-mail: monica.beltrame@unimi.it
tel +39-0250315025
fax +39-0250315044

Keywords: *sox13*, zebrafish, ISV, angiogenesis, Notch pathway

Bulleted highlights:

- Zebrafish *sox13* is expressed in the central nervous system and transiently in the developing vasculature
- *sox13* knockdown impairs angiogenesis in different vascular beds
- ISV defects in *sox13* morphants are apparently linked to altered Notch signaling

Abstract

Members of the SOX (Sry-related HMG box) family of transcription factors are found throughout the animal kingdom and are involved in many developmental processes. A role of Sox13 role in T-cell differentiation has been clearly shown in mouse. *Sox13* expression has been also reported in arteries during late somitogenesis in mouse and in the developing vasculature in *Xenopus*. McGary and colleagues proposed Sox13 as a new potential player in angiogenesis.

We identified the zebrafish *SOX13* ortholog and we decided to characterize its function during embryo development via morpholino-induced knockdown. We report here *sox13* expression in the posterior lateral plate mesoderm and transiently in the forming axial vessels. In *sox13* morphants angiogenesis is largely affected in several vascular beds, and we decided to focus our attention on primary ISVs and DLAVs formation. Diverse classes of ISVs phenotype has been observed with increasingly severe phenotype, leading to partially formed or completely absent DLAVs. The expression of the Notch-controlled gene *ephrinB2* is slightly upregulated in *sox13* morphants, and it is reported that Notch pathway hyper-activation inhibits normal angiogenesis, similarly to *sox13* knockdown. We were able to rescue ISVs migration and DLAVs formation by treating *sox13* morphants with DAPT, a Notch pathway inhibitor.

Our data suggest that Sox13 could act as modulator of the Notch signaling pathway in angiogenetic processes.

Introduction

The establishment of a functional cardiovascular system is one of the earliest events that occurs during embryogenesis. An accurate knowledge of the mechanisms that regulate the correct patterning of a functional vascular network is really relevant, in particular if we consider that in many pathological conditions the formation of vascular vessels is regulated by the same processes and molecules (Folkman, 1995). In the last two decades the zebrafish has emerged as an innovative model system to go deeper into the anatomical processes and the molecular mechanisms that regulate the assembly of a primary vascular network and its successive remodelling.

At the onset of circulation, at around 24 hours post fertilization (hpf), the main axial vessels which originate through vasculogenesis are formed and luminizated in zebrafish embryos (Isogai et al., 2001). During vasculogenesis, under the influence of VegfA, angioblasts migrate from the lateral plate mesoderm (LPM) towards the midline to give rise to the dorsal aorta (DA) and the posterior cardinal vein (PCV) (Lawson and Weinstein, 2002). Recently, it has been shown that two different populations of angioblasts reside in the LPM: one medial layer of cells which correspond to the arterial progenitors of the DA, and a second lateral layer, which gives rise to the venous endothelial cells of the PCV (Kohli et al., 2013). When the DA and PCV are assembled, a set of primary sprouts emerge from the DA and migrate towards the dorsal region of the embryo, following each vertical somite boundary, and give rise to the primary intersomitic vessels (ISVs) (Isogai et al., 2003). When the primary sprouts have reached the dorsal portion of the embryo they branch rostrally and

caudally to connect with their neighbors to form the dorsal longitudinal anastomotic vessels (DLAVs) (Isogai et al., 2003).

An ISV sprout is composed by two different types of cells: the tip and the stalk cells. The tip cell is located in the apical portion of the sprout and it is characterized by long dynamic filopodial extensions, indispensible for the correct growth and migration of the vessel (Gerhardt et al., 2003; Siekmann and Lawson, 2007b). The stalk cells are behind the tip cells and are important to make up the base of the sprout and maintain the connection with the vessel of origin (Siekmann and Lawson, 2007a). Regulation of the correct identity of each of these cells should be fine-tuned. Tip cell differentiation is induced by VegfA signaling, which induces an endothelial cell to acquire a motile and invasive behavior (Gerhardt et al., 2003). Vegfr2 activation stimulates the up-regulation of the Notch ligand Delta-like4 (Dll4) in the tip cells inducing an up-regulation of the Notch signaling in the neighboring cells, that acquire a stalk cell identity through a lateral inhibition mechanism (Leslie et al., 2007; Siekmann and Lawson, 2007b; Jakobsson et al., 2010). Notch activation in the stalk cells suppresses angiogenetic activity and Vegfr-3/Flt4 activity (Siekmann and Lawson, 2007b) (Tammela et al., 2008).

Members of the Sry-related HMG box (SOX) family of transcription factors are found throughout the animal kingdom and play widespread roles during development (Bowles et al., 2000; Schepers et al., 2002; Kamachi and Kondoh, 2013). SoxF proteins are expressed in endothelial cells during mouse vascular development and they are involved in the regulation of different aspects of vascular development (Francois et al., 2010; Kamachi and Kondoh, 2013). In zebrafish, *sox7* and *sox18* play redundant role in the establishment of proper arteriovenous identity (Cermenati et al., 2008; Herpers et al., 2008; Pendeville et al., 2008). The

SoxD protein Sox13 is known to be involved in the regulation of T-cell differentiation by promoting gammadelta T-cell development while opposing alphabeta T-cell identity (Melichar et al., 2007). During T-cell differentiation SOX13 acts by directly binding TCF1 and preventing it from binding to target genes (Melichar et al., 2007; Marfil et al., 2010). In literature, we found some hints that suggest a possible involvement for Sox13 in vascular development. High expression of *Sox13* in arterial walls was reported during mouse embryonic development (Roose et al., 1998). In 2010, McGary and colleagues performed a limited functional characterization of Sox13. The knockdown of human *SOX13* by siRNA disrupted tube formation in HUVECs and *Xenopus sox13* morpholino-knocked down embryos presented defects in vascular tree formation (McGary et al., 2010).

We identified the zebrafish *SOX13* ortholog and we report here that it is transiently expressed in the developing vasculature. We characterized its role during embryonic development via morpholino-induced knockdown. In *sox13* morphants angiogenesis is largely disrupted in several vascular beds, and we focused our attention on primary ISVs and DLAVs formation. We collected data that suggest that ISVs defects in *sox13* morphants could be provoked by an incorrect Notch signaling.

Our results therefore point to an involvement of Sox13 in ISVs angiogenesis in zebrafish as a modulator of Notch signaling.

Materials and methods

Zebrafish lines and maintenance

Zebrafish were raised and maintained according to established techniques (Westerfield, 1993). The following strains were used: AB (from the Wilson lab, UCL, London, UK), tg(*gata1*:dsRed)^{sd2};(*kdrl*:EGFP)^{s843} (from Massimo Santoro lab, Università di Torino, Italy), tg(*fli1a*:EGFP)^{y1} (Lawson and Weinstein, 2002) (from the Lawson lab, University of Massachusetts Medical School, MA).

In silico translation of zebrafish *sox13* coding sequence

We partially sequenced the naa14b10 EST clone (Vihtelic et al., 2005) from 5' and 3'. Based on sequencing results and on available genomic data we introduced a C at position 1852 in the predicted RNA sequence available under accession number XR_082631.1 (gi:292619084).The corrected sequence was then translated *in silico* using StriderX.

Alignments and phylogenetic analysis

Sox13 proteins alignment by CLUSTAL W was processed by BOXSHADE 3.21 (cut-off for shading: 80%) @ ch.EMBnet.org. SoxD protein sequences alignment was made by Muscle and unambiguously aligned regions were identified by Gblocks. Bootstrapping annotated at each node was carried out on 1000 replicates. The tree was rooted using Drosophila SoxC as outgroup. Sequences used are listed in table S1.

RT-PCR

RNA samples were extracted with ToTALLY RNA isolation kit (Ambion), treated with DNAse I RNAse free (Roche), and retrotranscribed with

SuperScriptII Reverse Transcriptase (Invitrogen, Life Technologies), according to the manufacturers' instructions. PCR reactions were performed using the following primers:

sox13-Fw: 5' – GCAGGCCCACAGAAGCACG - 3';

sox13-Rv: 5' – TATCATGGGCTCTGCCGCCT – 3';

actb1a-Fw: 5' – TGTTTTCCCCTCCATTGTTGG – 3';

actba1-Rv: 5' – TTCTCCTTGATGTCACGGAC – 3'.

Phenotypic and statistical analysis

To avoid an altered analysis due to the growth defects, *sox13* morphants were not analyzed and fixed at the same time of controls, but when they reached the same somite-stage or a comparable morphology within 1 dpf. In the text and figures, this is specified indicating the hours post fertilization at which the analysis was perfomed for the different samples.

Statistical analyses were performed with Student's *t*-test or one-way ANOVA followed by Dunnett's Multiple Comparison post-test, when needed, using GraphPad PRISM version 5.0 (GraphPad, San Diego, CA). In the graphs, statistically highly significant data, with a p value <0.001, are marked by ***.

***In situ* analysis, IHC and imaging**

Whole mount *in situ* hybridizations were carried out as described, (Thisse et al., 1993; Patterson et al., 2005). For the *sox13* antisense probe, a 1.3 kb *Sal*I/*Xho*I fragment from the EST clone naa14b10 was subcloned into pBSKS^{+}; the resulting plasmid was digested with SalI and transcribed with T3 RNA Polymerase (Roche). We synthesized probes as described in the following papers: *cdh5*, *etv2/etsrp*, *notch3*, *flt4* and *efbnB2a* (Cermenati et

al., 2008), *notch1b* (Westin and Lardelli, 1997). Images were taken with a Leica MZFLIII epifluorescence stereomicroscope equipped with a DFC 480-R2 digital camera or with a Leica microscope equipped with a Leica 480 digital camera and the LAS imaging software (Leica, Wetzlar, Germany). Confocal microscopy was performed on a Leica TCS SP2 AOBS microscope, equipped with an argon laser, or a Zeiss 510 microscope. Images were processed using the Adobe Photoshop software (Adobe, San Jose, CA). IHC for znp1 were carried out as described (Brusegan et al., 2012).

Morpholinos and RNA microinjections

Antisense morpholinos were purchased from Gene Tools (LLC, Philomath, OR).

sox13-sMO: 5' – GAGAACGCTCCTATAAACAGAGATA – 3';

sox13-sMO2: 5' – CTCCCAAGAAGCCTGGAGAGTGAAA – 3'

MOs, diluted in Danieau buffer (Nasevicius and Ekker, 2000), were injected at 1- to 2-cell stage. Escalating doses of each MO were tested for phenotypic effects; we routinely injected 0,5 pmol/embryo both for sox13-sMO and sox13-sMO2; as control for unspecific effects, each experiment was performed in parallel with a std-MO (standard control oligo) with no target in zebrafish embryos. Co-injection with 0,75 pmol/embryo p53-MO was tried to exclude aspecific effects (Robu et al., 2007). RT-PCR to test the molecular effects on RNA processing of *sox13*-sMO and *sox13*-sMO2 injection were performed on total RNA extracted from *sox13* morphants and controls using the following primers:

sox13-EX2Fw: 5' – TCCCAGCAGTCCTCCCGCT - 3';

sox13-EX4/5R: 5'–TGCCAAACTCTCTGGGGTTCCT–3' for *sox13*-sMO

sox13-8/9EXFw: 5’ – CGCCAGCACACCAGCCAACC – 3’
sox13-EX12R: 5’ – TGGCCAGAAGGAGTTCGGG – 3’ for *sox13*-sMO2

For *sox13* RNA injection, a pCS2+/sox13 plasmid was created by PCR amplification of the pBSKS/sox13 construct using the primers listed herafter, followed by the digestion of the amplified fragment with *Bam*HI and *Xba*I and subcloned in pCS2+ vector cut with *Bam*HI and *Xba*I. The pCS2+/sox13 plasmid a fragment was digested with *Not*I and transcribed with mMessage mMachine Sp6 transcription kit (Ambion). Rescue experiments were performed with the coinjection, into 1-cell stage embryos, of 0,5 pmol/embryo *sox13*-sMO and 100 pg/embryo *sox13* RNA diluted in Danieau buffer.

*sox13*F+*Bam*HI: 5’ –CGGGATCCAAGCGTATGTTATTAACTCGC – 3’
T7 promoter: 5’ – TAATACGACTCACTATAGGG – 3’

DAPT treatments

A 25 mM stock solution of DAPT (γ-secretase inhibitor IX; Calbiochem) in DMSO was diluited in E3 1X embryo medium at 100 µM. *sox13*-MO3 and std-MO morphants were dechorionated and treated with DAPT from 18-20 ss to 30 hpf at 30°C. As controls, *sox13*-sMO and std-MO injected embryos were treated with E3 1X embryo medium containing the same concentration of DMSO carrier only (0,8%).

Results

We identified a *bona fide sox13* in zebrafish

We identified a putative *Sox13* ortholog in zebrafish by searching expressed sequence tag (EST) and genomic databases. Zebrafish *sox13* is located on chromosome 11 and it is organized in 14 exons and 13 introns. We performed an *in silico* translation of the nucleotide sequence, because no protein sequence was deposited in the databases, and aligned it with other Sox13 proteins of different species (Fig. 1A). Our sequence codes for the typical domains of known SoxD proteins: a leucine-zipper and a neighboring glutamine-rich sequence stretch, which was named Q box (Kido et al., 1998), in the N-terminal portion, and the HMG-box DNA binding domain in the C-terminus (Fig. 1A). To be sure that our sequence was more similar to Sox13 proteins than the other SoxD proteins we performed a phylogenetic analysis comparing our putative Sox13 with Sox5 and Sox6 proteins of different species (Fig. 1B). The analysis showed that our putative zebrafish Sox13 gather together with the other Sox13 and not with Sox5 nor Sox6 proteins (Fig. 1B).

sox13 is mainly expressed in the central nervous system, but also in the developing vasculature

Characterization of *sox13* expression by RT-PCR revealed that *sox13* transcripts were present from the first developmental stages up to 5 days post fertilization (dpf), which was the last stage we analyzed (Fig. 2A). A *sox13* signal is detectable by whole mount *in situ* hybridization (WISH) from the earliest developmental stages (data not shown). We analysed in

detail its spatial distribution from mid somitogenesis to the early larval stages (Fig. 2B, C and data not shown). *sox13* was widely expressed in the developing central nervous system (CNS) at all analyzed stages. From the mid somitogenesis, *sox13* appeared to be expressed in a series of regions of the most anterior portions of the CNS, i.e. the forebrain and the midbrain (Fig. 2B a). On the contrary, the region of the anterior midbrain-hindbrain boundary was negative for *sox13* (Fig. 2B b), while an intense signal was detectable in the following region of the hindbrain (Fig. 2B a,b,c), and in the rhombomeres boundaries at 30 hpf (Fig. 2B c). In the spinal cord, *sox13* signal appeared more intense in the upper layers and in the ventral portion of the neural tube, and less in the central part (Fig. 2B, d). At mid-somitogenesis, *sox13* was weakly expressed in the lateral plate mesoderm, which is the region where angioblasts reside (Fig. 2C e,f,g). At 20 somite stage a *sox13* signal was clearly detectable in both forming axial vessels, the dorsal aorta and the cardinal vein (Fig. 2C h). At 22 hpf, *sox13* expression was mainly detectable in the dorsal aorta, in the region where the caudal vein plexus will develop and in the intermediate cell mass (ICM; Fig. 2C, i). After this stage, the signal of *sox13* in axial vessels substantially decreased. *sox13* expression in the adult organs has been detected in ovary (Fig. 2A), kidney, gills and gut and, at a low level, in liver, heart and muscle by RT-PCR (data not shown).

sox13 knockdown affects different aspects of zebrafish embryogenesis

To investigate the role of *sox13* during zebrafish development we performed knockdown experiments, using two independent splice-blocking morpholinos (sMOs). The first one, *sox13*-sMO, was designed to cause the loss of all functional domains (coiled-coil domain and HMG-box), the

second one, *sox13*-sMO2, only the HMG-box. We analyzed RNA processing defects by RT-PCR (Fig. S1). The injection of *sox13*-sMO caused the loss of the wild-type mRNA and the formation of two aberrant isoforms of the transcript (Fig. S1A, B). We determined by sequencing that the predominant aberrant transcript was characterised by the partial retention of the second intron, through the activation of a cryptic splice site. The second one, less represented, by the skipping of the third exon (Fig. S1A and data not shown). In both cases, a premature stop codon was introduced. The injection of *sox13*-sMO2 caused the reduction of the wild-type transcript (Fig. S1B). Aberrant isoforms have been observed at an higher number of amplification cycles (data not shown).

In literature, it is reported that *Sox13*-null mice present severe growth defects (Melichar et al., 2007). *sox13* knockdown slightly affected embryo growth in a dose dependent manner (data not shown). To analyse if this defect was an off-target effect mediated through p53 activation (Robu et al., 2007), we coinjected *sox13*-sMO with p53-MO. No significant ameliorations were observed after this coinjection (Fig. S2A). *sox13* morphants presented motility defects, in particular they did not react to touch-response stimuli. To determine if this defects were due to an altered formation of the motoneurons, we decided to perform an IHC assay using an anti-synaptotagmin2 antibody (znp1). At around 30 hpf primary motoneurons in *sox13* morphants were formed, but appeared thinner than controls, and at 2 dpf less arborized in their ventral portion (Fig. S2B). *sox13* knockdown did not affect embryos circulation, however some defects in hematopoietic processes were observed (data not shown).

In *sox13* morphants angiogenesis was largely disrupted in different vascular beds. A range of ISVs defects were observed, leading to partially formed or completely absent DLAVs (Fig. 3 a'). The structure of the

caudal vein plexus was severly reduced, losing the classical honeycomb-like aspect at 2 dpf (Fig. 3 b'). The SIV basket was strongly reduced at 3 dpf (Fig. 3 c'). In this study, we decided to focus our attention on the defects caused by *sox13* knockdown to ISVs and DLAVs.

sox13 is involved in ISVs angiogenesis

Vasculogenesis was mildly affected in *sox13* morphants (Fig. S3A). At 12 somites the angioblast marker *etv2*/*etsrp* revealed a partial or complete loss of the lateral layer of *etsrp* positive cells in posterior LPM (Fig. S3A, a'). In addition, *etv2*/*etsrp* ISHs showed that the migration of endothelial cell precursors from the LPM towards the midline is partially affected (Fig. S3A, b',b''). However, at around 24 hpf, the pan-endothelial marker *cdh5* showed that the two main axial vessels were formed (Fig. 4A). At the same stage, ISV defects were already detectable. Primary sprouts from the artery were already stained in the controls, but in *sox13* morphants they were still undetectable (Fig. 4A). At around 29 hpf, ISV signals were still absent in some regions of the trunk or only partially developed in *sox13* morphants (Fig. 4A). ISVs defects were analyzed *in vivo* at around 30 hpf considering ten consecutive trunk ISVs, up to the anus, and classified as normal, reduced and absent ISVs (Fig. 4B). In *sox13* morphants around half of the ISVs are affected (Fig. 4C), with statistically highly significant differences with respect to controls (Fig. S3B). Qualitatively similar results, though with a lower penetrance, were obtained by injecting an independent splice-blocking MO, *sox13*-sMO2 (Fig. S3C). A statistical analysis showed that the differences between morphants and controls were already highly statistically significant (Fig. S3C). A rescue assay was performed to verify the specificity of *sox13*

knockdown defects. The coinjection of *sox13* RNA with *sox13*-sMO led to a statistically highly significant rescue of the ISV phenotype (Fig. 4B,C and S3B).

sox13 could act as a Notch signaling modulator

We decided to analyze a series of endothelial markers by WISH to better characterize the *sox13* morphants phenotype (Fig. S4). At around 24 hpf, an increased signal of *notch1b* was detectable both in neural districts and in the DA, on the other hand *notch3*, which is expressed in the same regions, seemed to be unaffected in *sox13* morphants (Fig. S4). At around 29 hpf the venous marker *flt4* appeared unaffected in the PCV (Fig. S4). We noticed that, at around 30 hpf, the signal of the arterial marker *ephrinB2a* was slightly increased in the trunk region in a significant portion of the *sox13* knocked-down embryos (Fig. 5A and S4). On the other hand, the *ephrinB2a* signal in the cranial region seemed comparable between *sox13* morphants and controls (Fig. 5A). In zebrafish, an improper expression of *ephrinB2a* could be related to a defective Notch signaling (Lawson et al., 2001), and Notch hyper-activation inhibits angiogenesis (Siekmann and Lawson, 2007b). We decided to investigate if the Notch pathway was incorrectly modulated in *sox13* knockdown conditions by treating *sox13* morphants with an inhibitor of Notch signaling (DAPT). We analyzed the effects of DAPT treatment on *sox13* morphants by observing ISV angiogenesis *in vivo* (Fig. 5B). Embryos were treated with DAPT just before the beginning of the ISVs sprouting at 18 somites and analyzed at around 30 hpf and at 2 dpf. At around 30 hpf, we report a statistically highly significant rescue of ISV defects in *sox13* morphants treated with DAPT (Fig. 5C and S5A). At 2 dpf ISVs defects in *sox13* morphants were

slightly decreased. (Fig. S5B). However, the difference between morphants and controls were statistically highly significant and successfully rescued with the DAPT treatment (Fig. S5B). At 2 dpf, we analysed the defects in DLAV formation. We counted direct DLAV connections between adjacent ISVs, limiting the analysis to ten consecutive trunk ISVs, up to the anus. *sox13* morphants lost a great number of these connections (Fig. 5D). The DAPT treatment could significantly rescue also this defect (Fig. 5D).

Discussion

In zebrafish, as in other vertebrates, intersomitic vessels are among the first angiogenic vessels to form (Isogai et al., 2003). The correct acquisition of the tip and stalk identity and the control of their migration are finely tuned by the interplay of different signaling pathways (Gerhardt et al., 2003; Leslie et al., 2007; Siekmann and Lawson, 2007b; Herbert and Stainier, 2011). The Notch pathway acts in this puzzle by influencing the endothelial cells of a single sprout to acquire a tip or stalk identity through a lateral inhibition mechanism (Leslie et al., 2007; Jakobsson et al., 2010). Consequently, an incorrect modulation of the Notch signaling pathway could severely affect angiogenetic processes (Siekmann and Lawson, 2007b; Siekmann and Lawson, 2007a). We proposed here a role for Sox13 as a modulator of Notch signaling during ISVs angiogenesis in zebrafish.

Sox13 belongs to the SOX family of transcription factors and in literature its role in the differentiation of T cells in mouse, by modulating the Wnt pathway, is well described (Melichar et al., 2007; Turchinovich and Hayday, 2011; Gray et al., 2013; Ouyang et al., 2014). In literature, some hints were present, pointing to a possible involvement for Sox13 in vascular development (Roose et al., 1998; McGary et al., 2010). However this aspect of Sox13 function has been not investigated in depth so far. We use zebrafish as a model system to further investigate this point. We identified a *Sox13* putative ortholog in zebrafish, which presented the typical domains of the other Sox13 proteins. When we carried out WISH analysis to determine *sox13* expression pattern in zebrafish, we observed that *sox13* was predominantly expressed in the central nervous system. A strong expression in neural regions has been reported also in mice embryos

(Wang et al., 2005; Wang et al., 2006). However, we detected a *sox13* signal also in vascular districts. During mid-somitogenesis, *sox13* is slightly expressed in the lateral plate mesoderm and in the forming axial vessels during late somitogenesis. Interestingly, when we knocked down *sox13* with a splice-blocking morpholino, the expression of the angioblasts marker *etv2*/*etsrp* resulted affected, as the migration towards the midline of angioblasts was perturbed in *sox13* morphants. Angioblasts in the LPM are distributed into two layers; recently it has been proposed that the population which resides in medial one gives rise to the DA, while the lateral one migrates to form the PCV (Kohli et al., 2013). In a significant number of *sox13* morphants we observed that the external layer, which should correspond to venous endothelial cell precursors, disappeared. However, *in vivo* observations at the following stages and ISH analysis with *cdh5* showed that both the DA and the PCV were substantially formed. Our data suggest that *sox13* knockdown could mildly affect zebrafish vasculogenesis, but that this defect could be recovered. We described also a *sox13* expression in the DA at 22 hpf, just before its expression became undetectable in endothelial cells by ISH. Interestingly, this moment is crucial for the beginning of primary ISVs sprouting from the DA (Isogai et al., 2003). We report here that *sox13* knockdown affects ISVs angiogenesis with increasingly severe phenotypes, leading to partially formed or completely absent DLAV. At around 30 hpf a half of the ISVs considered for the analysis were affected in *sox13* morphants; at 2 dpf these defects were less pronounced, suggesting that part of the phenotype is linked to a specific angiogenesis delay. We were able to obtain analogous results with another independent splice-blocking morpholino, but with a lower penetrance. This correlates also with a more reduced molecular activity of *sox13*-sMO2, compared with *sox13*-sMO, in altering *sox13* pre-mRNA processing, possibly explain the reduced effect

in vivo effect. The specifity of the knockdown phenotype we observed is further supported by the fact that we were able to rescue the ISVs defects by the coinjection of *sox13*-sMO with *sox13*-RNA.

Notch1b and Notch3 in zebrafish are both expressed in the neural tube and in the DA, however they have a diverse involvement in zebrafish vascular development. Notch1b is mainly involved in the specification of tip and stalk identity, while Notch3 have a crucial role in arterial-venous differentiation (Lawson and Weinstein, 2002; Geudens et al., 2010). We observed that *sox13* knockdown selectively altered *notch1b* signal, which appeared slightly increased in *sox13* morphants. Furthermore, the signal of the Notch-controlled gene *ephrinB2* is slightly increased in *sox13* morphants too. The expression of the venous marker *flt4* in the PCV in *sox13* morphants is comparable to control embryos, suggesting that the arterial-venous identity is not grossly affected in *sox13* morphants. In literature it is described that Notch signaling hyper-activation inhibits normal angiogenesis (Siekmann and Lawson, 2007b). We reasoned that our data could suggest an incorrect modulation of the Notch signaling during ISVs angiogenesis due to *sox13* knockdown. We confirmed a link between Sox13 and Notch pathway by the rescue of ISVs defects by treating *sox13* morphants with a Notch signaling inhibitor.

In conclusion, we report here for the first time a detailed analysis that partially elucidates Sox13 role in vascular development, with a particular attention to its pro-angiogenic activity in ISVs formation. Our data point to a Sox13 engagement in this process by the modulation of the Notch signaling pathway. We are convinced that our work will be useful also to better understand the contribution of SOX proteins in vascular development in vertebrates.

Acknowledgements

We want to thank Graeme Wistow (NIH/NEI) to kindly provide us the *sox13* EST clone. We acknowledge financial support by Regione Lombardia (grant SAL-01 to M. Beltrame) and by Fondazione Cariplo (grant 2011-0555 to M. Beltrame).

References

Bowles J, Schepers G, Koopman P. 2000. Phylogeny of the SOX family of developmental transcription factors based on sequence and structural indicators. Dev Biol 227:239-255.

Brusegan C, Pistocchi A, Frassine A, Della Noce I, Schepis F, Cotelli F. 2012. Ccdc80-l1 Is involved in axon pathfinding of zebrafish motoneurons. PLoS One 7:e31851.

Cermenati S, Moleri S, Cimbro S, Corti P, Del Giacco L, Amodeo R, Dejana E, Koopman P, Cotelli F, Beltrame M. 2008. Sox18 and Sox7 play redundant roles in vascular development. Blood 111:2657-2666.

Folkman J. 1995. Angiogenesis in cancer, vascular, rheumatoid and other disease. Nat Med 1:27-31.

Francois M, Koopman P, Beltrame M. 2010. SoxF genes: Key players in the development of the cardio-vascular system. Int J Biochem Cell Biol 42:445-448.

Gerhardt H, Golding M, Fruttiger M, Ruhrberg C, Lundkvist A, Abramsson A, Jeltsch M, Mitchell C, Alitalo K, Shima D, Betsholtz C. 2003. VEGF guides angiogenic sprouting utilizing endothelial tip cell filopodia. J Cell Biol 161:1163-1177.

Geudens I, Herpers R, Hermans K, Segura I, Ruiz de Almodovar C, Bussmann J, De Smet F, Vandevelde W, Hogan BM, Siekmann A, Claes F, Moore JC, Pistocchi AS, Loges S, Mazzone M, Mariggi G, Bruyere F, Cotelli F, Kerjaschki D, Noel A, Foidart JM, Gerhardt H, Ny A, Langenberg T, Lawson ND, Duckers HJ, Schulte-Merker S, Carmeliet P, Dewerchin M. 2010. Role of delta-like-4/Notch in the formation and wiring of the lymphatic network in zebrafish. Arterioscler Thromb Vasc Biol 30:1695-1702.

Gray EE, Ramirez-Valle F, Xu Y, Wu S, Wu Z, Karjalainen KE, Cyster JG. 2013. Deficiency in IL-17-committed Vgamma4(+)

gammadelta T cells in a spontaneous Sox13-mutant CD45.1(+) congenic mouse substrain provides protection from dermatitis. Nat Immunol 14:584-592.

Herbert SP, Stainier DY. 2011. Molecular control of endothelial cell behaviour during blood vessel morphogenesis. Nat Rev Mol Cell Biol 12:551-564.

Herpers R, van de Kamp E, Duckers HJ, Schulte-Merker S. 2008. Redundant roles for sox7 and sox18 in arteriovenous specification in zebrafish. Circ Res 102:12-15.

Isogai S, Horiguchi M, Weinstein BM. 2001. The vascular anatomy of the developing zebrafish: an atlas of embryonic and early larval development. Dev Biol 230:278-301.

Isogai S, Lawson ND, Torrealday S, Horiguchi M, Weinstein BM. 2003. Angiogenic network formation in the developing vertebrate trunk. Development 130:5281-5290.

Jakobsson L, Franco CA, Bentley K, Collins RT, Ponsioen B, Aspalter IM, Rosewell I, Busse M, Thurston G, Medvinsky A, Schulte-Merker S, Gerhardt H. 2010. Endothelial cells dynamically compete for the tip cell position during angiogenic sprouting. Nat Cell Biol 12:943-953.

Kamachi Y, Kondoh H. 2013. Sox proteins: regulators of cell fate specification and differentiation. Development 140:4129-4144.

Kido S, Hiraoka Y, Ogawa M, Sakai Y, Yoshimura Y, Aiso S. 1998. Cloning and characterization of mouse mSox13 cDNA. Gene 208:201-206.

Kohli V, Schumacher JA, Desai SP, Rehn K, Sumanas S. 2013. Arterial and venous progenitors of the major axial vessels originate at distinct locations. Dev Cell 25:196-206.

Lawson ND, Scheer N, Pham VN, Kim CH, Chitnis AB, Campos-Ortega JA, Weinstein BM. 2001. Notch signaling is required for arterial-venous differentiation during embryonic vascular development. Development 128:3675-3683.

Lawson ND, Weinstein BM. 2002. Arteries and veins: making a difference with zebrafish. Nat Rev Genet 3:674-682.

Leslie JD, Ariza-McNaughton L, Bermange AL, McAdow R, Johnson SL, Lewis J. 2007. Endothelial signalling by the Notch ligand Delta-like 4 restricts angiogenesis. Development 134:839-844.

Marfil V, Moya M, Pierreux CE, Castell JV, Lemaigre FP, Real FX, Bort R. 2010. Interaction between Hhex and SOX13 modulates Wnt/TCF activity. J Biol Chem 285:5726-5737.

McGary KL, Park TJ, Woods JO, Cha HJ, Wallingford JB, Marcotte EM. 2010. Systematic discovery of nonobvious human disease models

through orthologous phenotypes. Proc Natl Acad Sci U S A 107:6544-6549.

Melichar HJ, Narayan K, Der SD, Hiraoka Y, Gardiol N, Jeannet G, Held W, Chambers CA, Kang J. 2007. Regulation of gammadelta versus alphabeta T lymphocyte differentiation by the transcription factor SOX13. Science 315:230-233.

Nasevicius A, Ekker SC. 2000. Effective targeted gene 'knockdown' in zebrafish. Nat Genet 26:216-220.

Ouyang K, Leandro Gomez-Amaro R, Stachura DL, Tang H, Peng X, Fang X, Traver D, Evans SM, Chen J. 2014. Loss of IP3R-dependent Ca(2+) signalling in thymocytes leads to aberrant development and acute lymphoblastic leukemia. Nat Commun 5:4814.

Patterson LJ, Gering M, Patient R. 2005. Scl is required for dorsal aorta as well as blood formation in zebrafish embryos. Blood 105:3502-3511.

Pendeville H, Winandy M, Manfroid I, Nivelles O, Motte P, Pasque V, Peers B, Struman I, Martial JA, Voz ML. 2008. Zebrafish Sox7 and Sox18 function together to control arterial-venous identity. Dev Biol 317:405-416.

Robu ME, Larson JD, Nasevicius A, Beiraghi S, Brenner C, Farber SA, Ekker SC. 2007. p53 activation by knockdown technologies. PLoS Genet 3:e78.

Roose J, Korver W, Oving E, Wilson A, Wagenaar G, Markman M, Lamers W, Clevers H. 1998. High expression of the HMG box factor sox-13 in arterial walls during embryonic development. Nucleic Acids Res 26:469-476.

Schepers GE, Teasdale RD, Koopman P. 2002. Twenty pairs of sox: extent, homology, and nomenclature of the mouse and human sox transcription factor gene families. Dev Cell 3:167-170.

Siekmann AF, Lawson ND. 2007a. Notch signalling and the regulation of angiogenesis. Cell Adh Migr 1:104-106.

Siekmann AF, Lawson ND. 2007b. Notch signalling limits angiogenic cell behaviour in developing zebrafish arteries. Nature 445:781-784.

Tammela T, Zarkada G, Wallgard E, Murtomaki A, Suchting S, Wirzenius M, Waltari M, Hellstrom M, Schomber T, Peltonen R, Freitas C, Duarte A, Isoniemi H, Laakkonen P, Christofori G, Yla-Herttuala S, Shibuya M, Pytowski B, Eichmann A, Betsholtz C, Alitalo K. 2008. Blocking VEGFR-3 suppresses angiogenic sprouting and vascular network formation. Nature 454:656-660.

Thisse C, Thisse B, Schilling TF, Postlethwait JH. 1993. Structure of the zebrafish snail1 gene and its expression in wild-type, spadetail and no tail mutant embryos. Development 119:1203-1215.

Turchinovich G, Hayday AC. 2011. Skint-1 identifies a common molecular mechanism for the development of interferon-gamma-secreting versus interleukin-17-secreting gammadelta T cells. Immunity 35:59-68.

Vihtelic TS, Fadool JM, Gao J, Thornton KA, Hyde DR, Wistow G. 2005. Expressed sequence tag analysis of zebrafish eye tissues for NEIBank. Mol Vis 11:1083-1100.

Wang Y, Bagheri-Fam S, Harley VR. 2005. SOX13 is up-regulated in the developing mouse neuroepithelium and identifies a sub-population of differentiating neurons. Brain Res Dev Brain Res 157:201-208.

Wang Y, Ristevski S, Harley VR. 2006. SOX13 exhibits a distinct spatial and temporal expression pattern during chondrogenesis, neurogenesis, and limb development. J Histochem Cytochem 54:1327-1333.

Westerfield M. 1993. The zebrafish book. University of Oregon Press, Eugene, OR.

Westin J, Lardelli M. 1997. Three novel Notch genes in zebrafish: implications for vertebrate Notch gene evolution and function. Dev Genes Evol 207:51-63.

Figure legends

Fig. 1. We identified the *Sox13* putative ortholog in zebrafish

(**A**) Alignement of Sox13 protein sequences of different species. The leucine zipper (LZ) and Q-box region and the family-specific HMG box DNA-binding domain are highlighted. (**B**) Phylogenetic analysis of SoxD proteins. Sequences used for these analyses are reported in Table S1.

Fig. 2. *sox13* was expressed in the central nervous system and transiently in the forming axial vessels

(**A**) *sox13* and *actb1a* temporal expression analysis by RT-PCR on total RNA extracted from ovary and different embryonic and larval stages. The size of the obtained PCR fragments is indicated. Negative and positive controls are showed in the right-most lanes. (**B-C**) *sox13* spatial expression was analyzed by WISH at different developmental stages. (**B**) *sox13* was largely expressed in the central nervous system. Distinct portion in the fore- (F), mid-(M) and hindbrain (H) were marked, but the anterior portion of the midbrain-hindbrain boundary (MHB) was clearly negative for a *sox13* signal (**a-b**). At 30 hpf *sox13* clearly marked the rhombomeres boundaries (**c**, white arrowhead). In the spinal cord, *sox13* signal appeared more intense in the upper layers and in the ventral wall of the neural tube (**d,** black arrowhead). (**C**) *sox13* was expressed in the LPM (**e-g**; black arrowheads) and in the forming axial vessels (**h**,**i**; white arrowheads). Lateral (**a**,**c**,**d**,**e**,**h**,**i**; embryos are shown anterior to the left), frontal (**b**), dorso-lateral (**f**) and caudal (**g**) views.

Fig. 3. Angiogenesis was disrupted in several vascular beds in *sox13* morphants

(**a**,**a'**) ISVs were severely affected in *sox13* morphants compared to controls; at around 30 hpf ISVs could be reduced or totally absent (**a'**) and also DLAV formation was highly compromised (**a'**, white stars). (**b**,**b'**) The caudal vein plexus was strongly reduced in *sox13* morphants at 2 dpf and it lost the braided structure typical of this stage (white brackets). (**c**,**c'**) At 3 dpf, the comparison of the SIV basket between *sox13* morphants and controls highlighted the presence of severe defects also in this structure, which strongly reduced is *sox13* morphants (**c'**, white arrowhead). Representative confocal images of the trunk (**A**), the caudal region (**B**), lateral views, and the SIV basket over yolk (**C**), dorso-lateral view. The tg(*gata1*:dsRed)^{sd2};(*kdrl*:EGFP)^{s843} (**A**,**B**) and the tg(*fli1a*:EGFP)^{y1} (**C**) lines were used for the analysis. Embryos were injected with 0,5 pmol/embryo of *sox13*-sMO.

Fig. 4. ISV angiogenesis was affected in *sox13* morphants

(**A**) The pan-endothelial marker *cdh5* showed by WISH assay that the DA and the PCV were formed in *sox13* morphants. At around 24 hpf ISVs sprouting were absent so far in *sox13* morphants (black arrowhead); at 29 hpf some ISVs were present, but undeveloped with respect to controls. Numbers on the left indicate the numbers of embryos which presented the illustrated phenotypes (**B**) Representative confocal images of the trunk region, lateral view. At around 30 hpf we classified ten consecutive ISVs in the trunk up to the anus as fully formed, reduced (white arrowhead) or totally absent (white star). *sox13* knockdown could be rescued by the coinjection of 0,5 pmol/embryo of *sox13*-sMO with 100 pg/embryo of *sox13* RNA. The tg(*gata1*:dsRed)^{sd2};(*kdrl*:EGFP)^{s843} was used for the analysis. (**C**) Graphical analysis of ISVs phenotype at around 30 hpf in

controls, *sox13* morphants and *sox13* morphants coinjected with *sox13* RNA. White bar indicate normal ISV, light blue reduced ISV and blue totally absent ISVs. Cumulative data of three independent experiments are shown.

Fig. 5. *sox13* could modulate Notch signaling

(**A**) WISH assay showed that *ephrinB2a* signal was slightly increased in the trunk of *sox13* morphants at around 30 hpf. The staining in the cranial region was comparable between *sox13* morphants and controls. Numbers on the left indicate the numbers of embryos which presented the illustrated phenotypes (**B**) Representative confocal images of the trunk region, lateral view, of tg(*gata1*:dsRed)^{sd2};(*kdrl*:EGFP)^{s843} embryos. The treatment of *sox13* morphants with 100 µM of the Notch inhibitor DAPT partially rescued ISV angiogenetic defects. Embryoa were injected with 0,5 pmol/embryos of *sox13*-sMO. (**C**) Graphical analysis of ISVs phenotype at around 30 hpf in controls, *sox13* morphants and *sox13* morphants treated with the DAPT. White bar indicate normal ISV, light blue reduced ISV and blue totally absent ISVs. Cumulative data of three independent experiments are shown. (**D**) Statistical analysis of direct DLAV connections between adjacent ISVs in ten consecutive trunk ISVs, up to the anus, in controls, *sox13* morphants and *sox13* morphants treated with the DAPT at 2 dpf. Statistically highly significant data, with a p value <0.001, are marked by ***.

Figure legends of supplementary figures

Fig. S1. Molecular effects of *sox13* knockdown

(**A**) Diagram of the regions targeted by *sox13*-sMO and *sox13*-sMO2 and readout of processing defects induced by *sox13*-sMO injection (in blue and red). (**B**-**C**) RT-PCR on total RNA extracted from *sox13* morphants and controls injected with *sox13*-sMO (**B**) and *sox13*-sMO2 (**C**). The size of the obtained PCR fragments are 362 bp in controls and around 250 bp and 400 bp in *sox13* morphants (**B**); 454 bp in both *sox13* morphants and controls (**C**). PCR fragment reffered to actb1 is 560 bp (**B**,**C**). The injection of the *sox13*-sMO caused the skipping of exon 3 and the partial retention of the intron 2 (**A**, **B**). The injection of the *sox13*-sMO2 caused the decrease of the wild-type form in sox13 morphants (**C**).

Fig. S2. *sox13* knockdown affects different aspects of embryo development

(**A**) The coinjection of 0,5pmol/embryo of *sox13*-sMO with 0,75 pmol/embryo of p53-MO did not ameliorate defects in the embryo morphology. Brightfield, lateral views. (**B**) IHC staining of motoneurons with anti alfa-synaptotegmin-2 Ab (znp1). In sox13 morphants primary motoneurons are thinner than controls at around 30 hpf and appeared less arborized in their ventral portion at 2 dpf. Lateral flat-mount preparation of the trunk region overhanging the yolk extension.

Fig. S3. *sox13* knockdown mildly affects vasculogenesis and significantly affects ISVs angiogenesis

(**A**) *etv2*/*etsrp* ISHs at 12 somites stage. The external layer of *etsrp* positive cells in posterior LPM present in controls was completely lost in a big

portion of *sox13* morphants (**a**,**a'**, black arrowhead) and the the angioblasts migration from the LPM towards the midline (**b**), was severely (**b'**) or mildly (**b''**) affected in *sox13* morphants. Numbers on the left indicate the numbers of embryos which presented the illustrated phenotypes. Lateral (**a**,**a'**) and dorsal (**b**,**b'**.**b''**) views. (**B**) Statistical analysis of ISVs phenotype at around 30 hpf in controls, *sox13* morphants and *sox13* morphants coinjected with *sox13* RNA. (**C**) Graphical and statistical analysis of ISVs phenotype at around 30 hpf in controls and *sox13* knocked down embryos with 0,5 pmol/embryo of *sox13*-sMO2. Cumulative data of three independent experiments are shown. Statistically highly significant data, with a p value <0.001, are marked by ***. White bar indicate normal ISV, light blue reduced ISV and blue totally absent ISVs (**B**,**C**).

Fig. S4. Analysis of arterial and venous markers in *sox13* morphants and control embryos

(**A**) Analysis of arterial and venous markers by WISH at different developmental stages. The signal of *notch1b* and *ephrinB2a* appeared increased in the trunk of *sox13* morphants. *notch3* and *flt4* expression is gross comparable between controls and *sox13* morphants. Numbers on the left indicate the numbers of embryos which presented the illustrated phenotypes. Lateral views, trunks details, anterior to left.

Fig. S5. Statistical analysys of DAPT treatment at around 30 hpd and 2 dpf

(**A**) Statistical analysis of ISVs phenotype at 30 dpf in controls, *sox13* morphants and *sox13* morphants treated with DAPT. (**B**) Graphical and statistical analysis of ISVs phenotype at 2 dpf in controls, *sox13* morphants and *sox13* morphants treated with the DAPT. White bar indicate normal ISV, light blue reduced ISV and blue totally absent ISVs. Cumulative data

of three independent experiments are shown. Statistically highly significant data, with a p value <0.001, are marked by ***. (**A**,**B**).

Figure 1

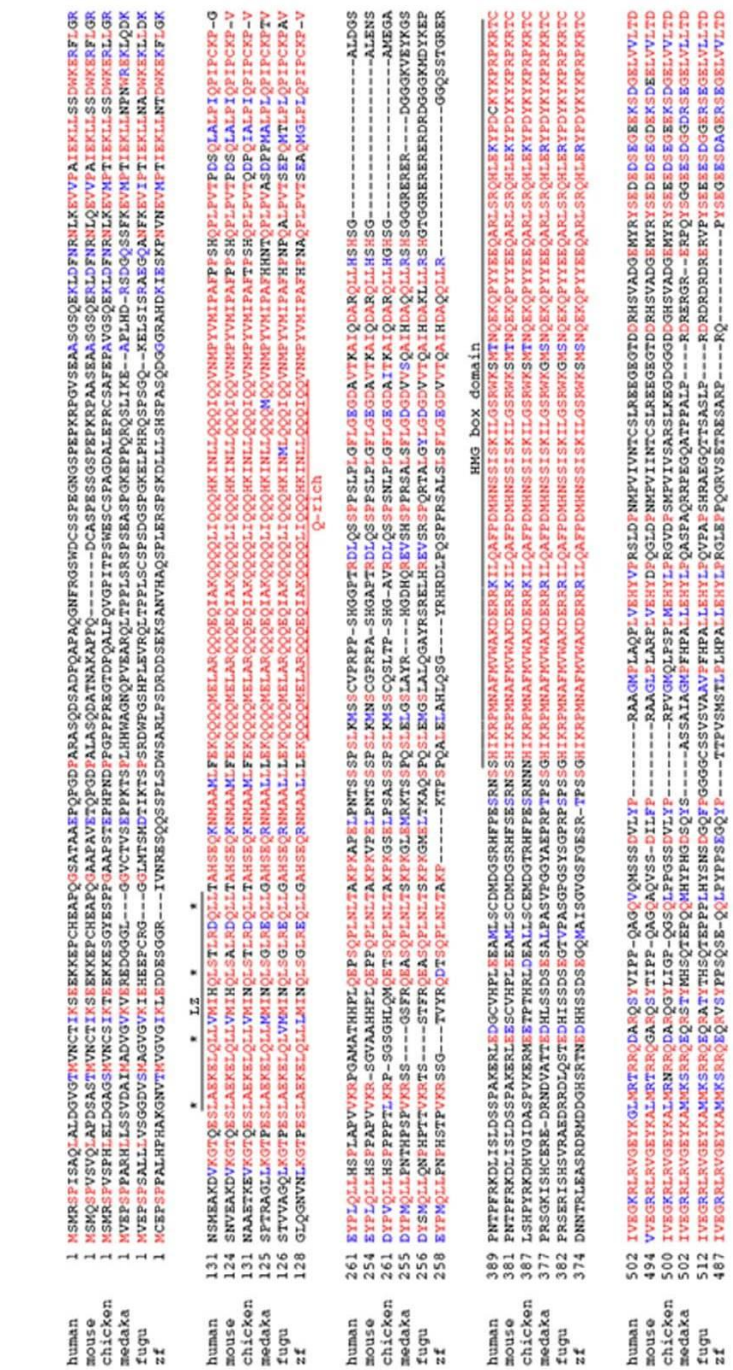

B

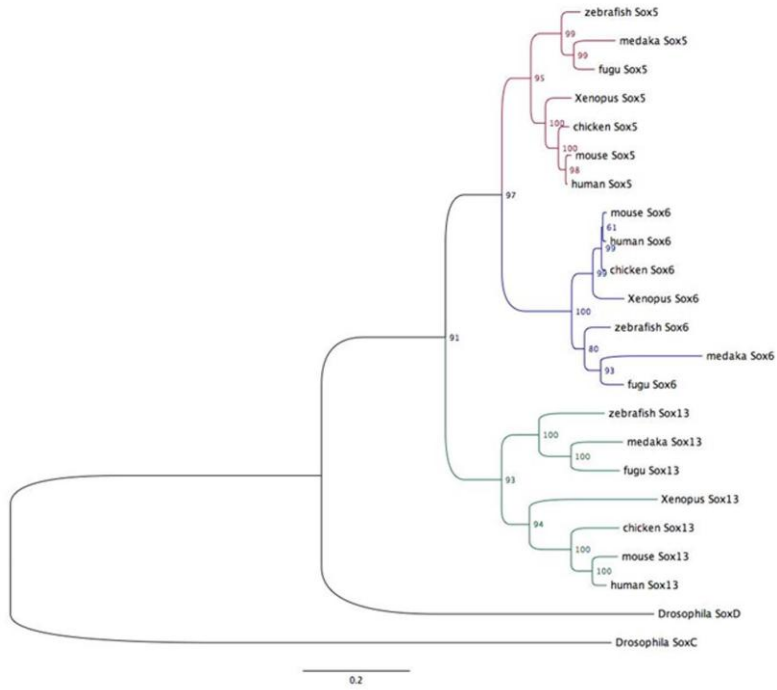
zebrafish Sox5
medaka Sox5
fugu Sox5
Xenopus Sox5
chicken Sox5
mouse Sox5
human Sox5
mouse Sox6
human Sox6
chicken Sox6
Xenopus Sox6
zebrafish Sox6
medaka Sox6
fugu Sox6
zebrafish Sox13
medaka Sox13
fugu Sox13
Xenopus Sox13
chicken Sox13
mouse Sox13
human Sox13
Drosophila SoxD
Drosophila SoxC
0.2

Figure 2

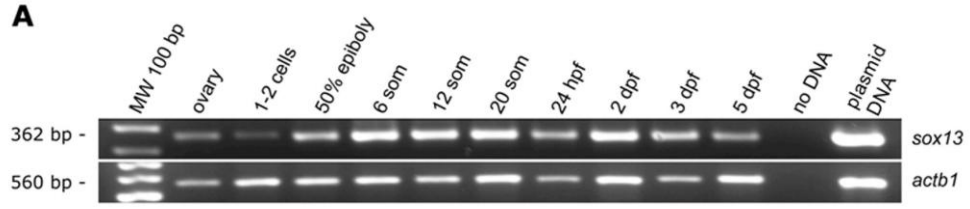
A
MW 100 bp
ovary
1-2 cells
50% epiboly
6 som
12 som
20 som
24 hpf
2 dpf
3 dpf
5 dpf
no DNA
plasmid DNA
362 bp -
560 bp -
sox13
actb1

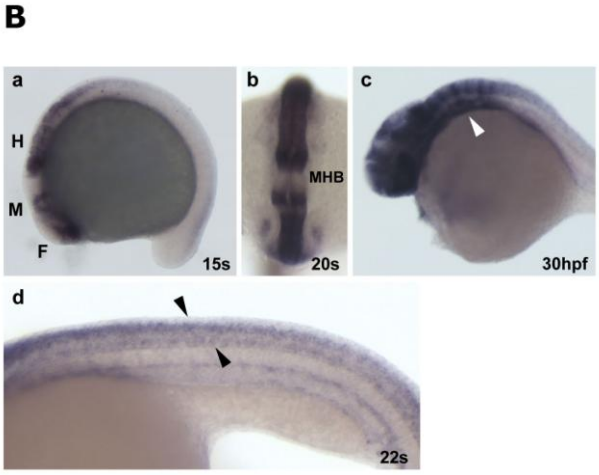
B
a
H
M
F
15s
b
MHB
20s
c
30hpf
d
22s

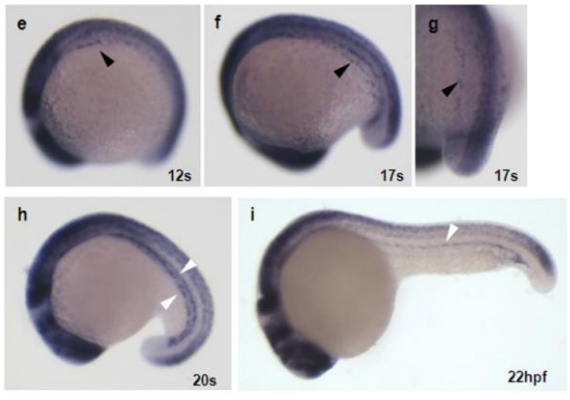
C
e
12s
f
17s
g
17s
h
20s
i
22hpf

Figure 3

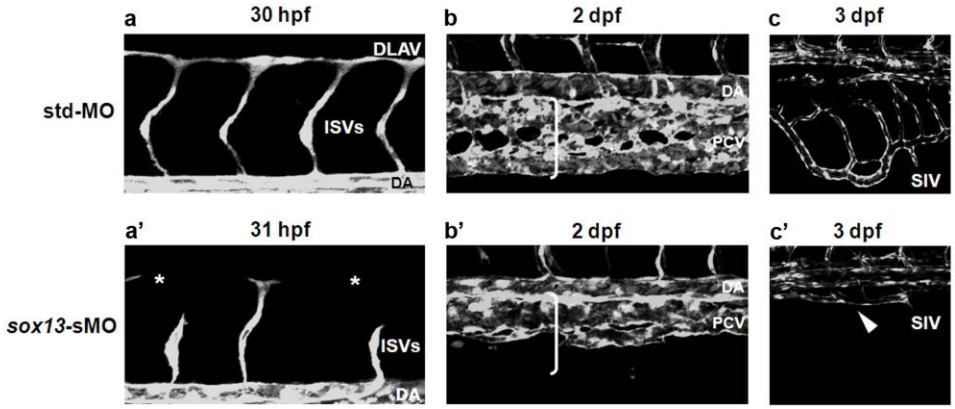
a
30 hpf
b
2 dpf
c
3 dpf
std-MO
DLAV
ISVs
DA
DA
PCV
SIV
a'
31 hpf
b'
2 dpf
c'
3 dpf
sox13-sMO
*
*
ISVs
DA
DA
PCV
SIV

Figure 4

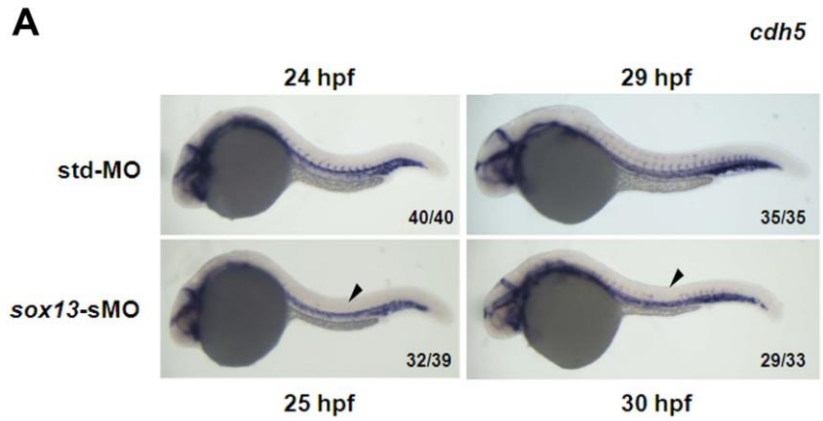
A
cdh5
24 hpf
29 hpf
std-MO
40/40
35/35
sox13-sMO
32/39
29/33
25 hpf
30 hpf

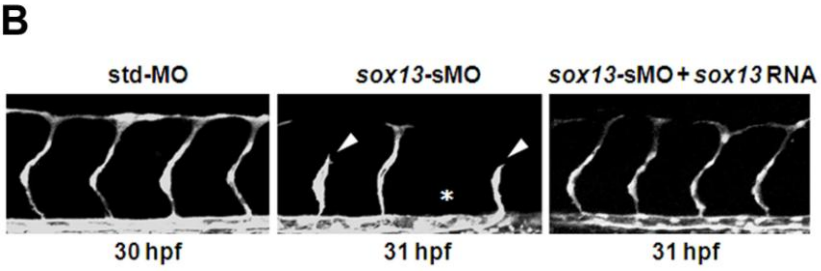
B
std-MO
sox13-sMO
sox13-sMO + sox13 RNA
30 hpf
31 hpf
31 hpf

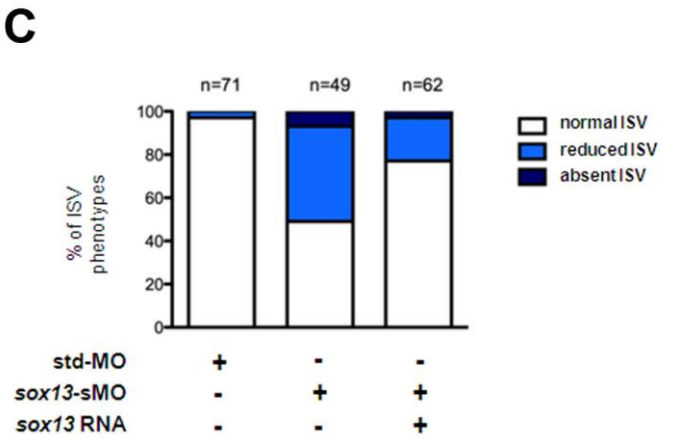
C
n=71
n=49
n=62
% of ISV phenotypes
100
80
60
40
20
0
normal ISV
reduced ISV
absent ISV
std-MO + - -
sox13-sMO - + +
sox13 RNA - - +

Figure 5

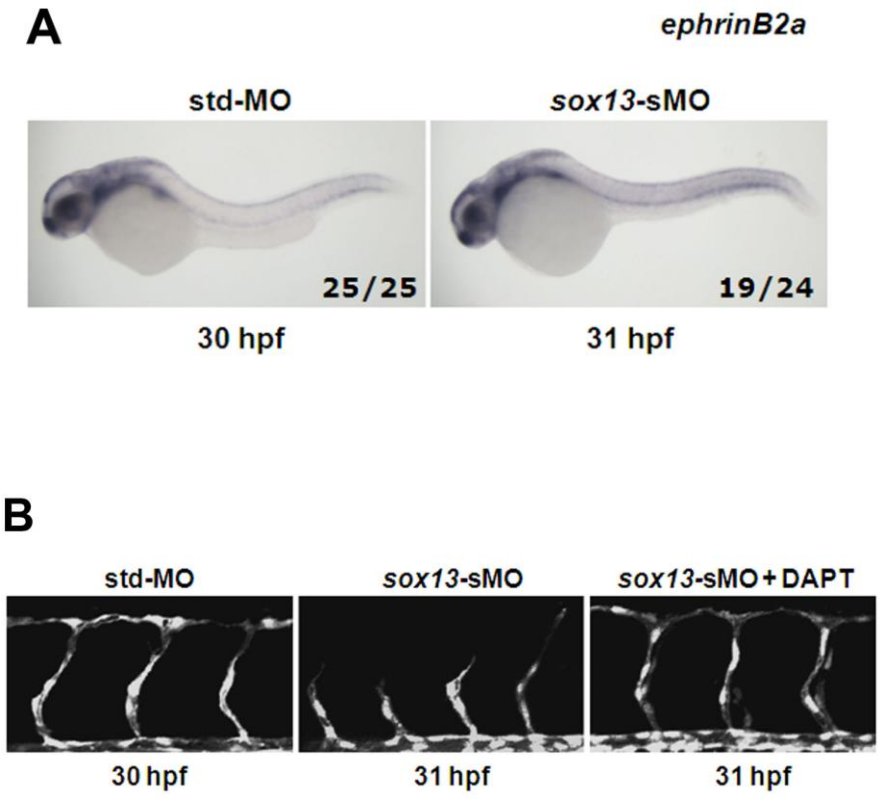
A
ephrinB2a
std-MO
sox13-sMO
25/25
19/24
30 hpf
31 hpf
B
std-MO
sox13-sMO
sox13-sMO + DAPT
30 hpf
31 hpf
31 hpf
C
n=35
n=54
n=56
100
80
60
40
20
0
% of ISV phenotypes
normal ISV
reduced ISV
absent ISV
std-MO + - -
sox13-sMO - + +
DAPT 100 mM - - +

D

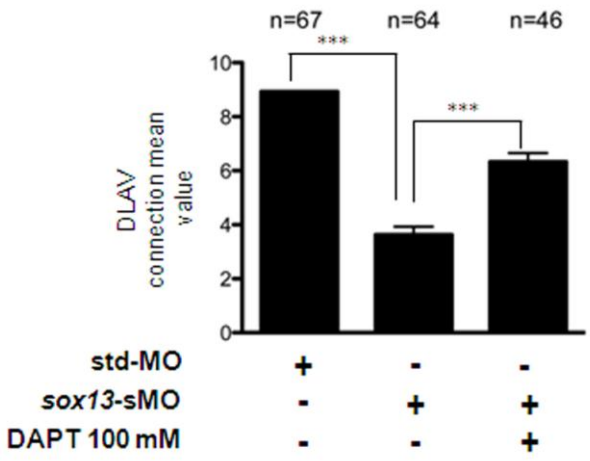
n=67
n=64
n=46
***
***
10
8
6
4
2
0
DLAV connection mean value
std-MO + - -
sox13-sMO - + +
DAPT 100 mM - - +

Supplementary figure 1

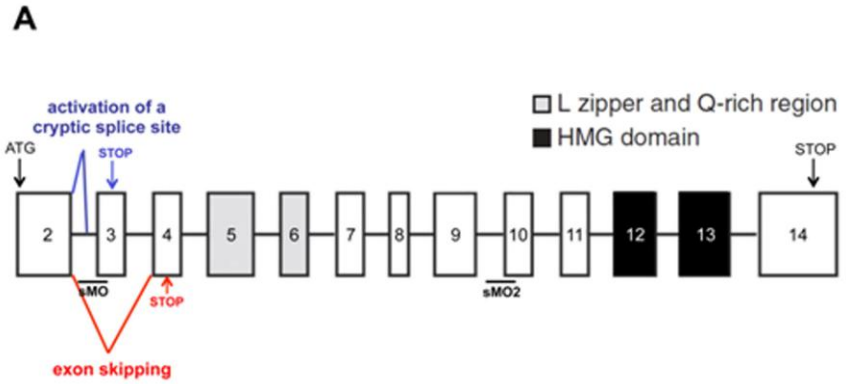

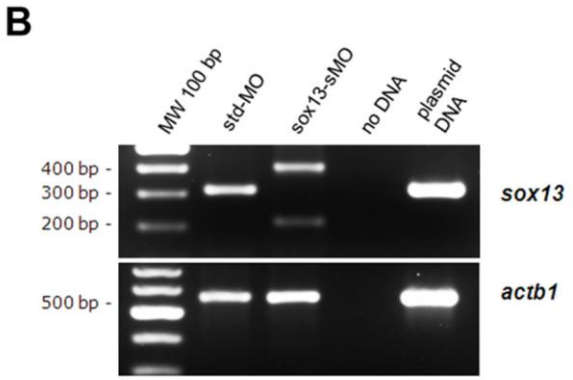

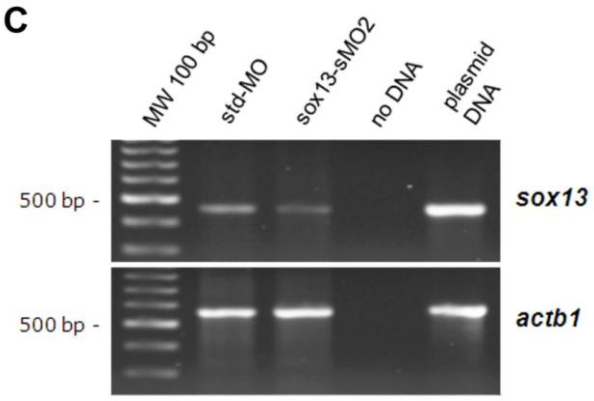

Supplementary figure 2

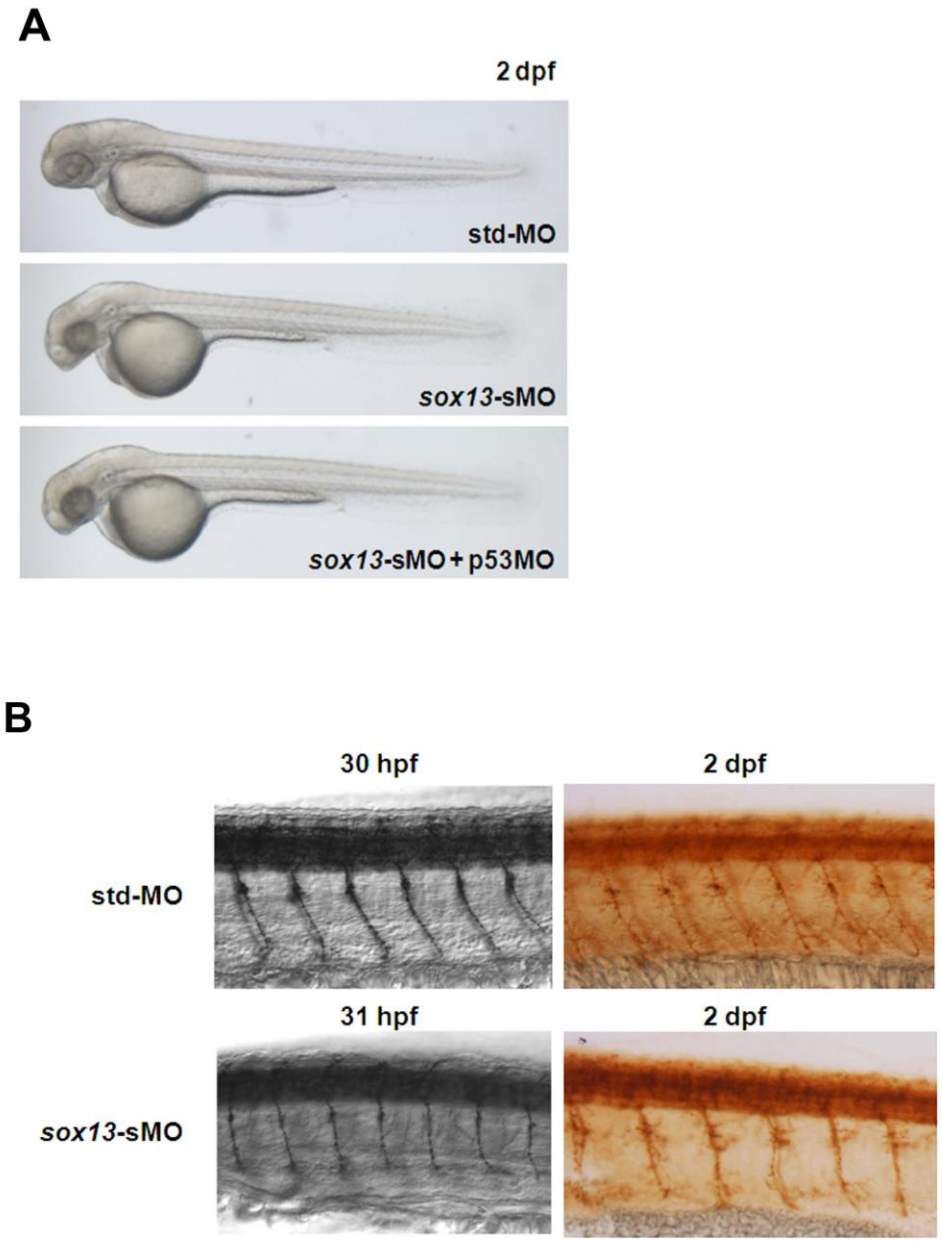

Supplementary figure 3

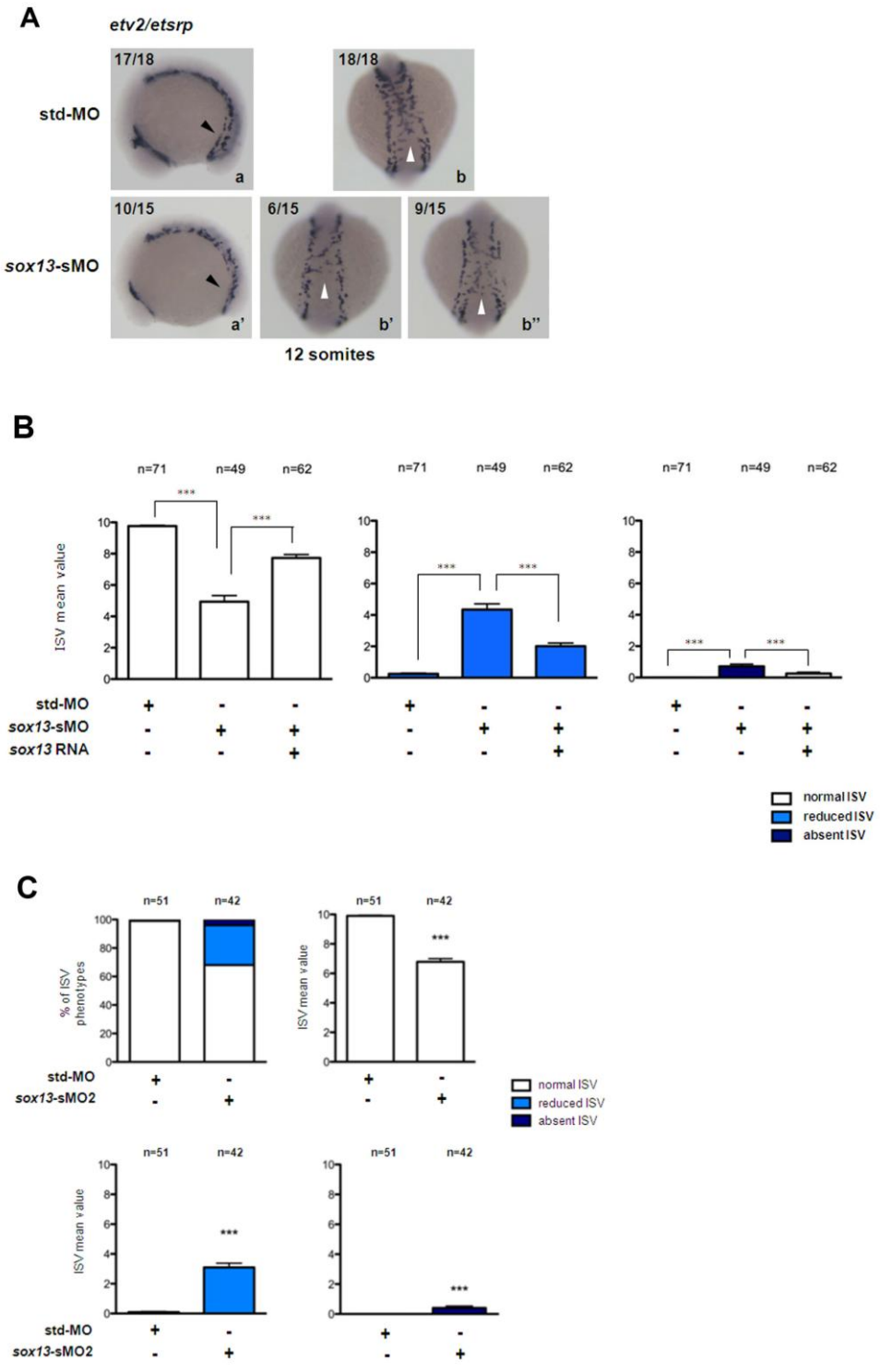

Supplementary figure 4

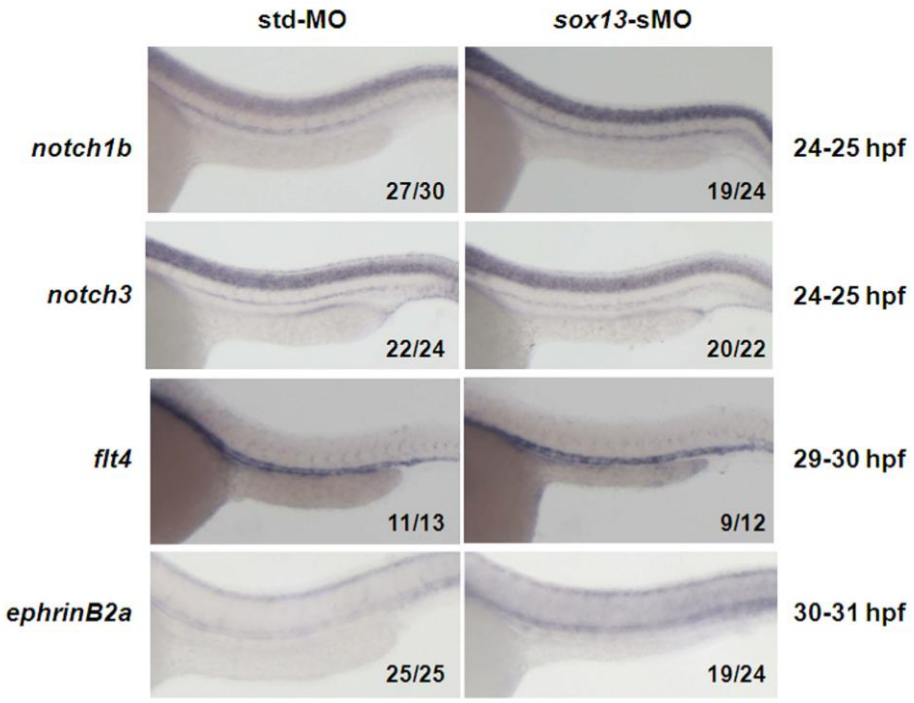

Supplementary figure 5

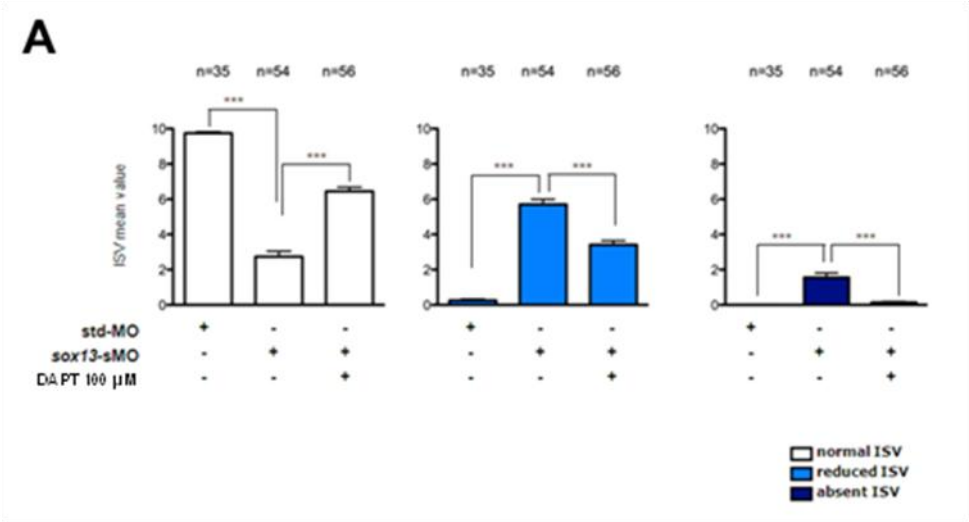

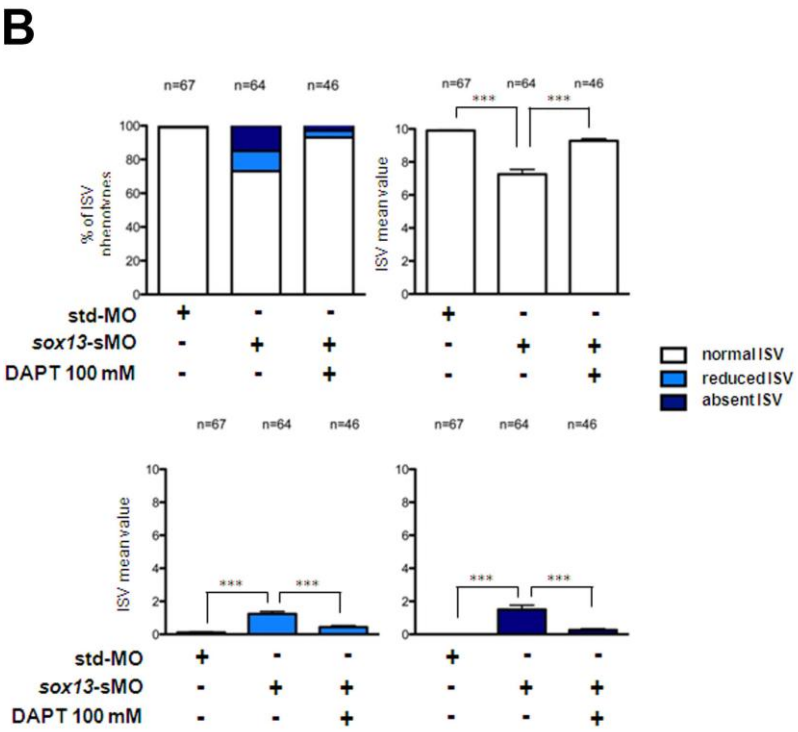

Table S1

Accession numbers of the sequences used for Sox13 protein alignment and SoxD alignments for phylogenetic analysis.

Species	Gene	NCBI ref. sequence
Zebrafish	Sox5	NP_001028757.1
(*Danio rerio*)	Sox6	NP_001116481.1
	Sox13	*In silico* translation
Fugu	Sox5	XP_003977577.1
(*Takifugu rubripes*)	Sox6	XP_003970005.1
	Sox13	XP_003973791.1
Medaka	Sox5	NP_001116382.1
(*Oryzias latipes*)	Sox6	NP_001158340.1
	Sox13	XP_004069090.1
Xenopus	Sox5	NP_001122130.1
(*Xenopus tropicalis*)	Sox6	NP_001116887.1
	Sox13	NP_001017004.1
Chicken	Sox5	NP_001004385.1
(*Gallus gallus*)	Sox6	XP_004941454.1
	Sox13	XP_003642770.2
Mouse	Sox5	NP_035574.2
(*Mus musculus*)	Sox6	NP_001264255.1
	Sox13	NP_035569.2
Human	Sox5	NP_008871.3
(*Homo sapiens*)	Sox6	NP_001139291.1
	Sox13	AAD50120.1

Part III

Sox13 is involved in primitive erythropoieis in zebrafish

Abstract

Sox13 is known to be involved in the regulation of T-cell differentiation by promoting gammadelta T cell development while opposing alphabeta T cell differentiation (Melichar et al., 2007). In zebrafish, we verified that *sox13* knockdown affects T cell markers. On the other hand, a possible implication of Sox13 in other aspects of the hematopoietic development has never been proposed. Sox13 expression has not been reported until now in the erythropoietic tissues in mouse and a role in erythropoiesis was so far excluded (Dumitriu et al., 2006). We report here, for the first time, *sox13* expression in the region were primitive erythrocyte progenitors accumulate and differentiate. We collected data, using different approaches, suggesting a role for *sox13* in primitive erythrocyte differentiation during zebrafish development. Our next step is to shed light on the molecular pathways in which Sox13 acts during primitive erythropoiesis. We are also interested in analysing if definitive hematopoieisis occurs correctly in *sox13* morphants.

Results and Discussion

sox13 is expressed in primitive erythropoietic tissues

During the characterization of *sox13* expression in zebrafish by WISH, we observed a signal in the ICM both in whole mount and in

histological sections. This expression is well detectable at 22 hpf (Fig. 1). At this developmental stage, erythrocyte progenitors accumulate in the ICM after the migration from the lateral plate mesoderm, which is the region where they primarily differentiate from the hemangioblasts. We reasoned that, due to this expression, *sox13* could be involved in erythrocyte differentiation and we decided to better investigate this aspect.

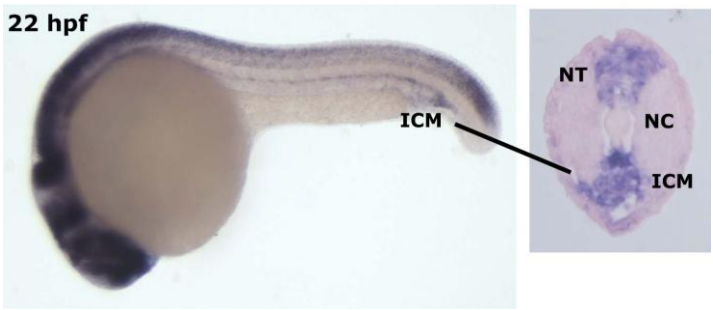

Fig. 1: *sox13* is expressed in the ICM. We detected a *sox13* signal in the region of the ICM by WISH (left panel). Right panel: histological section of the same embryo (nt:neural tube, nc:notochord, icm: intermediate cell mass).

sox13 knockdown affects T-cell markers

Zebrafish hematopoiesis consists of two waves. During the primitive wave (6-30hpf) erythrocytes and some myeloid cells are generated; in the definitive wave (30hpf-adult) all blood lineages are defined (Paik and Zon, 2010). We decided to investigate the role of *sox13* in zebrafish development using a morpholino knockdown approach. I performed knockdown experiments injecting independently two different types of morpholino. A translation-blocking morpholino was used to inhibit the translation of both maternal and zygotic transcripts to obtain a dose-dependent decrease of Sox13 protein levels. To check the specificity

of the phenotypes I observed, I also performed knockdown assays using two splice-blocking morpholino. With all these three morpholinos I observed the same defects that I will describe in the following paragraphs. As a starting point of this study, we decided that it would be interesting to observe if Sox13 is involved in T cell development also in zebrafish. The thymus arises from the third pharyngeal pouch. To determine if the development of the organ starts correctly I analyzed the expression of the pharyngeal marker *nkx2.3*, which appears unaffected in *sox13* morphants at 2.5 dpf (Fig. 2 – upper panel). Instead, *sox13* knockdown affects the expression of T cells marker such as *rag1* and *ikaros* (Fig. 2 – lower panel and data not shown). These data suggest a possible involvement for *sox13* in T cell development also in zebrafish. However, we cannot elucidate a possible role in the differentiation of the diverse sub-populations as in mouse, because the specific markers are not available in zebrafish.

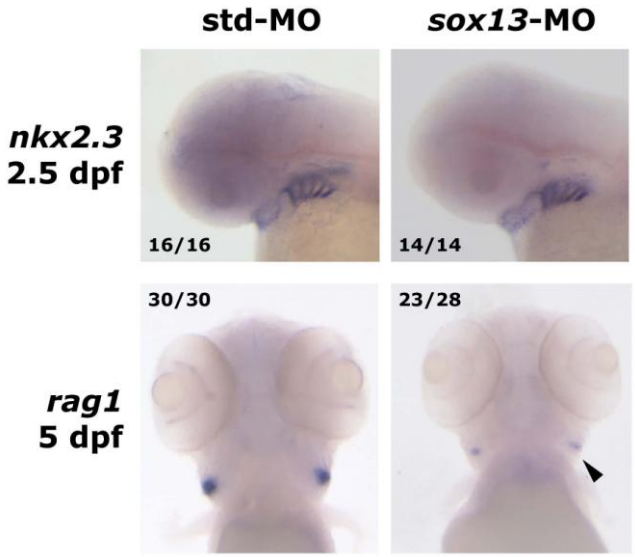

Fig. 2: The *nkx2.3* pharyngeal pouch marker is unaffected in *sox13* morphants at 2.5 dpf (upper panel). *sox13* knockdown causes instead the reduction of thymus markers, such as *rag1* (lower panel; black arrowhead) at 5 dpf.

sox13 morphants show a reduction in the number of differentiated erythrocytes

I performed *in vivo* analysis using the transgenic line (kdrl:GFP;gata1:dsRed) that expresses GFP under the endothelial specific promoter *kdrl*/*flk1*/*vegfr2*, which allows visualization of the vascular tree, and dsRed under the erythroid specific promoter *gata1* to monitor blood circulation. I observed blood circulation in *sox13* morphants both in bright field and by fluorescence. I did not detect circulatory defects in *sox13* morphants and the amount of blood circulating cells is not grossly affected compared to control embryos (Fig. 3 - left panel). Then, I performed the o-dianisidine staining, which detects the hemoglobin activity of the erythrocytes, to verify the differentiation levels of the circulating blood

cells. In *sox13* morphants the staining is remarkably reduced compared to control embryos. We concluded that in *sox13* morphants the circulation is not grossly affected, however circulating cells do not have reached the same differentiation stage of control embryos.

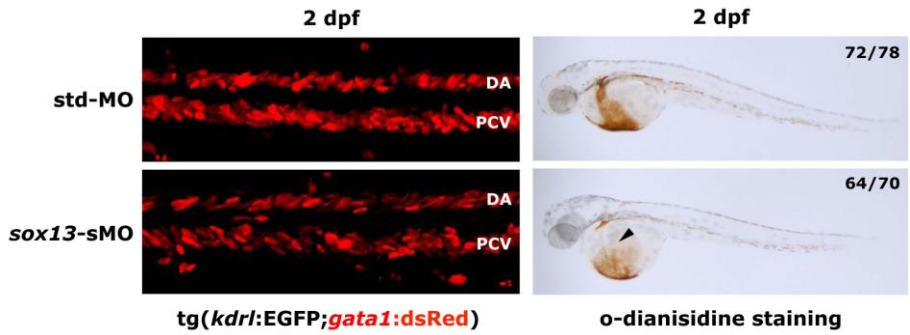

Fig. 3: On the left, confocal images of tg(*kdrl*:EGFP;*gata1*:dsRed) embryos show no gross defects in the amount of blood circulating cells in *sox13* morphants compared to control embryos. On the right, the o-dianisidine staining is remarkably reduced in *sox13* morphants (black arrowhead).

ISH analysis of early erythroid markers suggests defects in erythrocyte differentiation

I decided to analyze a series of molecular markers to better characterize my preliminary observations. At two different time points, I compared the expression of *gata1*, the early erythroid marker for excellence, and of *hbbe3*, the only exclusive embryonic globin, between *sox13* morphants and control embryos. At 22 hpf both *gata1* and *hbbe3* signals in *sox13* morphants seem to be comparable to control embryos (Fig. 4 – left panel). At 2 dpf, *gata1* expression is normally undetectable by ISH in control embryos. However a signal of *gata1* which corresponds to the accumulation of erythrocytes on the yolk is clearly visible in *sox13*

morphants (Fig. 4 – right panel). At the same stage, *hbbe3* signal appears more intense in *sox13* morphants (Fig. 4 – right panel). The persistent or increased signal of some early erythroid markers that are normally absent or less expressed at 2 dpf confirms defects in erythrocyte differentiation upon *sox13* knockdown.

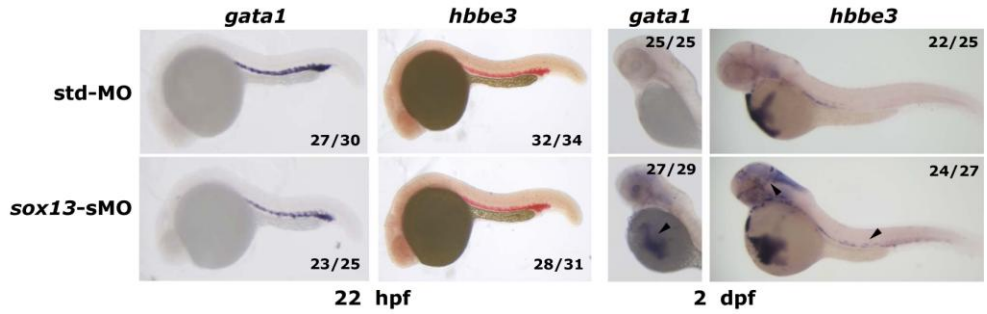

Fig. 4: Analysis of early erythrocyte markers. *gata1* and *hbbe3* at 22 hpf (left panel) and at 2 dpf (right panel). Black arrowheads indicate the anomalous persistence of the signals in *sox13* morphants.

I decided to analyze also some myeloid markers to investigate if defects in primitive hematopoieis in *sox13* morphants are specific of the erythroid lineage. I analyzed the expression of *pu.1/spi1b* and *l-plastin/lcp1* at around 22 hpf and I did not detect any significant difference between *sox13* morphants and controls (Fig. 5), pointing to a specific defect on the erythroid lineage.

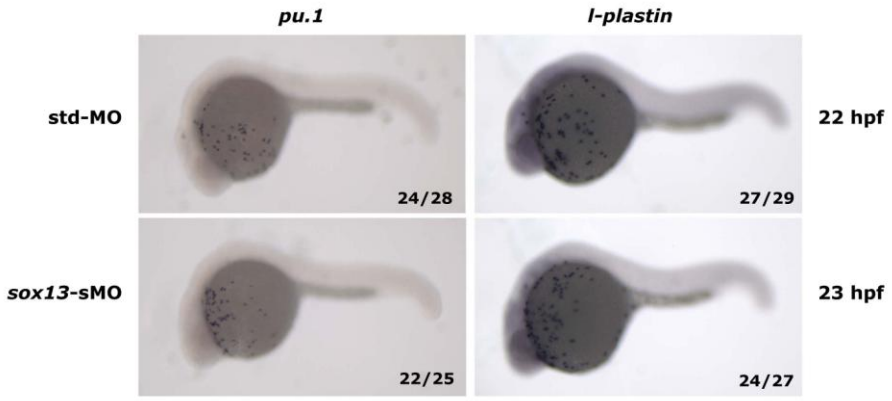

Fig. 5: Some myeloid markers appear unaffected in *sox13* morphants.

We reasoned that it will be important to analyze also the cell lineages of the definitive hematopoieis. We have already described that T cells development is affected in *sox13* morphants. As a very preliminary analysis, I checked for some marker (*runx1* and *gfi1aa*) of the AGM (aorta-gonad-mesonephros region), which is the region where definitive hematopoietic stem cells arise. Both of them seemed not to be grossly affected in sox13 morphants (Fig. 6), but more analyses have to be carried out.

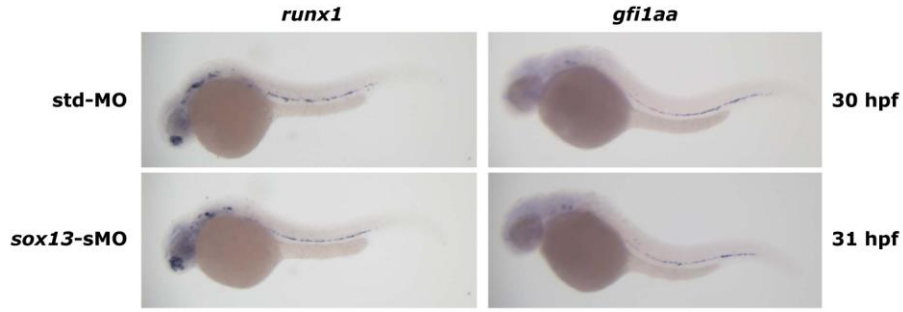

Fig. 6: Preliminary data show that the expression of two AGM markers is not grossly affected.

Blood smears and FACS analysis support the hypothesis of differentiation defects

Erythrocyte differentiation is characterized by changes in cell size, in nuclear shape and in cytoplasmatic staining (Fig. 7 – upper panel). I decided to analyze *sox13* morphants circulating cells by blood smears assay at 3 dpf. However, I ran into some difficulties to set up the blood smears procedures and no cells counts are available yet. Preliminary cytological analysis showed that *sox13* morphants erythroid cells maintain a morphology which is more similar to the aspect of an immature cell. They are big round-shaped, have a large and open nucleus and a more basophilic cytoplasm (Fig. 7 – right lower panel). On the other hand, most cells in the control embryos have a morpholgy which is more similar to mature erythrocyte. These cells are rugby-ball shaped and a little bit smaller than progenitors, the nucleus is more condensed and cytoplasm is acidophilic (Fig. 7 – left lower panel, black arrowheads).

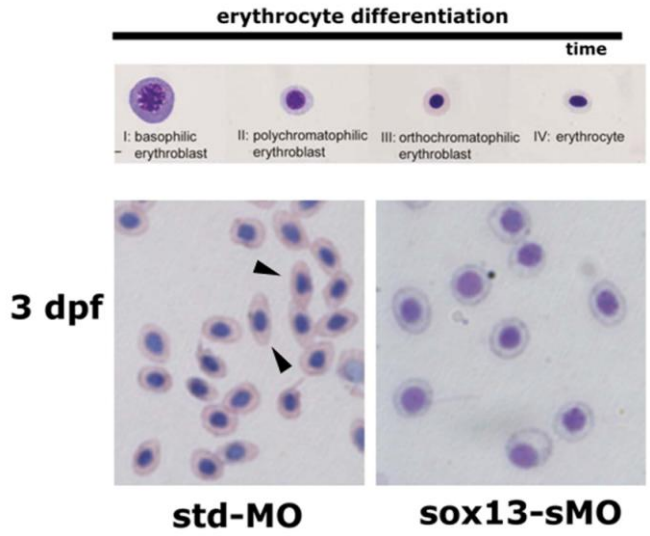

Fig. 7: Cytological analysis confirms erythrocyte differentiation defects in *sox13* morphants (lower panel). Time course of the primitive erythrocyte differentiation (upper panel). Details of blood smears of sox13 morphants and control embryos; black arrowhead indicate more mature cells in control embryos.

Using flow cytometry, it is possible to distinguish cell populations by size and granulosity, which influence forward scatter (FSC) and side scatter (SSC) parameters in FACS plot. We reasoned that this technique could be an additional control to validate the different nature of blood circulating cells in *sox13* morphants, as progenitors and more mature cells have a different size and morphology. FACS sorting assay is largely used in zebrafish for the analysis of adult blood cells, but it is not so usual for embryos (Traver et al., 2003; Hsu et al., 2004; Pimtong et al., 2014). For this analysis I dissociated embryos of the tg line (kdrl:GFP;gata1:dsRed), to easily analyse the erythropoietic component. In a very preliminary analysis we observed that dsRed+ cells of *sox13* morphants sample spread in a different way compared to control embryos (Fig. 8 – right panel). In

particular, cells are less accumulated in a region on the left side of the plot (Fig. 8 – right panel, black arrowhead). In the FACS plot from adult kidney marrow, which is the erythropoietic organ in the adult zebrafish, in this region accumulate mature erythrocytes (Traver et al., 2003). We are planning to perform other experiment at different time points using this assay to check if dsRed+ cells spread different between *sox13* morphants and control embryos throughout erythrocyte differentiation.

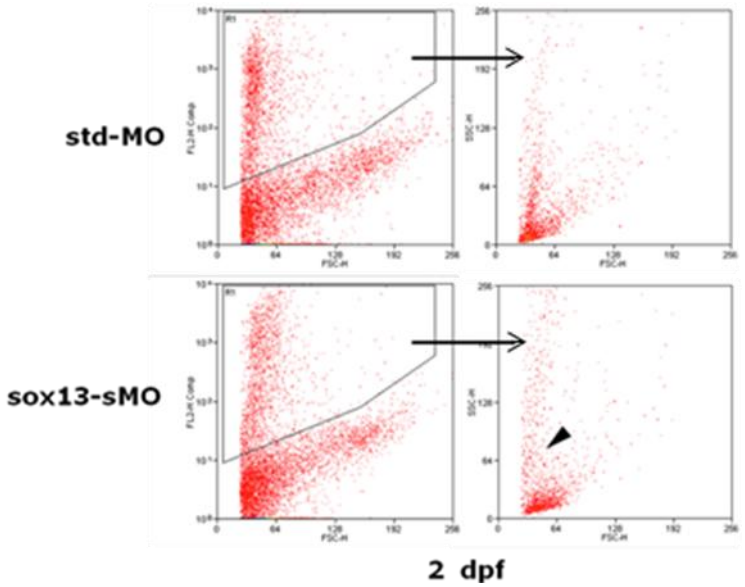

Fig. 8: Flow cytometry analysis of *sox13* morphants reveals a different distribution of erythrocytes. Plots on the left show dsRed+ and GFP+ cells. In R1 plots dsRed+ cells are selected. dsRed + cells correspond to 12,5% and 8,3% of the total counted events in controls and *sox13* morphants, respectively. On the right, dsRed+ cells spread into the plots according to FSC and SSC parameters. Black arrowhead indicates the region where dsRed+ cells are less accumulated.

Conclusion and future perspectives

We propose here for the first time an involvement for Sox13 in primitive erythropoieisis. Our data report a *sox13* expression in the ICM, where primitive erythrocyte progenitors accumulate before entering circulation. Loss-of-function assays using a morpholino approach revealed that *sox13* knocked-down embryos present defects in erythrocyte differentiation, pointing to a role for Sox13 in this process.

Our next goal is to shed light on the molecular pathways in which *sox13* is involved during primitive erythropoiesis. We previously demonstrated that Sox13 could modulate the Notch pathway activity during intersomitic vessels angiogenesis in zebrafish. Interestingly, Notch signaling is a key factor in inhibiting the differentiation of hematopoietic stem cells (Cheng et al., 2008) and, in zebrafish, an enhanced Notch activation has been shown to result in primitive erythroid differentiation defects (Bresciani et al., 2010). We want to verify if the defects in primitive erythrocytes differentiation provoked by *sox13* knockdown could be caused by an uncorrect modulation of the Notch signalling pathway.

Materials and methods

Zebrafish lines and maintenance

Zebrafish were raised and maintained according to established techniques (Westerfield, 1993). The following strains were used: AB (from the Wilson lab, UCL, London, UK), Tg(*gata1*:dsRed)^{sd2};(*kdrl*:EGFP)^{s843} (from Massimo Santoro lab, Università di Torino, Italy).

Morpholinos microinjections

Antisense morpholinos were purchased from Gene Tools (LLC, Philomath, OR).

sox13-MO: 5' – GGCTCACACATTCAACTCCAAAAGA – 3'(translation blocking MO, targeting the AUG region);

sox13-sMO: 5' – GAGAACGCTCCTATAAACAGAGATA – 3'(splice-blocking MO, targeting the i2e3 splice site);

sox13-sMO2: 5' – CTCCCAAGAAGCCTGGAGAGTGAAA – 3'(splice-blocking MO, targeting the i9e10 splice site).

MOs, diluted in Danieau buffer (Nasevicius and Ekker, 2000), were injected at 1- to 2-cell stage. Escalating doses of each MO were tested for phenotypic effects; as control for unspecific effects, each experiment was performed in parallel with a std-MO (standard control oligo) with no target in zebrafish embryos.

In situ analysis, histological section, o-dianisidine staining and imaging

Whole mount *in situ* hybridization were carried out as described, (Thisse et al., 1993; Patterson et al., 2005). We synthesized probes as described in the following papers: *nkx2.3* (Trede et al., 2008), *rag1* (Willett et al., 1997), *gata1* (Detrich et al., 1995), *hbbe3* (Ganis et al., 2012), *pu.1* (Bennett et al., 2001), *l-plastin* (Herbomel et al., 1999), *runx1* (Kalev-Zylinska et al., 2002), *gfi1aa* (Cooney et al., 2013). Histological sections were carried out as described (Cermenati et al., 2008). O-dianisidine staining was carried out as described (Detrich et al., 1995). Images were taken with a Leica MZFLIII epifluorescence stereomicroscope equipped with a DFC 480-R2 digital camera or with a Leica microscope equipped with a Leica 480

digital camera and the LAS imaging software (Leica, Wetzlar, Germany). Confocal microscopy was performed on a Leica TCS SP2 AOBS microscope, equipped with an argon laser, or a Zeiss 510 microscope. Images were processed using the Adobe Photoshop software (Adobe, San Jose, CA).

Blood smears

Embryos were anesthetized in 0,02% tricaine and dissected directly on slides. Preparations were treated as described (Bresciani et al., 2010).

Embryo dissociation and FACS analysis

Embryos were dissociated essentially as described (Ma et al., 2010). Sample were analysed using a BD *FACSCalibur*™ and the collected data analysed and elaboreted with Summit 4.3.

Acknowledgements

I want to thank Cristina Fugazza for the FACS analysis and Antonella Ronchi and Erica Bresciani for helpful discussions and suggestions.

References

Bennett CM, Kanki JP, Rhodes J, Liu TX, Paw BH, Kieran MW, Langenau DM, Delahaye-Brown A, Zon LI, Fleming MD, Look AT. 2001. Myelopoiesis in the zebrafish, Danio rerio. Blood 98:643-651.

Bresciani E, Confalonieri S, Cermenati S, Cimbro S, Foglia E, Beltrame M, Di Fiore PP, Cotelli F. 2010. Zebrafish numb and numblike are involved in primitive erythrocyte differentiation. PLoS One 5:e14296.

Cermenati S, Moleri S, Cimbro S, Corti P, Del Giacco L, Amodeo R, Dejana E, Koopman P, Cotelli F, Beltrame M. 2008. Sox18 and Sox7 play redundant roles in vascular development. Blood 111:2657-2666.

Cheng X, Huber TL, Chen VC, Gadue P, Keller GM. 2008. Numb mediates the interaction between Wnt and Notch to modulate primitive erythropoietic specification from the hemangioblast. Development 135:3447-3458.

Cooney JD, Hildick-Smith GJ, Shafizadeh E, McBride PF, Carroll KJ, Anderson H, Shaw GC, Tamplin OJ, Branco DS, Dalton AJ, Shah DI, Wong C, Gallagher PG, Zon LI, North TE, Paw BH. 2013. Teleost growth factor independence (gfi) genes differentially regulate successive waves of hematopoiesis. Dev Biol 373:431-441.

Detrich HW, 3rd, Kieran MW, Chan FY, Barone LM, Yee K, Rundstadler JA, Pratt S, Ransom D, Zon LI. 1995. Intraembryonic hematopoietic cell migration during vertebrate development. Proc Natl Acad Sci U S A 92:10713-10717.

Dumitriu B, Patrick MR, Petschek JP, Cherukuri S, Klingmuller U, Fox PL, Lefebvre V. 2006. Sox6 cell-autonomously stimulates erythroid cell survival, proliferation, and terminal maturation and is thereby an important enhancer of definitive erythropoiesis during mouse development. Blood 108:1198-1207.

Ganis JJ, Hsia N, Trompouki E, de Jong JL, DiBiase A, Lambert JS, Jia Z, Sabo PJ, Weaver M, Sandstrom R, Stamatoyannopoulos JA, Zhou Y, Zon LI. 2012. Zebrafish globin switching occurs in two developmental stages and is controlled by the LCR. Dev Biol 366:185-194.

Herbomel P, Thisse B, Thisse C. 1999. Ontogeny and behaviour of early macrophages in the zebrafish embryo. Development 126:3735-3745.

Hsu K, Traver D, Kutok JL, Hagen A, Liu TX, Paw BH, Rhodes J, Berman JN, Zon LI, Kanki JP, Look AT. 2004. The pu.1 promoter drives myeloid gene expression in zebrafish. Blood 104:1291-1297.

Kalev-Zylinska ML, Horsfield JA, Flores MV, Postlethwait JH, Vitas MR, Baas AM, Crosier PS, Crosier KE. 2002. Runx1 is required for zebrafish blood and vessel development and expression of a human RUNX1-CBF2T1 transgene advances a model for studies of leukemogenesis. Development 129:2015-2030.

Ma AC, Chung MI, Liang R, Leung AY. 2010. A DEAB-sensitive aldehyde dehydrogenase regulates hematopoietic stem and progenitor cells development during primitive hematopoiesis in zebrafish embryos. Leukemia 24:2090-2099.

Melichar HJ, Narayan K, Der SD, Hiraoka Y, Gardiol N, Jeannet G, Held W, Chambers CA, Kang J. 2007. Regulation of gammadelta versus alphabeta T lymphocyte differentiation by the transcription factor SOX13. Science 315:230-233.

Nasevicius A, Ekker SC. 2000. Effective targeted gene 'knockdown' in zebrafish. Nat Genet 26:216-220.

Paik EJ, Zon LI. 2010. Hematopoietic development in the zebrafish. Int J Dev Biol 54:1127-1137.

Patterson LJ, Gering M, Patient R. 2005. Scl is required for dorsal aorta as well as blood formation in zebrafish embryos. Blood 105:3502-3511.

Pimtong W, Datta M, Ulrich AM, Rhodes J. 2014. Drl.3 governs primitive hematopoiesis in zebrafish. Sci Rep 4:5791.

Thisse C, Thisse B, Schilling TF, Postlethwait JH. 1993. Structure of the zebrafish snail1 gene and its expression in wild-type, spadetail and no tail mutant embryos. Development 119:1203-1215.

Traver D, Paw BH, Poss KD, Penberthy WT, Lin S, Zon LI. 2003. Transplantation and in vivo imaging of multilineage engraftment in zebrafish bloodless mutants. Nat Immunol 4:1238-1246.

Trede NS, Ota T, Kawasaki H, Paw BH, Katz T, Demarest B, Hutchinson S, Zhou Y, Hersey C, Zapata A, Amemiya CT, Zon LI. 2008. Zebrafish mutants with disrupted early T-cell and thymus development identified in early pressure screen. Dev Dyn 237:2575-2584.

Westerfield M. 1993. The zebrafish book. University of Oregon Press, Eugene, OR.

Willett CE, Cherry JJ, Steiner LA. 1997. Characterization and expression of the recombination activating genes (rag1 and rag2) of zebrafish. Immunogenetics 45:394-404.

Appendix

Acronyms

AGM	aorta-gonad-mesonephros
aISV	arterial intersomitic vessels
ALM	anterior lateral plate mesoderm
BEC	blood vascular endothelial cells
BMP	bone morphogenetic protein
CA	caudal artery
CHT	caudal hematopoietic tissue
CNS	central nervous system
CV	caudal vein
CVP	caudal vein plexus
DA	dorsal aorta
DC	duct of Cuvier (= common cardinal vein or CCV)
DLAV	dorsal longitudinal anastomotic vessel
DLLV	dorsal longitudinal lymphatic vessel
dpf	days post-fertilization
E	embryonic day
EC	endothelial cell
EMP	erythroid-myeloid progenitors
F	forebrain
FL	facial lymphatics
H	hindbrain
HLT	hypotrichosys-lymphedema-telangiectasia
HLTRS	hypotrichosys-lymphedema-telangiectasia-renal defect syndrome
HMG	high mobility group

hpf	hours post-fertilization
HSC	hematopoietic stem cell
ICM	intermediate cell mass
IL	intestinal lymphatics
ISH	*in situ* hybridization
ISLV	intersomitic lymphatic vessels
ISV	intersomitic vessels
LDA	lateral dorsal aorta
LEC	lymphatic endothelial cells
LL	lateral lymphatics
LPM	lateral plate mesoderm
M	midbrain
MHB	midbrain-hindbrain boundary
MO	morfolino
PCV	posterior cardinal vein
PLM	posterior lateral plate mesoderm
PL	parachordal lymphangioblasts
s	somite
SIA	sub-intestinal artery
SIV	sub-intestinal vein
TD	thoracic duct
VEGF	vascular endothelial growth factor
vISV	venous intersomitic vessel
WISH	whole-mount *in situ* hybridization

Zebrafish embryo developmental stages